RECORD
1999/4

GOVERNMENT OF
WESTERN AUSTRALIA

GSWA EMPRESS 1 AND 1A WELL COMPLETION REPORT YOWALGA SUB-BASIN OFFICER BASIN WESTERN AUSTRALIA

compiled by M. K. Stevens and S. N. Apak

GEOLOGICAL SURVEY OF WESTERN AUSTRALIA

DEPARTMENT OF MINERALS AND ENERGY

GEOLOGICAL SURVEY OF WESTERN AUSTRALIA

Record 1999/4

GSWA EMPRESS 1 AND 1A WELL COMPLETION REPORT Yowalga Sub-basin, Officer Basin Western Australia

compiled by

M. K. Stevens and S. N. Apak

with contributions from

J. Backhouse, K. A. R. Ghori, K. Grey, P. J. Havord, K. Martin, I. Ruddock, and S. Shevchenko

Perth 1999

REFERENCE
The recommended reference for this publication is:
STEVENS, M. K., and APAK, S. N., (compilers), 1999, GSWA Empress 1 and 1A well completion report, Yowalga Sub-basin, Officer Basin, Western Australia: Western Australia Geological Survey, Record 1999/4, 110p.

National Library of Australia Card Number and ISBN 0 7309 6632 1

Printed by Optima Press, Perth, Western Australia

Copies available from:

Information Centre
Department of Minerals and Energy
100 Plain Street
EAST PERTH, WESTERN AUSTRALIA 6004
Telephone: (08) 9222 3459 Facsimile: (08) 9222 3444
www.dme.wa.gov.au

Contents

Appendices

Plates

Figures

Digital dataset (in pocket)

Digital well log information and text

GSWA Empress 1 and 1A well completion report Yowalga Sub-basin, Officer Basin Western Australia

compiled by
M. K. Stevens and S. N. Apak

with contributions from
J. Backhouse, K. A. R. Ghori, K. Grey, P. J. Havord, K. Martin, I. Ruddock, and S. Shevchenko

Abstract

Empress 1 and 1A are two vertical stratigraphic drillholes located in the Yowalga Sub-basin of the Officer Basin in Western Australia. Empress 1 was designed to further define the petroleum source potential of the Neoproterozoic and lower Palaeozoic rocks of the Officer Basin. Empress 1 was cored from 105 to 612.9 m, but was abandoned as a result of technical difficulties. Empress 1A was continuously cored from 210.5 to 1624.6 m total depth. The drillhole penetrated unnamed strata (Cainozoic), the Paterson Formation, Lennis Sandstone, Table Hill Volcanics (Palaeozoic), an unnamed unit (Neoproterozoic), ?Lupton Formation (Supersequence 3), Kanpa, Hussar, Browne, and ?Lefroy Formations (Supersequence 1), and pre-Officer Basin strata.

Potassium–argon dating indicates ages of 484 ± 4 Ma for the Table Hill Volcanics and 1058 ± 13 Ma for the volcanic rocks within the pre-Officer Basin sequence. No hydrocarbons were encountered in the drillhole.

The Kanpa and Hussar Formations of Supersequence 1, which consist mainly of interbedded siliciclastic rocks (mudstone to sandstone) and stromatolitic dolomite, show overall shoaling-upward characteristics. Oil-prone organic-rich beds are present within thinly laminated mudstones in facies associated with the dolomitic carbonates of the Kanpa Formation in Empress 1A. TOC and Rock-Eval analyses, conducted on core samples, revealed that three samples from the Kanpa Formation have good oil- and gas-generating potential. The Kanpa and Hussar Formations also have good reservoir potential in medium- to coarse-grained sandstone with greater than 15% core porosity and permeability of hundreds of millidarcies. Potentially effective seals formed within the Kanpa and Hussar Formations. Empress 1 and 1A shows that all the elements of a petroleum system are present in the Yowalga Sub-basin.

KEYWORDS: hydrocarbon potential, stratigraphy, drill hole data, well logs, diamond drilling, source beds, reservoir data, stromatolites, Paterson Formation, Lennis Sandstone, Table Hill Volcanics, Lupton Formation, Kanpa Formation, Hussar Formation, Browne Formation, Lefroy Formation, Yowalga Sub-basin, Officer Basin

Introduction

The Geological Survey of Western Australia's (GSWA) vertical diamond drillhole Empress 1 was designed to test the source-rock potential of the Neoproterozoic sequences within the Yowalga Sub-basin of the western Officer Basin. Empress 1 and the re-drilled Empress 1A are part of GSWA's program of investigating the petroleum potential of Western Australia's onshore sedimentary basins.

Empress 1 and 1A is located on the WESTWOOD* 1:250 000 map sheet at latitude 27°03'13"S, longitude 125°09'24"E, 375 km northeast of Laverton by the Great Central Road (Fig. 1). Empress 1 was cored from 105 to 612.9 m, but abandoned at 615 m due to technical problems. Empress 1A was respudded 6 m away from Empress 1 and fully cored from 210.5 m to a total depth (TD) of 1624.6 m. No hydrocarbons were encountered. The drillhole intersected the Paterson Formation (79 – 131.9 m), Lennis Sandstone (131.9 – 201.3 m), Table Hill Volcanics (201.3 –286 m), an unnamed unit (286 – 317.1 m), ?Lupton Formation (317.1 – 483 m), and Supersequence 1 strata, which includes the Kanpa, Hussar, Browne, and ?Lefroy Formations (483 – 1540.2 m). An unconformity at 1540.2 m separates the Officer Basin succession from the presently unnamed pre-Officer Basin succession. The drillhole intersected 54.6 m of fine-grained basaltic rocks from 1570 to 1624.6 m (TD).

The following additional information related to Empress 1 and 1A has been placed in the GSWA S-series files under reference number S20424: wireline logs at 1:200 and 1:500 scale; porosity and permeability reports; 1:100-scale logging sheets; core photographs; daily drilling reports; final petrography report by K. Martin; and a sample list.

The depths of core cited within this Record are, unless otherwise specified, those reported by the drillers as modified by the wellsite geologist. However, in the composite log (Plate 1), although the depths cited in the core descriptions are core depths, the lithologies have been adjusted to match the log depth. In practice, no adjustment was made above the 210.5 m depth and in converting from core to log depths. The adjustment was always positive and varied from +0.7 m at 210.5 m to +2.9 m at 1570 m (Appendix 1).

The term dolomite is used in lithological descriptions to refer to carbonates that commonly do not effervesce in 10% hydrochloric acid, and only weakly effervesce, if at all, in concentrated hydrochloric acid. However, many of the dolomites are stained red by alizarin red S, which indicates that there is at least some limestone in the dolomites.

At the base of the PQ core interval in Empress 1, the rig datum was raised by 0.7 m to install the blow-out preventer stack, thus 294.2 m (base PQ core) is equivalent to 294.9 m (top HQ core). As Empress 1 was not wireline logged, this does not affect the composite log (Plate 1).

---

* Capitalized names refer to standard map sheets.

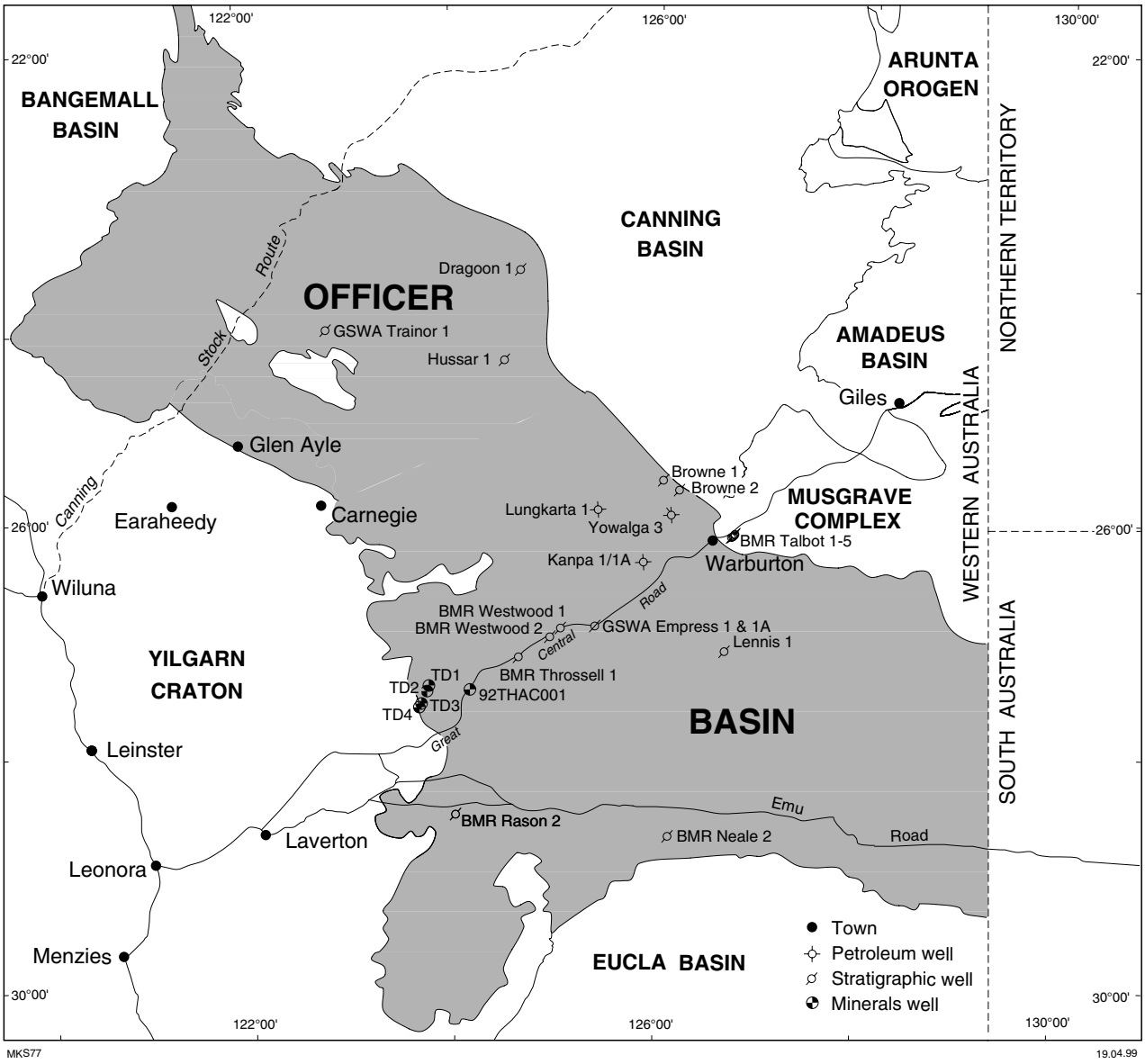

Figure 1. Location of petroleum exploration and stratigraphic wells in the Officer Basin referred to in the text

Drillhole history

General data Empress 1

Location:	Latitude 27°03'13"S, Longitude 125°09'24"E
	AGD84 Zone 51J, 713917E, 7005774N (from differential GPS)
Derivation of name:	WESTWOOD, Empress Spring
Total depth:	615 m
Date spudded:	21 June 1997
Reached TD:	4 July 1997

Logging of hole:	not logged
Date completed:	13 July 1997
Elevation:	461 m AHD (from differential GPS)
Status:	Plugged and abandoned

General data Empress 1A

Location:	Latitude 27°03'13"S, Longitude 125°09'24"E
	AGD84 Zone 51J, 713912E, 7005777N (from differential GPS)
Derivation of name:	WESTWOOD, Empress Spring
Total depth:	1624.6 m
Date spudded:	13 July 1997
Reached TD:	23 August 1997
Logging of hole:	24 to 27 August 1997
Date completed:	28 August 1997
Elevation:	461 m AHD (from differential GPS)
Status:	Plugged and abandoned

Drilling data Empress 1

Drilling contractor:	Western Deep Hole Drilling, 15 Catalano Rd, Canning Vale, W.A. 6155	
Rig:	UDR 3000 (Rig no. 8)	
Hole size:	0 – 16 m	215.9 mm with 11.5 m of 177.8 mm (7") casing left in hole
	16 – 105 m	152.4 mm with PW casing
	105 – 294.2 m	122.6 mm with PF casing (PQ coring)
	294.9 – 615 m TD	96.1 mm open hole (HQ coring)
Core recovery:	PQ 105 – 294.2 m	(94% recovery)
	HQ 294.9 – 615 m TD	(93% recovery)
	(Appendix 1)	
Hole deviation:	Maximum of 1.2° from vertical (Appendix 1; Table 1.2)	

Drilling data Empress 1A

Drilling contractor:	Western Deep Hole Drilling, 15 Catalano Rd, Canning Vale, W.A. 6155	
Rig:	UDR 3000 (Rig no. 8)	
Hole size:	0 – 21 m	215.9 mm with 21 m of 177.8 mm (7") casing left in hole
	21 – 210.5 m	159 mm with PW casing

	210.5 – 649.8 m	122.6 mm with PF casing (PQ coring)
	649.8 – 1624.6 m TD	96.1 mm open hole (HQ coring)
Core recovery:	PQ 210.5–649.8 m	(98% recovery)
	HQ 649.8–1624.6 m TD	(about 100% recovery)
	(Appendix 1)	
Hole deviation:	Maximum of 2° from vertical (Appendix 1; Table 1.3)	

Logging Empress 1A

Logging contractor:	BPB Slimline Services, 47 Felspar St, Welshpool, W.A. 6106	
Logs run:	Compensated density, gamma ray, caliper	650–1580 m
	Compensated density, gamma ray, caliper	210–310 m
	Multi-channel sonic	650–1580 m
	Multi-channel sonic	210–310 m
	Dual resistivity	650–1580 m
	Dual resistivity	210–310 m
	Dipmeter (4 arm)	650–1580 m
	Dipmeter (4 arm)	210–310 m
	Limestone-neutron porosity, gamma ray	0–1580 m
	Limestone-neutron porosity, gamma ray	0–310 m

The wireline logs are of very good quality except in zones of significant overgauge hole, such as the Browne Formation halite. The depth matching of core to logs is considered to be good and, where tie points could be established, the match was within 0–3 m.

Regional setting

The Neoproterozoic to Phanerozoic Officer Basin is a large, episutural intracratonic basin, which extends 1500 km from the southeastern flank of the Pilbara Craton to the central west of South Australia. The western Officer Basin is overlain by the Gunbarrel Basin, which is defined as the Palaeozoic and Mesozoic successions floored by the Table Hill Volcanics, which were previously included in the Officer Basin (Hocking, 1994). As used herein, the term western Officer Basin includes the Gunbarrel Basin.

In Western Australia, the Officer Basin is dominated by northwest-oriented structural trends, and its fault-bounded northern margin is defined by the Musgrave and Rudall metamorphic complexes, and the Anketell–Warri Gravity Ridge (Fig. 2). The southern margin of the Officer Basin is defined where Neoproterozoic to Phanerozoic strata are eroded, and older units, including the Yilgarn and Pilbara Cratons, Albany–Fraser Orogen, Earaheedy and Bangemall Basins, are

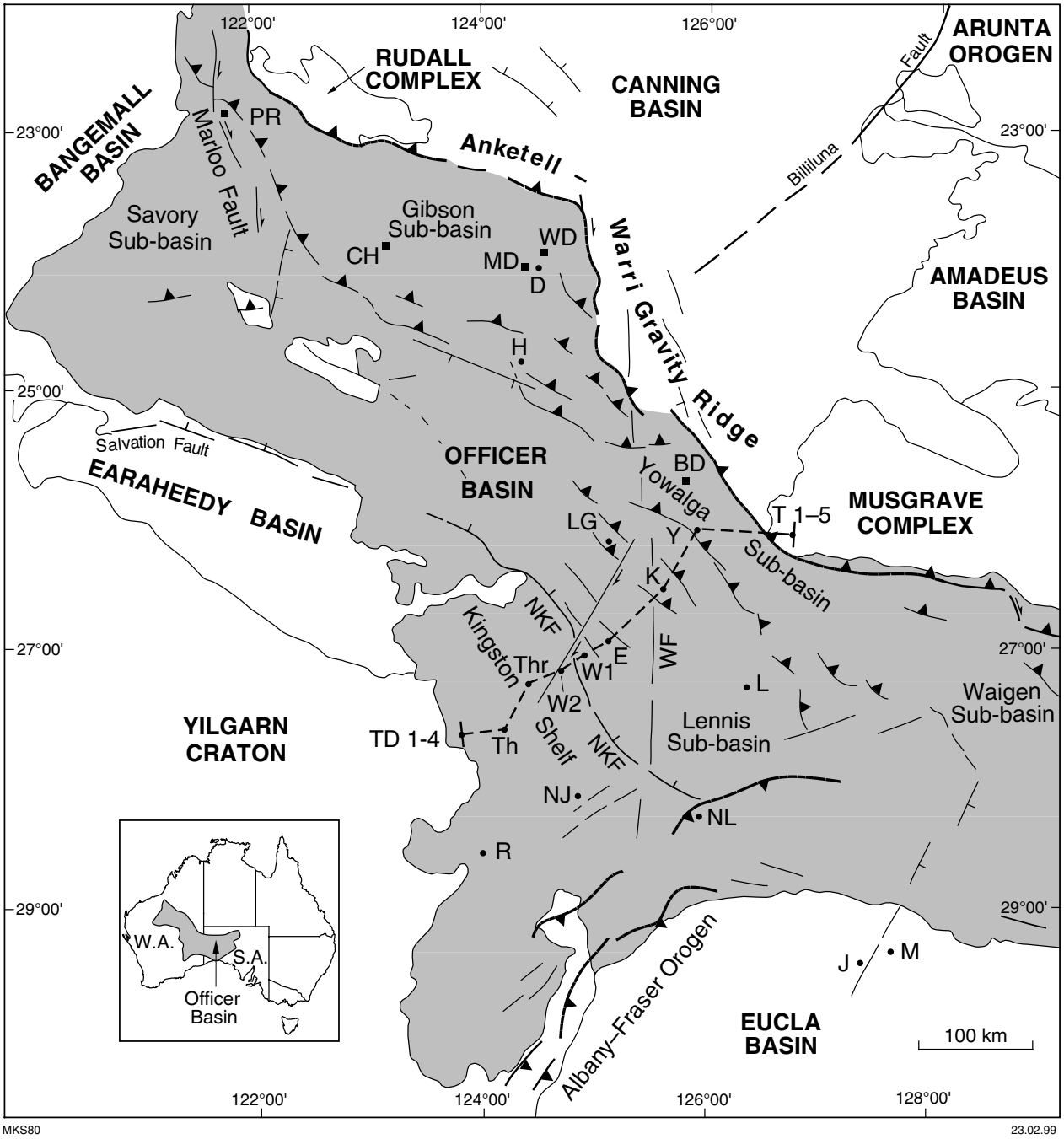

BD	Browne Diapir	LG	Lungkarta	T	BMR Talbot 1–5
CH	Constance Headland	M	Mason 1	Th	BMR Thac 001
D	Dragoon	MD	Madley Diapir	Thr	BMR Throssell 1
E	Empress 1/1A	NJ	NJD 1	W1	BMR Westwood 1
H	Hussar	NKF	North Kingston Fault	W2	BMR Westwood 2
J	Jubilee 2	NL	BMR Neale 1A - 1B	WD	Woolnough Diapir
K	Kanpa 1A	PR	Poisonbush Range	WF	Westwood Fault
L	Lennis 1	R	BMR Rason 2	Y	Yowalga 3

Cross-section

Figure 2. The location and major structural elements of the Officer Basin with exploration and stratigraphic wells referred to in the text (modified after Perincek, 1996b)

exposed. Parts of the southern margin of the basin are concealed by Mesozoic to Cainozoic strata of the Eucla Basin.

The Officer Basin is considered to be part of the Neoproterozoic Centralian Superbasin, which also includes the Amadeus Basin, Ngalia Basin, and part of the Georgina Basin (Walter and Gorter, 1994). Walter and Veevers (1997) discussed the palaeogeographic and tectonic settings of Neoproterozoic strata throughout Australia. Formations of the Officer Basin and correlations between the sub-basins are shown in Figure 3. Empress 1and 1A were drilled near the southern margin of the Yowalga Sub-basin on a broad structural shelf (Fig. 4), which has been relatively tectonically stable since the Neoproterozoic.

Local geology and geophysics

Empress 1 and 1A were drilled near the northern margin of WESTWOOD (Kennewell, 1977a) and hence, both this sheet and YOWALGA (1:250 000) to the north (Kennewell, 1977b) are relevant to the local geology. Cainozoic sediments make up about 90% of the land surface with the remaining area consisting of scattered outcrops of the Lower Cretaceous Samuel Formation and Paterson Formation (previously known as Early Permian). There are three outcrops of Table Hill Volcanics in the northwestern part of YOWALGA (1:250 000), about 90 km northwest of Empress 1 and 1A. The Table Hill Volcanics consist of tholeiitic basalt, which was previously considered to be Early Cambrian in age (Compston, 1974). Potassium–argon dating suggests that an Early Ordovician age is more appropriate (Appendix 2). The nearest pre-Cainozoic outcrops to the well site are 7 km to the south and southeast, and are mapped as thin beds of Samuel Formation overlying Paterson Formation.

Structural dips in the Phanerozoic rocks within the region are gentle. The Paterson and Samuel Formations are virtually flat lying over large areas (Kennewell, 1977a). The only significant structure recognized at the surface near Empress 1 and 1A is the Westwood Fault Zone (Fig. 2), which is a series of prominent northerly trending faults extending almost across WESTWOOD. The presence of a prominent scarp to the west, a depression area immediately east of the fault zone, and the photo-interpreted eastward dip of sediments exposed in the scarp indicate that the rocks are downthrown to the east. The throw on the fault zone is not known, but its effect on flat-lying Cretaceous sediments and the local topography suggests a maximum movement of several tens of metres since Cretaceous time (Kennewell, 1977a). The northernmost known extent of this fault is 43 km southeast of the wellsite.

Subsurface control prior to the drilling of Empress 1 and 1A consisted of two statigraphic drillholes, BMR Westwood 1 and Westwood 2 located 33 km west and 45 km west-southwest of the wellsite respectively, waterbore WTDB 1 drilled at the wellsite for drilling and campsite water, and petroleum exploration well Kanpa 1A located 74 km northeast of the wellsite (Fig. 2 and Plate 2).

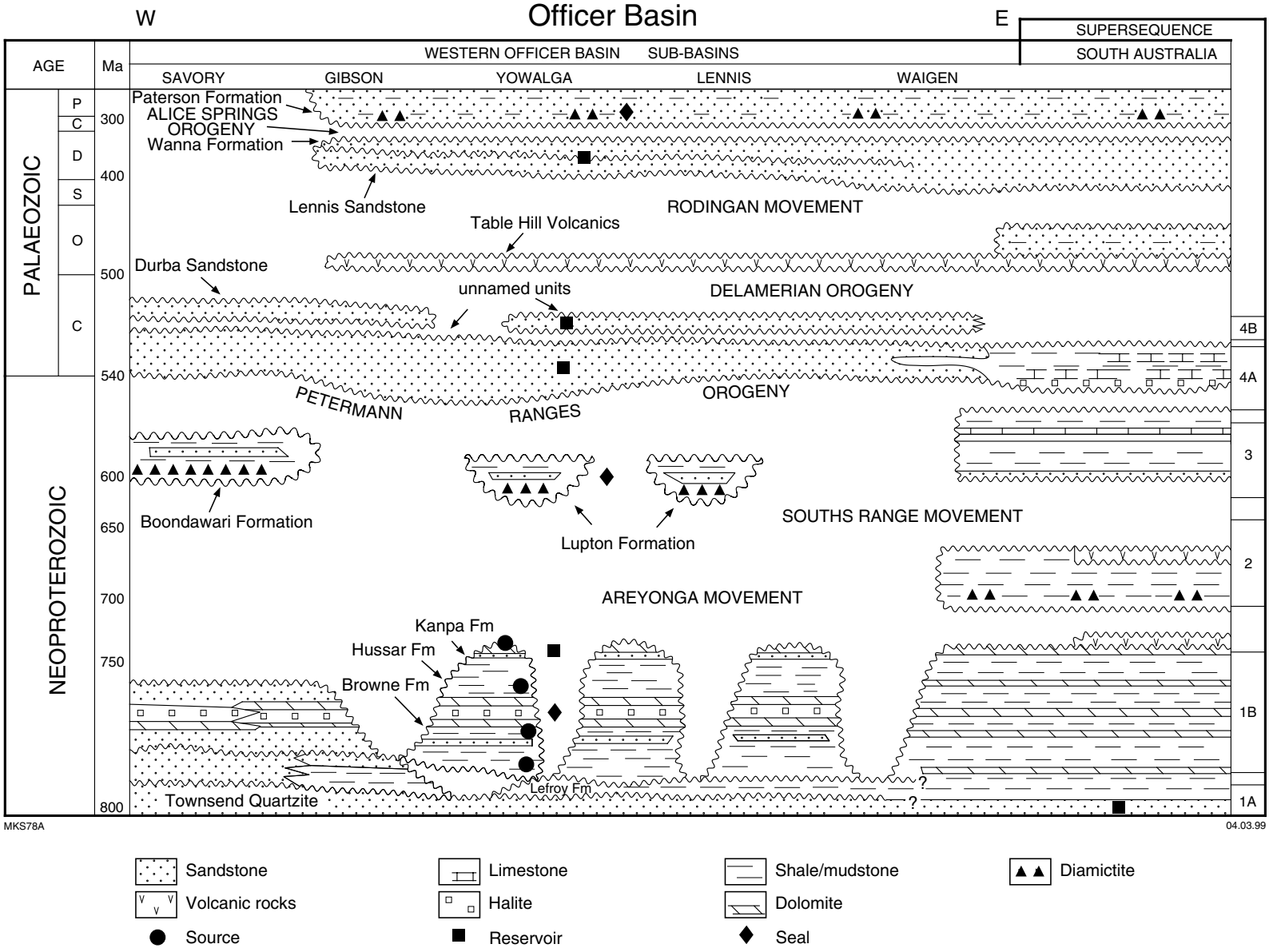

Figure 3. Stratigraphic correlation of the Palaeozoic and Neoproterozoic units in the Officer Basin

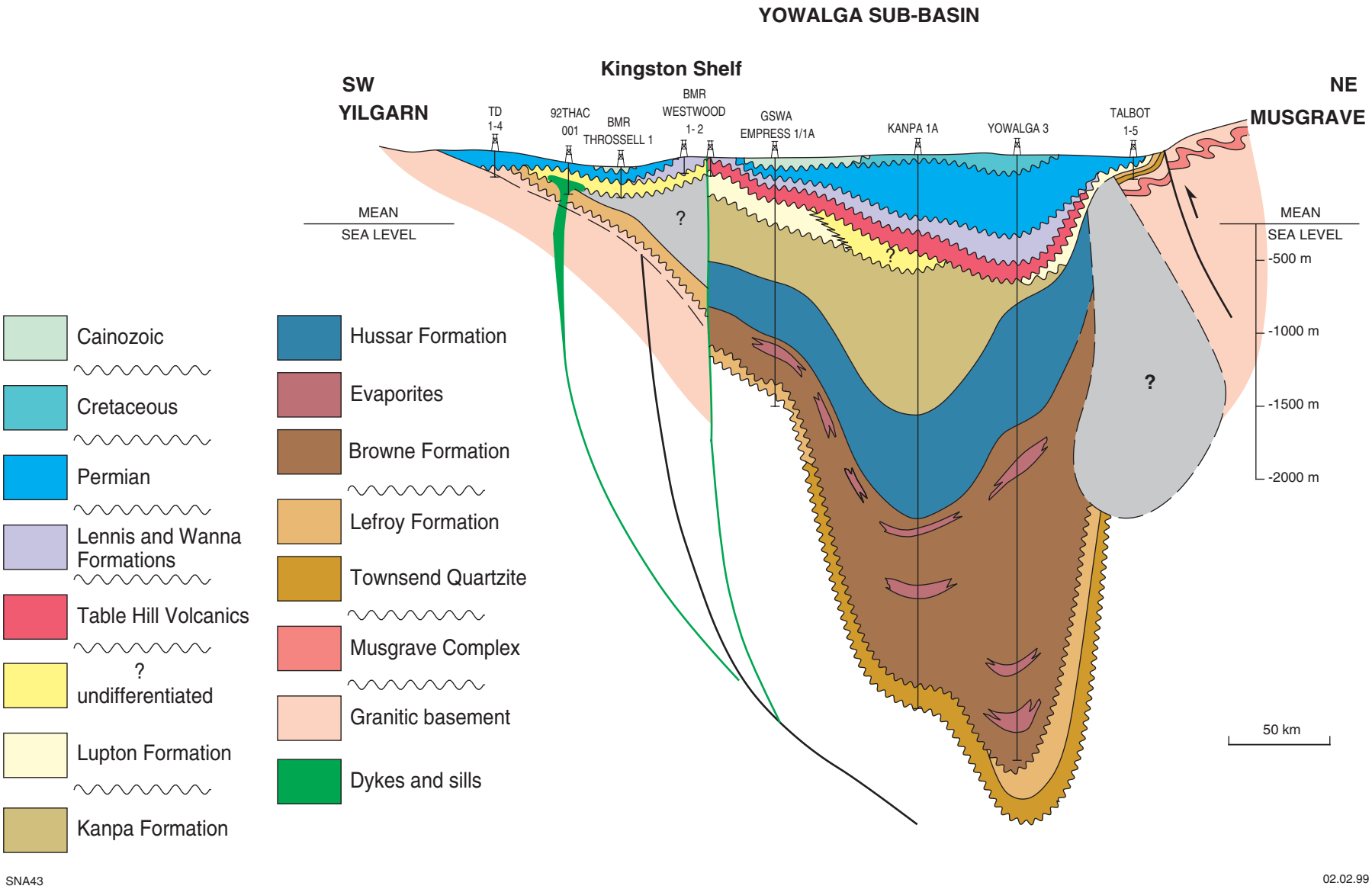

Figure 4. Regional well correlation across the Kingston Shelf and Yowalga Sub-basin (SW–NE). For well location see Figure 1

Empress 1 was originally planned to be drilled on a seismic line in the Yowalga Sub-basin to penetrate completely the Neoproterozoic succession, including the Browne Formation, in a drillhole less than 2000 m deep. However, a suitable site could not be identified on the seismic grid. Therefore, it was decided to site Empress 1 using existing gravity data and, to a lesser extent, regional aeromagnetic data. The final location of Empress 1 was chosen between Westwood 1 and Kanpa 1A, where gravity modelling suggested that Neoproterozoic and Phanerozoic strata would be about 1200 m thick. The gravity and aeromagnetic data did not indicate the presence of faults or dykes (Shevchenko and Iasky, 1997; Appendix 3).

Drillhole geology

Stratigraphy

Empress 1 and 1A were spudded in Cainozoic sand and intersected the Upper Carboniferous Paterson Formation at 79 m, Lennis Sandstone at 132 m, Table Hill Volcanics at 201 m, Neoproterozoic sedimentary rocks from 286 to 1540 m, and pre-Officer Basin sedimentary rocks and basalt from 1540 to 1624.6 m TD.

A composite log of Empress 1 and 1A is presented in Plate 1 and summarized in Figure 5. The ages of units encountered in the well were previously poorly controlled, but the presence of palynomorphs in the Paterson Formation and in many of the post-Browne Formation units, the identification of two stromatolite assemblage biozones, and radiometric dating of three units has resulted in a considerable increase in knowledge of ages for the Neoproterozoic units of the Officer Basin in general, as well as for this drillhole. The following descriptions of the stratigraphic units are derived from cuttings descriptions from 1 to 16 m in Empress 1A and from 16 to 105 m in Empress 1, and core logging from 105 to 210.5 m in Empress 1 and from 210.5 to 1624.6 m (TD) in Empress 1A. Petrographic examination of 11 samples and their petrographic descriptions are presented in Appendix 4. A summary of the petrography of porosity core plugs and other samples, extracted from Martin (in prep.), is presented in Appendix 5.

Geochronology

Palynology

Palynomorphs were recorded in samples from the drillhole (Appendices 6 and 7). Palynology has been applied effectively to date Palaeozoic and Neoproterozoic rocks. All other rocks were barren.

Stromatolite biostratigraphy

More than 70 stromatolite horizons have been identified in Empress 1A. The presence of three stromatolite assemblages (the *Acaciella australica* and the *Baicalia burra* Assemblages, and the

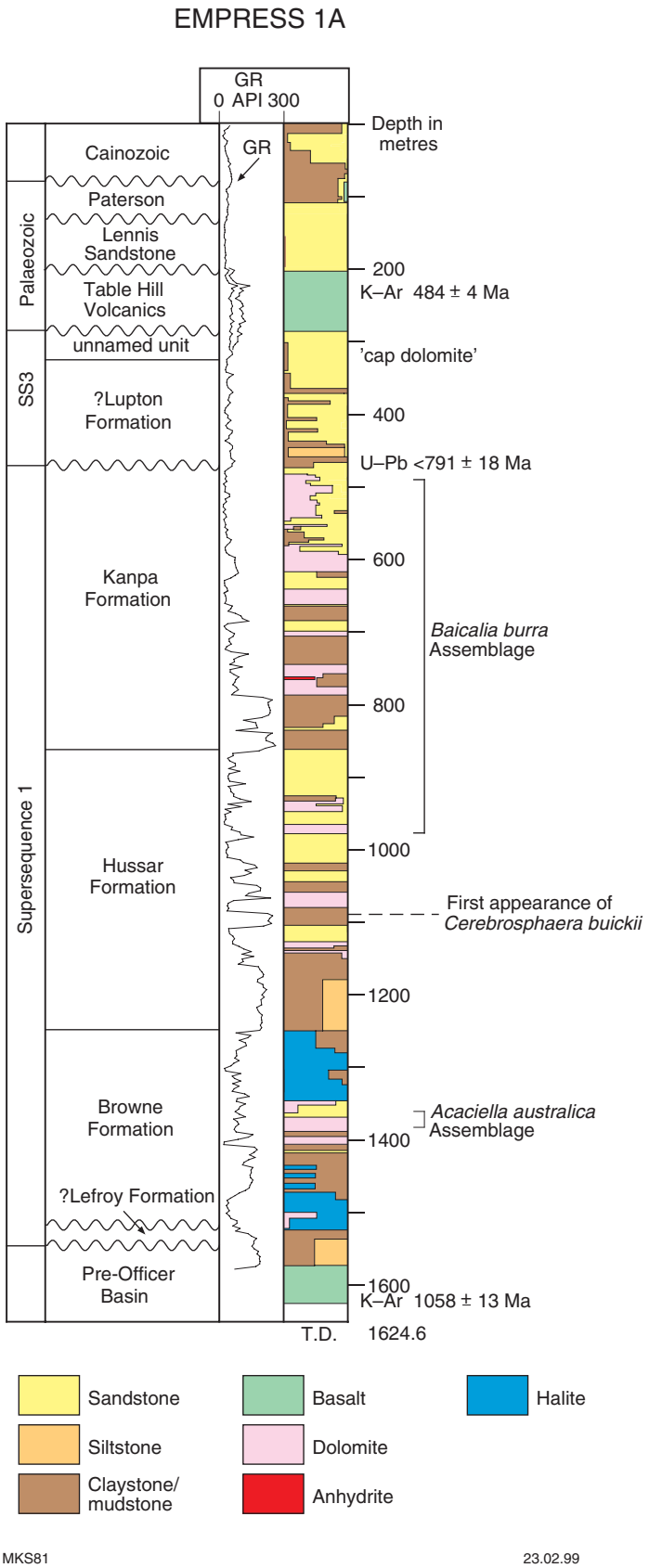

Figure 5. Empress 1 and 1A stratigraphy (for lithological description see Plate 1)

?*Elleria minuta* horizon) allows correlation within the Officer Basin and with other Neoproterozoic successions. The stromatolites also provide useful information about palaeoenvironments (Appendix 8).

Zircon U–Pb

One sample was processed to concentrate sedimentary zircon grains (Nelson, in prep.). The sample from 457.5 m is a diamictite from the ?Lupton Formation. These sedimentary zircon grains were dated by the U–Pb method using a Sensitive High-Resolution Ion Microprobe (SHRIMP).

Thirty-nine analyses were obtained from 35 zircons. A detrital grain gave weighted mean $^{207}Pb/^{206}Pb$ and $^{206}Pb/^{238}U$ ages of 791 ± 18 and 788 ± 26 Ma respectively. These are interpreted as the maximum possible ages for the deposition of the diamictite. The remaining analyses are interpreted to be from detrital grains, with the age groups consistent largely with an origin from either the Musgrave Complex or the Albany–Fraser Orogen.

K–Ar

Two core samples of basalts were dated using the K–Ar method (Appendix 2). The first sample (215.9 – 216.49 m) is from the Table Hill Volcanics. This sample consists predominantly of plagioclase laths and augite crystals. The rock is commonly fresh and contains opaque minerals and translucent, reddish-brown limonitic material. An age of 484 ± 4 Ma was determined for the Table Hill Volcanics.

The second sample (1601.57 – 1602.24 m) is from the pre-Officer Basin succession. This sample consists of plagioclase laths and granular pyroxene. Overall, the rock is very fresh and commonly unaltered. The basalt age from the pre-Officer Basin succession is 1058 ± 13 Ma (Appendix 2).

Cainozoic rocks

Unnamed unit — 0 to 79 m

This unnamed unit is described from cuttings in Empress 1A from 1 to 16 m and in Empress 1 from 16 to 79 m. The uppermost interval (1–5 m) consists of fine-grained, moderate-red–brown clay and sand. The next interval, from 5 to 15 m, consists of a fining-upward cycle and grades from sand and sandstone, through mudstone, to moderate-brown clay and silt at the top. The next interval, from 15 to 27 m, also consists of a fining-upward cycle with similar lithologies to those from 5 to 15 m. Minor pebbles of ferruginous sandstone are present between 15 and 27 m in Empress 1A. The next interval, from 27 to 61 m, consists of a weak, coarsening-upward cycle and grades from clay with minor, very fine to fine grained sand at the base, through clay with up to 20% sandstone in parts and rare quartz granules, to mud and mudstone with very fine grained sandstone at the top. The colours in this interval are predominantly red, yellow, and brown at the top, moderate yellow–green in the middle, and moderate green–grey at the base. The next interval,

from 61 to 73 m, consists of medium-grey clay. The basal interval, from 73 to 79 m, consists of about 80% moderate-grey–brown clay with the remainder including very fine to fine grained sand, and granules and pebbles of mudstone and basalt.

There is no internal evidence for the age of this unit, but it is interpreted as Cainozoic. The unit consists predominantly of poorly sorted, fluvial clastic rocks and poorly to moderately sorted, lacustrine clay deposits. The sediments coarsen upward from the base of the unit to 25 m, and above this depth the sediments fine upward. The sediments are unconsolidated to moderately consolidated in parts, and are weathered to a depth of about 60 m.

It is possible that lower parts of this unit could be very poorly consolidated, Lower Cretaceous sedimentary rocks, such as the Bejah Claystone and Samuel Formation. However, both of these units are interpreted as marine deposits, with the Samuel Formation described as a dominantly moderate to well sorted, micaceous, carbonaceous, and glauconitic unit (Jackson and van de Graaff, 1981), which is not compatible with the cuttings descriptions.

Palaeozoic rocks

Paterson Formation — 79 to 131.9 m (Late Carboniferous)

The description of the Paterson Formation is taken from Empress 1 cuttings (79–105 m) and core (105 – 131.9 m). The formation consists predominantly of clay, mudstone, sandstone, and conglomerate. The uppermost interval, from 79 to 86 m, consists of a poorly defined, fining-upward cycle and grades from predominantly sandstone with clay at the base to predominantly clay with sandstone at the top. The next interval, from 86 to 105 m, consists predominantly of light-grey and moderate-yellow–brown clay, with the amount of very fine to fine grained, moderate-brown to light-grey sandstone decreasing from about 40% at the top to 5% at the base.

The cored interval, from 105 to 109 m, consists of dark-grey and moderate-brown sandy and pebbly mudstone. The basal interval, from 109 to 131.9 m, includes polymictic, pebble to boulder conglomerate interbedded with sandstone and minor mudstone. The sandstone is fine to very coarse grained, very poorly to well sorted, and massive to planar laminated. The conglomerate beds, which are 0.2 – 2.6 m thick, are extremely poorly sorted and interpreted to be diamictites.

The mudstone and sandstone are disrupted and contorted in parts; these features are interpreted to be a result of either syndepositional slumping or subglacial deformation. There is a fault and two zones of tectonic breccia at 108 – 110.4 m. These are the only significant faults recognized in Empress 1 from the Officer Basin succession, other than those in the Table Hill Volcanics. These breccias may also have been caused by subglacial deformation.

Palynology indicates a latest Carboniferous age for the Paterson Formation in Empress 1 (Appendix 6). Previous palynological investigations of the Paterson Formation in the western Officer Basin suggested a Stage 2 assignment. The Paterson Formation in Hunt Oil Browne 1,

Browne 2, Yowalga 1; BMR Wanna 1, Neale 2, Rason 2; and shothole NMF 23 were all assigned to Stage 2 by Kemp (1976) with a suggested age of Asselian to early Sakmarian. A recent review (Archbold, 1998) placed Stage 2 in the Asselian (earliest Permian). Thus, the Late Carboniferous age reported here is the oldest known for the Paterson Formation from the western Officer Basin, but is well within the reported age range of the interval previously placed in the Grant Group from the Canning Basin. Apak and Backhouse (1998) redefined the interval previously referred to as the Lower Grant Group, to the Reeves Formation. The Reeves Formation has an age ranging from the late Visean to Stephanian. The assemblages from Empress 1 correlate with the uppermost part of the Reeves Formation of the Canning Basin.

The Paterson Formation is widespread in the Officer Basin and consists of three facies: diamictite; cross-bedded, coarse-grained pebbly sandstone; and well-bedded claystone, siltstone, and fine-grained sandstone. These are interpreted, respectively, as tillites, fluvioglacial outwash, and lacustrine deposits with some possible marine influence (Jackson and van de Graaff, 1981). The basal interval, from 109 to 131.9 m, in Empress 1 is interpreted as fluvioglacial outwash, and is either tillite or reworked, glaciogenically derived sediments. The interval from 79 to 109 m consists predominantly of lacustrine deposits.

The contact between the Paterson Formation and underlying Lennis Sandstone is well defined in the core from Empress 1 at 131.9 m, but is indistinguishable in the cuttings descriptions from Empress 1A.

Lennis Sandstone — 131.9 to 201.3 m (?Devonian)

The description of the Lennis Sandstone is taken from Empress 1 core from 131.9 to 201.3 m. The unit consists of sandstone with minor mudstone and conglomerate. The uppermost interval, from 131.9 to 156.4 m, consists of fine- to medium-grained, light-grey quartzose sandstone. This interval is commonly massive but poorly planar bedded in parts. The Lennis Sandstone in this interval is moderately to well sorted with only minor mud forming the matrix, and has good porosity and permeability.

The interval from 156.4 to 198.9 m consists predominantly of sandstone, as from 131.9 to 156.4 m, with minor interlaminated and thinly interbedded mudstone, and rare, very coarse grained to granular bands about 1 cm thick. The colour grades from light grey above 179 m, to moderate yellow–brown below 180 m. Cross-bedding, with foreset dips of 10–20°, is common between 189 and 196 m.

The basal interval, from 198.9 to 201.3 m, consists of polymictic pebble to cobble conglomerate with a fine- to medium-grained sandstone matrix.

The Lennis Sandstone in Empress 1 lies between the Table Hill Volcanics and the Paterson Formation, thus limiting it to a Palaeozoic age. Based on fission-track analysis in other wells, the

Lennis Sandstone was assigned a Devonian–Carboniferous age (Green and Gleadow, 1984). Based on limited evidence, Jackson and van de Graaff (1981) suggested a shallow-marine depositional environment with minor subaerial exposure for this unit.

Table Hill Volcanics — 201.3 to 286 m (Early Ordovician)

The Table Hill Volcanics consist of fine- to coarse-grained basalt, which is amygdaloidal, vesicular, and massive in parts. Descriptions are taken from Empress 1 core (201.3 – 210.5 m), and Empress 1A core (210.5 – 286 m). The formation consists of six volcanic flows that vary in thickness from 7.8 to 22.9 m, with grain size increasing with depth. Flow thickness typically increases upwards. The flows have been informally sequentially numbered from one at the base, to six at the top. Amygdales are abundant at all the tops and some of the bases of these flows, and are typically filled with either quartz, calcite, green clay, or combinations of these minerals. These minerals also formed as vein and fracture fillings. Dark-green, crystalline zeolites were identified in some amygdales. Xenoliths of sandstone and quartzite are present in some of the basalts.

The uppermost flow (number six, 201.3 – 219.1 m) consists of amygdaloidal basalt. The top 5 cm of this flow is interpreted to be extensively weathered and the underlying 0.7 m of basalt to be slightly weathered. A K–Ar age of 484 ± 4 Ma was obtained near the base of this flow. Flow five (219.1 – 242 m) consists of vesicular and amygdaloidal basalt, and the grain size increases with depth. This flow has a sharp, brecciated top in Empress 1A, but in Empress 1 the contact is transitional. Flow four (242–256 m) consists of vesicular and amygdaloidal basalt that grades with increasing depth to massive, coarse-grained basalt. It has a transitional top. Flow three (256 – 268.1 m) consists of vesicular and amygdaloidal basalt, which grades with increasing depth to massive, coarse-grained basalt with grain size decreasing below 262 m. The basal 20 cm of the flow consists of amygdaloidal basalt and has a transitional top. Flow two (268.1 – 275.9 m) consists of amygdaloidal basalt, which grades with increasing depth to massive, coarse-grained basalt, but includes amygdaloidal basalt from 271.9 to 272.3 m and in the basal 1.9 m of the flow. This flow has a sharp top. The basal flow (number one, 275.9 – 286 m) consists of amygdaloidal basalt that grades with increasing depth to massive, coarse-grained basalt, but has amygdaloidal basalt in the basal 0.5 m of the flow. This flow has a faulted and brecciated top. A fault breccia with associated quartz and dolomite is located at 278.9 m.

Weathering was noted only in the uppermost flow. This implies that there was only a short time-interval between the flows, or that any evidence of weathering was destroyed by subsequent flows. In Empress 1, the basal contact of the formation is at 285.05 m with a flat-lying, 1 cm-thick sandstone underlying the basalt.

The gamma-ray and resistivity logs through the 72 m-thick Table Hill Volcanics in Westwood 1 are published in Jackson et al. (1975), and are of fair quality below 23 m. Possible correlation points have been established based on wireline log characteristics between the top of flow number

two in Empress 1A at 268.1 m with Westwood 1 at 51 m, and the top of flow number four in Empress 1A at 242 m with Westwood 1 at 26 m. If a similar thickness of volcanic rocks was extruded at both localities, it could be inferred that about 18 m of rock was lost as a result of erosion of the uppermost flow at Westwood 1. Jackson et al. (1975) reported only two flows in Westwood 1, which are separated by a 2 m-thick sandstone at about 23 m.

Previous work on radiometric dating of the Table Hill Volcanics was summarized by Perincek (1998). On the basis of seismic and stratigraphic correlations, Perincek (1998) suggested a Middle to Late Cambrian age for this unit. However, K–Ar radiometric dating (Appendix 2) indicates an Early Ordovician age (484 ± 4 Ma) for the Table Hill Volcanics. Based on palynological and geochemical estimates of the relatively low, thermal maturity of sediments (Appendices 7 and 9), this age is considered to be reliable.

The Early Ordovician age agrees well with K–Ar dates of 485 ± 20 to 475 ± 20 Ma for the Kulyong Formation (previously known as the Kulyong Volcanics) from the South Australian part of the Officer Basin (Morton and Drexel, 1997).

Neoproterozoic rocks

Unnamed unit — 286 to 317.1 m (?Ediacarian)

The description of this unnamed unit is taken from Empress 1A core. This unit consists predominantly of sandstone and has an upper unconformable contact with the Table Hill Volcanics and a transitional lower contact with the ?Lupton Formation. There is no internal evidence for the age of this unit.

The uppermost interval, from 286 to 286.8 m, consists of moderate-brown, ferruginous sandstone with a sharp, flat-lying upper contact. The uppermost 10 cm has been contact metamorphosed by the basal flow of the Table Hill Volcanics. The remainder of the interval has been weakly metamorphosed with a spotted hornfels texture. The underlying interval, from 286.8 to 311 m, consists of fine- to medium-grained sandstone with minor coarse to very coarse grained bands. The sandstone is predominantly moderate brown, quartzose, and subfriable. This interval coarsens upwards and has a sharp top. The interval is typically very fine to medium grained below 289 m. Minor mudstone interbeds from 1 mm to 2 cm thick form below 302.5 m. Sedimentary structures include planar bedding, which dips 3–5° to the west (from dipmeter data), and cross-bedding, with foreset dips of 10–29° to the north and west.

The interval from 311 to 315 m consists of very fine to fine grained, moderate-brown sandstone with minor interlaminated mudstone. Planar bedding dips 4–8°. The basal interval, from 315 to 317.1 m, consists of very fine to medium grained sandstone with minor coarse-grained, moderate-brown, subfriable, quartzose sandstone.

This unnamed unit was probably deposited on an open marine shelf. The lower two intervals, from 317.1 to 311 m, consist of a poorly defined, fining-upward cycle, which probably recorded a

transgression at the end of the Marinoan glaciation. The upper two intervals comprise a coarsening-upward cycle, which records a regression as a result of accommodation space being filled after a post-glacial sea-level rise.

?Lupton Formation — 317.1 to 483 m (Marinoan, Supersequence 3)

The ?Lupton Formation is described principally from Empress 1A core and consists predominantly of sandstone interbedded with mudstone, diamictite, and minor dolomite. The formation has a gradational contact with the overlying unnamed unit and an erosional, disconformable contact with the underlying Kanpa Formation. The uppermost interval, from 317.1 to 318.7 m, consists of interlaminated and interbedded sandstone, mudstone, and dolomite. The sandstone is fine to coarse grained and light grey to moderate brown. The mudstone is moderate brown, and the dolomites are laminated, stromatolitic, micritic, and light grey. Both the sandstone and mudstone are slightly dolomitic. This uppermost interval of the ?Lupton Formation has been interpreted to be the 'cap dolomite' that forms at the top of Marinoan glacial strata in the Amadeus and other basins (Walter, M. R., Preiss, W. V., and Grey, K., 1998, pers. comm.; Preiss et al., 1978). Dolomites were recognized at a comparable stratigraphic position in the Savory Sub-basin (Walter et al., 1994), and in the Kimberley region of Western Australia (Coats and Preiss, 1980).

The interval from 318.7 to 341.3 m consists of fine- to coarse-grained, moderate-brown sandstone with minor mudstone. Several fining-upward cycles, each about 1–2 m thick, are present. The sandstones are commonly moderately sorted and massive, weakly planar bedded, or cross-bedded. Minor soft-sediment slumping is present locally.

The sand from 334.8 to 336.6 m is very well sorted, well rounded, and unconsolidated. The underlying sandstone, from 336.6 to 340.2 m, is well laminated with bedding dips of 2–5°. These two poorly consolidated to unconsolidated beds represent a zone of core loss in Empress 1, and a zone of core loss in Empress 1A from 341.3 to 342.6 m.

The interval from 342.6 to 364 m consists of very poorly sorted, fine- to medium-grained, but locally coarse-grained, moderate-brown, pebbly and muddy sandstone. It is interpreted to be a diamictite. The pebbles are angular to subrounded and consist predominantly of dolomite with some quartz and granite. The pebbles gradually increase in size with depth to about 4 cm at 345.5 m, and gradually increase in abundance with depth to the base of this interval. The interval is commonly massive, but poorly defined bedding is present in parts with dips of 5°.

The interval from 364 to 369.6 m consists of moderate-brown, massive mudstone with reduction spots.

The interval from 369.6 to 387 m consists of sandy and muddy diamictite, which is similar to the interval from 342.6 to 364 m except that it is only slightly pebbly and has light-grey–green reduction spots below 377.7 m.

The interval from 387 to 407.7 m consists of interbedded sandstone, conglomerate, and mudstone, which are slightly dolomitic in parts. The sandstone is typically very fine to medium grained, moderately sorted, massive, and cross-bedded. Poorly defined fining-upward cycles are present locally.

The interval from 407.7 to 418.9 m consists predominantly of diamictite, similar to the interval from 342.6 to 364 m, with cross-bedding identified in the centre of the interval. Minor interbedded conglomerate and mudstone are present.

The interval from 418.9 to 423.5 m consists of interlaminated and interbedded mudstone and very fine to fine grained, moderate-brown sandstone. Sandstone beds up to 5 cm thick are present, but most beds are between 2 mm and 1 cm thick and consist of sandstone that fines upwards through mudstone to claystone. These beds are probably dilute, low-concentration turbidite deposits (Eyles and Eyles, 1998).

The interval from 423.5 to 459.2 m consists of interbedded diamictite, sandstone, mudstone, and conglomerate. The diamictite makes up about two thirds of the interval and is similar to the interval from 342.6 to 364 m. The mudstone is locally pebbly and sandy, and varies from being poorly to well sorted. Lithologies are commonly massive, but poorly defined bedding, which dips 3–6°, is present locally. Rare fining-upwards cycle, cross-bedding, ripples, and flame structures are also present.

The interval from 459.2 to 472.3 m consists of a poorly defined, fining-upward cycle and ranges from interbedded, poorly sorted sandstone, mudstone, and conglomerate, through interlaminated, slightly pebbly mudstone and claystone, to massive mudstone at the top. Many of the pebbles are dolomite but limonitic quartzite and ?basalt clasts are also present. Slickensides are present in the lower part of the interval, whereas contorted bedding is present in the upper part. The equivalent interval in Empress 1 is from 458.4 to 471.9 m and, although of similar thickness, shows considerable lithological variation from Empress 1A (Fig. 6). This interval in Empress 1 has a poorly sorted, basal sandstone bed that is 1 m thick (cf. 5.3 m in Empress 1A, Fig. 6). This bed is overlain by a poorly sorted, pebbly and sandy mudstone bed with ?limonite, which is 8.7 m thick (cf. 5.8 m in Empress 1A, Fig. 6). The uppermost 4.1 m in Empress 1 consists of well-bedded and moderately sorted pebbly sandstone, shale, and conglomerate, which includes contorted (slumped) bedding. In contrast, the equivalent zone in Empress 1A consists of shale and mudstone. The lithological variability between drillholes 6 m apart could be due to faulting, slumping, or channelling. The preferred interpretation is that the variation in the basal part of this interval is the result of slumping and possible debris flow, with the interval between 462.2 and 458.4 m in Empress 1 consisting of moderately sorted channel fill.

The basal interval, from 472.3 to 483 m, consists of moderately sorted, fine- to medium-grained, but locally coarse-grained, dark-brown sandstone. The basal 3 m of the interval is slightly

Figure 6. Comparison of a part of the ?Lupton Formation in Empress 1 and 1A. Note that separation between drillholes is 6 m at the surface

coarser grained with pebbles consisting predominantly of dolomite. The interval is commonly well layered with planar bedding dipping 4–8°, and minor cross-bedding with foresets dipping at about 15°.

The Lupton Formation outcrops about 170 km northeast of Empress 1 and 1A, with further exposures to the east along the southern edge of the Musgrave Block. In the type section located at Lupton Hills on COOPER (1:250 000), the formation consists of a lower unit, an unbedded, very poorly sorted, pebble to boulder conglomerate, and an upper unit of interbedded conglomerate, sandstone, and siltstone (Lowry et al., 1972). Elsewhere, the Lupton Formation is described as consisting mostly of fine-grained diamictite with scattered large boulders, but includes fine-grained, well-bedded sandstone and coarse-grained, cross-bedded sandstone (Jackson and van de Graaf, 1981). It is the fine-grained diamictite and associated lithologies that are considered to be correlatives with the interval discussed from Empress 1 and 1A, as no clasts larger than pebbles were recognized in the drillholes.

The ?Lupton Formation in Empress 1 and 1A consists of a wide variety of clastic lithologies ranging from unsorted diamictite, pebbly and sandy mudstone, moderately sorted sandstone, mudstone, conglomerate, and well-sorted, normally graded sandstone to claystone. Minor dolomite is present at the top of the formation. The strong brownish colour suggests a predominantly oxidizing depositional environment, but reduction spots and the grey to green colour show that parts of the environment were reducing. Some pebbles in the diamictites have striations, but these deposits are considered to be of glaciomarine origin rather than true tillites, and the well-laminated and graded, fine-clastic beds are considered to be distal turbidite deposits rather than lacustrine varves (Eyles and Eyles, 1998). A predominantly marine depositional environment is proposed with large volumes of glacially derived clastic rocks being rapidly deposited by debris flows and turbidity currents, with channelling and reworking of some of these deposits resulting in well-sorted, stratified deposits. The well-sorted, well-rounded sand from 334.8 to 336.6 m may be eolian or shoreface deposits.

Unfortunately, the SHRIMP U–Pb sedimentary zircon age of 791 ± 18 Ma from a diamictite at 457.5 m in Empress 1A (Nelson, in prep.), although confirming a Neoproterozoic age for the ?Lupton Formation, is too old to help determine if these glacial strata are either Supersequence 2 (Sturtian) or the preferred Supersequence 3 (Marinoan) age.

Kanpa Formation — 483 to 860.8 m; 484.1 to 862.7 m log depth (Supersequence 1)

The Kanpa Formation was intersected in Kanpa 1A, Hussar 1, and Lungkarta 1. Townson (1985) recognized the Kanpa and Steptoe Formations in Kanpa 1A, but the present authors grouped the two together as one formation. The lower contact of the Kanpa Formation is conformable with the Hussar Formation in Hussar 1 (Phillips et al., 1985). In Empress 1A, the Kanpa Formation conformably overlies the Hussar Formation at 861 m, and is unconformably overlain by the

?Lupton Formation at 483 m. The unconformity at 483 m represents a major time break; the upper parts of the Kanpa Formation have been significantly karstified.

The description of the Kanpa Formation is taken from Empress 1A core and consists predominantly of dolomite, mudstone, and sandstone. The uppermost interval, from 483 to 541.9 m, consists of interbedded dolomite, mudstone, and minor sandstone. The dolomite consists mostly of massive and laminated micrite with some beds of sand- and gravel-sized dolomite clasts. The beds are typically 1–4 m thick and many have sharp contacts. Erosional surfaces were noted at 525.8 and 540.06 m. Many of the dolomites show some porosity with intergranular, vuggy, and possibly oomoldic styles noted. Stromatolites, including *Baicalia burra* and *Tungusia wilkatana*, are common and some of them have been eroded and redeposited. The mudstones are typically light to dark grey and dolomitic. The sandstones are very fine to medium grained, light grey, quartzose, and dolomitic. Stylolites in the dolomites are rare and pyrite is present in a vug at 492.1 m. ?Gypsum is present at 492 m and ?anhydrite at 532 m. This interval was probably deposited above wave base on a restricted shallow-marine shelf with low clastic input. The interval is aggradational with sediment supply approximately balancing accommodation space. The top of the Kanpa Formation has been extensively karstified. The fine-grained strata from 494.8 to 496.4 m possibly represent cavern infill (Preiss, W. V., 1998, pers. comm.). The depth of karstification is unclear but extends to at least 504 m (i.e. 21 m below the unconformity at 483 m).

The interval from 541.9 to 616.7 m consists of interbedded sandstone, sand, mudstone, claystone, and dolomite and includes zones of significant core loss. Five zones of up to 1 m of core loss are present between 552 and 565 m. Sandstone and sand are the main lithologies above 578.6 m, with dolomite and mudstone more common below this depth. Claystone is the main lithology below 591.3 m. The sandstone and sand are typically fine to medium grained, but can vary from being very fine to coarse grained, moderate brown to light grey–green, and quartzose with good inferred porosity and permeability locally. ?Glauconite is present below 577 m. The mudstones are moderate brown and light green–grey. The claystone is dark grey below 598 m, has a weak bedding parting, and is hygroscopic. The dolomite is stromatolitic and similar to the interval above (483 – 541.9 m), except gravel-sized dolomite clasts are rare. Good oomoldic porosity is interpreted at 561.5 m. Evaporite minerals, predominantly ?anhydrite, are common from 576 to 593 m. Several fining-upward cycles, about 5–10 m thick are present with minor cross-bedding, ripples, and contorted bedding.

The interval from 541.9 to 616.7 m was probably deposited on a shallow-marine shelf in a ramp setting, with two coarsening-upward cycles and basal flooding surfaces (parasequences) recognized. The two parasequences occur from 572 to 616.7 m and 541.9 to 572 m. The claystone below 591.3 m was deposited in a quiet setting, either a restricted shallow-marine environment or a lagoon, deep enough to be consistently below wave base. Strata above 591.3 m were deposited in very shallow marine or lagoonal environments above storm wave-base.

The interval from 616.7 to 686 m is mainly dolomite interbedded with sandstone and mudstone. The dolomite is thinly parallel laminated, stromatolitic (*Baicalia burra* species), oolitic, brecciated, and contains intraformational, local erosive surfaces. Soft-sediment deformation is common within the dolomite. The sandstone, which is interbedded with dolomite, is grey to green, mainly medium grained, and cross-bedded. Dark-grey mudstone dominates towards the base of the interval. Although sandstones are mainly medium grained, they show slightly fining upward successions in the lower half, and coarsening-upward successions in the upper half of this interval. Lithological characteristics, evaporites, and chickenwire anhydrite (partly replaced by chert) within this interval suggest sea-level fluctuations within a shallow marine–sabkha environment.

The underlying interval (686–727 m) is a dolomite-dominated succession, containing the stromatolite *Baicalia burra*, with thin intercalations of sandstone. Mudstone and minor conglomerate are present. Dolomite is mainly light to medium grey, microcrystalline, locally brecciated, and contains stylolites and vuggy porosity, which was infilled by chert and evaporitic minerals (anhydrite). Stromatolites are locally broken, compacted, and truncated. In the uppermost part of the interval, dolomite is sharply overlain by mudstone, which has a thin, basal conglomeratic horizon. In the lower section, from 708 to 727 m, the dolomite is locally sandy and shows minor intraformational erosive surfaces, indicating that minor clastic sediments were transported into the area probably during storms.

The interval from 727 to 789 m comprises dolomite, mudstone, sandstone, minor siltstone, and evaporite. Light-brown, medium-grained, well-sorted sandstone interbedded with stromatolitic, partly brecciated evaporitic dolomite and mudstone dominate the interval between 727 and 746 m. There is a coarsening-upward cycle in the sandstone from 740 to 746 m.

From 746 to 789 m, the lithologies consist mainly of dolomite interbedded with mudstone and include minor, thin evaporite intercalations. Dolomite is stromatolitic, thinly parallel laminated, locally wavy bedded, and contains contorted bedding, stylolites, and chert and evaporite infilling the leached areas and fractures. Stromatolites are broken, compacted, and truncated, suggesting frequent sea-level fluctuations resulting in rapid facies changes.

The basal section of the Kanpa Formation (789–861 m) is predominantly mudstone with minor medium-grained, locally oxidized sandstone. Mudstone is light grey to greenish grey to dark grey from 748 to 848 m, and reddish brown from 848 to 861 m. Throughout this section, mudstone is silty, locally calcareous, sandy, and dolomicritic. Mudstone shows abundant soft-sediment deformation structures at a millimetre to centimetre scale. It contains very fine grained, wave-rippled, silty to sandy beds, and has numerous minor intraformational erosive surfaces (in particular, at the contact between mudstone and siltstone, and mudstone and sandstone beds). The basal Kanpa Formation is commonly massive, but shows very fine laminations. This section has been fractured and subsequently infilled with pyrite mineralization in places. Based on

sedimentary structures in the drillcore, the mudstone is a low-energy facies and was probably deposited in a lagoon or restricted shallow-marine environment. This interval, encountered in many wells (Perincek, 1996a,b), is laterally correlatable, and probably represents the lowest unit (unit D) of the Kanpa Formation informally defined by Townson (1985).

The Kanpa Formation was probably deposited in a sabkha to shallow-marine environment under oxidizing to slightly reducing conditions.

Rock-Eval pyrolysis indicates that samples from the Kanpa Formation between 737.4 and 768.2 m have fair hydrocarbon-generating potential (Appendix 9).

Hussar Formation — 860.8 to 1247.1 m; 862.7 to 1249.1 m log depth (Supersequence 1)

In Empress 1 and 1A, the Hussar Formation is conformably overlain by the Kanpa Formation at 860.8 m, and unconformably overlies the Browne Formation at 1247.1 m. The Hussar Formation comprises sandstone, dolomite, mudstone, and minor, locally developed conglomerate in Empress 1A.

The Hussar Formation was also penetrated in Hussar 1, Kanpa 1A, Lungkarta 1, and Yowalga 3. The upper contact of the Hussar Formation is conformable with the Kanpa Formation in Hussar 1, Kanpa 1A, Lungkarta 1, and Yowalga 3.

The uppermost interval (860.8 – 1013 m) comprises predominantly sandstone with thin interbeds of dolomite and mudstone. The interval from 861 to 927 m includes buff to reddish-brown, locally loosely cemented (at 886 m), thick sandstone beds interbedded with thin mudstones. Sandstones are dominantly quartz rich with minor opaque minerals and are locally cemented by dolomite. Vuggy porosity, which probably formed as a result of diagenetic dissolution, formed in heavily oxidized zones. Locally developed channel-cut surfaces, which are overlain by coarser grained sandstones, are also present. Sandstones are mostly medium grained, oxidized in parts, and show a slightly coarsening upward cycle; in particular, from 861 to 928 m. These strata are mainly massive, but locally cross-bedded and have strata inclined up to 15–20° between 880 and 890 m. Most of the sandstone beds are capped by thin mudstone layers. These facies assemblages indicate shallow-marine environments, probably within the shoreface area.

Thin mudstone layers are parallel to wavy bedded and interbedded with very thin silty laminae. They are sharply separated from sandstones and show abundant soft-sediment deformation structures and minor erosional surfaces. Graded beds within this mudstone section indicate fairly rapid deposition. The mudstone was probably deposited below wave base within a lagoon or restricted shallow-marine environment.

The interval from 927 to 1013 m consists predominantly of sandstone interbedded with mudstone and dolomitic beds. The sandstone is dominantly brown, medium grained, and thick

bedded above 980 m, but medium to coarse grained and massive below. It is unconsolidated from 985 to 989 m. Minor erosive surfaces are locally present and associated with granular beds. The dolomitic section is microcrystalline and stylolitic. The presence of oolites suggests a high-energy environment. From 966 to 978 m, the dolomite contains desiccation cracks and stromatolites. Both local erosive surfaces and dissolution breccias are common features within the dolomite. The laminae in the dolomite ranges from planar to wavy. The sedimentary succession from 861 to 1013 m was probably deposited in a mixed (dominantly siliciclastic), probably storm-influenced, shallow-marine, intertidal to subtidal environment.

The interval from 1013 to 1105 m is dominated by interbedded sandstone and mudstone (1013–1065 m), and dolomite and silty mudstone (1065–1105 m). The sandstone is well sorted, mainly massive, but locally cross-bedded. The core and gamma-ray log responses indicate that a few thin, coarsening-upward successions are capped by thin mudstone layers.

The lower part of the interval, from 1065 to 1105 m, comprises dolomite and silty mudstone. The dolomite consists of stylolites, stromatolites, soft-sediment deformation structures, local scour surfaces, and a thin conglomeratic bed. A stromatolite at 1077.4 m consists of almost horizontally inclined, closely spaced, irregular columns and is tentatively identified as *Tungussia* sp. nov. (this is labelled as unnamed branching columnar stromatolite in Plates 1 and 3). This form has not been identified in outcrop. An erosive contact with overlying, thinly laminated mudstone and small-scale desiccation fractures near the top of the unit suggest subaerial exposure. Mudstone deposits from 1045 to 1058 m and 1085 to 1105 m were probably deposited in a slightly deeper and lower energy environment.

The underlying succession (1105–1157 m) comprises mainly sandstone, dolomite, and mudstone. The upper section, from 1105 to 1133 m, is predominantly sandstone interbedded with thin oolitic and sandy dolomite beds. The gamma-ray log indicates that the sandstones formed in slightly coarsening upward successions. The sandstones are medium grained, well sorted, locally cross-bedded, oxidized, and contain minor cherts. The lower section (1133–1157 m) comprises dolomite and mudstone with minor sandstone interbeds. Dolomite is oolitic, conglomeratic, locally silicified, and vuggy. Fractures filled by evaporitic minerals are also common. Towards the base of the succession the dolomite grades to mudstone. The mudstone is silty, locally dolomitic, evaporitic, brecciated, light-grey mottled, and contains abundant soft-sediment deformation structures, small-scale wave-ripples, and desiccation fractures. Facies and sedimentological characteristics suggest a depositional environment ranging from sabkha to restricted shallow-marine for this interval.

The lowest interval (informal unit D of Townson, 1985), from 1157 to 1247.1 m, consists predominantly of silty mudstone interbedded with thin silty and rare thin, light-grey dolomite layers. This facies assemblage was probably laid down in very calm water in reducing conditions within a lagoon or restricted shallow-marine environment.

Browne Formation — 1247.1 to 1521.8 m; 1249.1 to 1524 m log depth (Supersequence 1)

Within the Officer Basin, the Browne Formation is composed of calcareous shale, anhydrite, gypsum, halite, sandstone, dolomite, and dolomitic limestone, and was previously intersected in Browne 1, Browne 2, Kanpa 1A, Yowalga 3, Dragoon 1, and Hussar 1. The Browne Formation is conformably overlain by the Hussar Formation in Hussar 1, Kanpa 1A, and Yowalga 3. The lower contact with the Townsend Quartzite is probably unconformable in Kanpa 1A (Townson, 1985).

The Browne Formation was fully penetrated in Empress 1A (275 m thick). The formation is conformably overlain by the Hussar Formation at 1247.1 m, and unconformably overlies the ?Lefroy Formation at 1521.8 m (1524 m log depth). The Browne Formation is composed of evaporites, stromatolitic dolomites, and red, fine-grained siliciclastic deposits.

The interval from 1247.1 m to 1351 m is mainly halite interbedded with mudstone and minor dolomite. The halite is white to translucent and orange–brown and includes mudstone inclusions. There are at least two types of halite in the Browne Formation: displacive halite, which forms within a siliciclastic matrix; and well-bedded, depositional halite up to 15 cm thick (El Tabakh, M., 1998, pers. comm.). The mudstone is reddish brown, slightly dolomitic, contains salt cubes, and has light-grey mottling and desiccation cracks. The dolomite is thinly laminated, fractured to brecciated, and includes large vugs infilled by salt crystals.

In the interval from 1351 to 1365 m, the Browne Formation includes dominantly reddish brown sandstone interbedded with siltstone, mudstone, and minor anhydrites.

Two dolomitic intervals between 1365 and 1403.7 m are separated by red silty mudstone. The upper dolomitic section (1365 – 1386.3 m) is multicoloured, locally siliceous, and includes minor mudstone layers. The older stromatolitic assemblage of Supersequence 1, dominated by *Acaciella australica*, was identified within the upper dolomitic section. Therefore, this section can be correlated with outcrops of the Woolnough Formation at Woolnough Diapir, and the Skates Hill Formation in the Savory Sub-basin (Grey, 1995; Stevens and Grey, 1997). The Browne Formation is considered to be an equivalent of the Loves Creek Member of the Bitter Springs Formation (Amadeus Basin) based on the stromatolite assemblage. The overall depositional environment indicated by the stromatolites is probably semi-emergent to shallow submergent (El Tabakh et al., in prep.).

The lower dolomitic section (1394.7 – 1403.7 m) is off-white to pink, massive, highly fractured, and contains salt inclusions within fractures and desiccation cracks. This section does not contain stromatolites and is probably equivalent to the Madley Formation, which outcrops in the Madley and Woolnough Diapirs. From 1406 to 1521.8 m, the Browne Formation is composed mainly of halite interbedded with mudstone and minor dolomite beds. The presence of massive salt and thick, reddish-brown claystone to siltstone-dominated deposits indicates a long period of a dry and

warm climate under hypersaline and oxidizing conditions during the deposition of this formation. The lithological characteristics of the Browne Formation are similar in other wells drilled in the Officer Basin. The Browne Formation was probably deposited in large, shallow lakes or a restricted inland sea.

?Lefroy Formation — 1521.8 to 1540.2 m; 1524 to 1543.3 m log depth (Supersequence 1)

The Lefroy Formation, at its type section, consists of grey to maroon, very argillaceous, micaceous shaly siltstone and sandstone (Lowry et al., 1972). In Empress 1A, the stratigraphic unit from 1521.8 to 1540.2 m, which consists of brownish and light-grey silty mudstone and a basal conglomerate, is believed to be, at least in part, equivalent to the Lefroy Formation. The ?Lefroy Formation unconformably lies between the Browne Formation and pre-Officer Basin strata. The ?Lefroy Formation is highly fractured and includes two volcanic layers; one at 1524.5 – 1526.5 m and the other at 1534.2 – 1535.3 m. The volcanic layers consist of relatively coarse grained, highly fractured basalt, which is transected by veins filled with quartz–chalcedony, carbonate, and limonitic material. The basalts are too highly altered for radiometric dating (Appendix 4; GSWA sample 154100). The basal conglomeratic horizon from 1539.6 to 1540.2 m is dominated by white quartz pebbles and separates the Officer Basin successions from the underlying pre-Officer Basin (pre-Centralian) strata.

?Mesoproterozoic rocks

Pre-Officer Basin succession (Pre-Centralian Superbasin) — 1540.2 to 1624.6 m TD; 1543.3 to 1624.6 m log depth

The pre-Officer Basin succession penetrated in Empress 1A, from 1540.2 to 1624.6 m (TD), is represented by mudstone with thin silty and sandy horizons, locally developed conglomerate, silty shale, and basalt. The mudstone is thinly laminated, brown to dark grey, silty, and is interbedded with silt and sandstone layers. From 1540 to 1570 m the unit is a silty shale composed mainly of clay minerals and silt-sized quartz grains. This unit is highly fractured, very dense, and thermally overmature. The succession from 1570 to 1624.6 m (TD) consists of fine-grained basaltic rock, which shows a variety of alteration features. The basalt is transected by some narrow veins filled with green chlorite. Thin-section examination indicates that the basalt shows slight variations in the degree of alteration, but is commonly unaltered. A K–Ar age of 1058 ± 13 Ma was determined for this basalt (1601.57 – 1602.24 m; Appendix 2). Similar age volcanic rocks have been identified from the Musgrave Complex northeast of Empress 1 and 1A, including volcanic rocks of the Tollu Group (Clarke et al., 1995) and the Kulgera Dyke Swarm (Camacho et al., 1991). Empress 1A was terminated within the basalt at 1624.6 m.

Petroleum geology

Petroleum exploration activities in the western Officer Basin were summarized by Townson (1985), Phillips et al. (1985), and Perincek (1998), and the petroleum potential of the eastern Officer Basin (within South Australia) was reviewed by Morton and Drexel (1997). Type II kerogens in the oil window are known in the Yowalga and Gibson Sub-basins (Ghori, 1998). Commercial quality reservoirs are noted in the Browne, Hussar, Kanpa, ?Lupton, unnamed, and Paterson Formations from log data. Sealing evaporites and shales are present throughout the sedimentary section in the Officer Basin.

Hydrocarbon shows

No oil shows were detected in Empress 1 and 1A. Minor fluorescence was observed, particularly from dolomites at various depths. These are all interpreted as either drilling contamination or mineral fluorescence. Rare ?bitumen was observed in organic petrology samples from 360.3 and 516.6 m (Appendix 9; Table 9.9). Bitumen-coated monazite has been tentatively identified in two thin sections (Martin, in prep.) at 1521.2 m (Browne Formation) and 639.8m (Kanpa Formation).

Source potential and maturity

A total of 88 total organic carbon (TOC) and 20 Rock-Eval analyses were conducted on core samples in Empress 1 and 1A. The Rock-Eval pyrolysis showed that six samples from the Kanpa Formation have fair to good hydrocarbon-generating potential. Their organic richness ranges from 1.52 to 0.51% TOC (Appendix 9). Maturation and hydrocarbon generation modelling of Empress 1A shows that source beds within the Kanpa Formation are currently in the main stages of oil generation. The basal section of interbedded clastic and volcanic rocks are overmature.

Reservoir character and seal potential

Porosity and permeability measurements were conducted on a total of 71 core samples. Mini-permeametry was measured on some core samples. Log analysis was carried out where open-hole logs were available over the Table Hill Volcanics, the upper part of the Neoproterozoic unnamed unit, the lower part of the Kanpa Formation, and the Hussar, Browne, and ?Lefroy Formations (Appendix 10).

The Lennis Sandstone has excellent porosity and permeability. The Table Hill Volcanics have nil to good porosity and very poor permeability. Sandstones of the Neoproterozoic unnamed unit have good porosity and excellent permeability.

The ?Lupton Formation has very poor to good porosity and good permeability in the moderately sorted sandstones. The basal sandstone of the ?Lupton Formation has excellent permeability (up to 1 darcy). Overlying mudstones and diamictites are interpreted to be potential seals.

Sandstones from the Kanpa and Hussar Formations have good porosities and permeabilities of hundreds of millidarcies (mD). The recognition of significant karstification of the dolomites at the top of the Kanpa Formation upgrades the reservoir potential of this unit. The computed maximum effective log porosities for the analysed interval of the Kanpa Formation is 34.9% and 28.2% for the Hussar Formation (Appendix 10). Thick mudstones in both formations provide seals for this reservoir-quality sandstone succession. The reservoir potential of the Browne Formation is commonly poor with porosities less than 15% and permeabilities less than 1 mD. Thick halite beds in the Browne Formation are considered to be potential seals.

Mineral potential

Twenty-two drillcore samples were analysed for nine elements (Ag, As, Ba, Co, Cu, Mn, P, Pb, and Zn) to investigate the mineral potential for both sedimentary-hosted and mafic-volcanic contact-hosted mineralization (Appendix 11). The values were not encouraging, but this does not necessarily downgrade the mineral potential of the region, as only limited sampling was done, and no focusing mechanism for mineralizing fluids was recognized in the drillhole.

Late generation malachite veinlets (0.05 mm wide) were identified in a thin section at 1574 m (Pirajno, 1999).

Contributions to geological knowledge

Investigation of the Empress 1 and 1A core significantly improved the understanding of both chronostratigraphic correlations and petroleum systems of the Officer Basin. Empress 1 and 1A are the first continuously cored drillholes through complete Neoproterozoic successions. Empress 1 and 1A are also the first drillholes to confirm the chronological succession of two distinct assemblages of stromatolites: the *Acaciella australica* and *Baicalia burra* Assemblages. In addition, distinctive, well-documented and well-constrained palynomorph assemblages of biostratigraphic significance are also present. These assemblages provide evidence for regional correlations and ages for Neoproterozoic rocks (Grey and Stevens, 1997). The application of SHRIMP U–Pb and K–Ar radiometric dating improves constraints on the ages of the Officer Basin strata. The age of the Table Hill Volcanics has been revised to Early Ordovician, which suggests a correlation with the Kulyong Formation from South Australia. The ‘cap dolomite’ represents a global synchronous geochemical event that marks the top of the Marinoan glacial succession. The identification of the ‘cap dolomite’ at the top of the ?Lupton Formation in Empress 1 and 1A suggests a Marinoan age for the Neoproterozoic glacial sequence.

On the basis of core data in Empress 1A, the Browne Formation was probably deposited in large, shallow lakes or in a restricted inland-sea environment that dominated the entire area, or a

large portion of the Officer Basin during this period. The facies assemblages from the Hussar Formation were deposited in very calm water under reducing conditions in a lagoon or restricted shallow-marine (subtidal) environment. The overlying Kanpa Formation was also probably deposited in a similar environment (sabkha to shallow marine) under oxidizing to slightly reducing conditions.

The reservoir potential of the sandstone in the Kanpa and Hussar Formations is commonly good. Shales more than 10 m thick in the ?Lupton, Kanpa, and Hussar Formations in Empress 1A may provide good seals. Thick halite beds in the Browne Formation are also excellent potential seals; however, subsalt reservoirs were not present in the drillhole.

Apatite fission-track and lamalginite and bitumen reflectance data indicate that the Neoproterozoic strata in the Yowalga Sub-basin probably reached maximum thermal maturity during the late Neoproterozoic to early Palaeozoic (600–300 Ma). The occurrence of another thermal event, probably during the Miocene (<40 Ma), may indicate a period of hot-fluid migration, which was probably associated with the migration of hydrocarbons (Appendix 9; Hegarty et al., 1998). TOC and Rock-Eval analyses indicate that the Kanpa Formation is mature for oil generation and has poor to good oil-generating potential in Empress 1A (Appendix 9; Ghori, 1998). Futhermore, the presence of rare bitumen is interpreted to indicate that oil migration has occurred through the Neoproterozoic succession.

Major unconformities are recognized at the base of the ?Lefroy Formation, ?Lupton Formation, Table Hill Volcanics, Lennis Sandstone, Paterson Formation, and Cainozoic strata. The Palaeozoic strata are flat lying, but the Neoproterozoic strata dip at about 5°, typically to the northeast. This suggests that Empress 1 and 1A were drilled on a broad structural shelf at the southern margin of the Yowalga Sub-basin, which has been relatively tectonically stable since the Neoproterozoic.

References

APAK, S. N., and BACKHOUSE, J., 1998, Re-interpretation of the Permo-Carboniferous succession, Canning Basin, Western Australia, *in* The sedimentary basins of Western Australia 2 *edited by* P. G. and R. R. PURCELL: Petroleum Exploration Society of Australia, Symposium, Perth, W.A., 1998, Proceedings, p. 683–694.

ARCHBOLD, N. W., 1998, Marine biostratigraphy and correlation of the West Australian Permian Basins, *in* The sedimentary basins of Western Australia 2 *edited by* P. G. and R. R. PURCELL: Petroleum Exploration Society of Australia, Symposium, Perth, W.A., 1998, Proceedings, p. 141–151.

CAMACHO, A., SIMONS, B., and SCHMIDT, P. W., 1991, Geological and palaeomagnetic significance of the Kulgera Dyke Swarm, Musgrave Block, N.T., Australia: Geophysical Journal International, v. 107, p. 37–45.

CLARKE, G. L., SUN, S.-S., and WHITE, R. W., 1995, Grenville-age belts and associated older terranes in Australia and Antarctica: Australian Geological Survey Organisation, Journal of Australian Geology and Geophysics, v. 16, p. 25–39.

COATS, R. P., and PREISS, W. V., 1980, Stratigraphic and geochronological reinterpretation of Late Proterozoic glaciogenic sequences in the Kimberley region, Western Australia: Precambrian Research, v. 13, p. 181–208.

COMPSTON, W., 1974, The Table Hill Volcanics of the Officer Basin — Precambrian or Palaeozoic?: Journal of the Geological Society of Australia, v. 21, p. 403–411.

EL TABAKH, M., GREY, K., and CARLSEN, G. M., in prep., Neoproterozoic stromatolite and dolomite deposits of the Browne Formation in the Officer Basin, Centralian Superbasin, Western Australia.

EYLES, N., and EYLES, C. H., 1998, Summary of Late Proterozoic glaciogenic succession in Empress 1, Officer Basin: Western Australia Geological Survey, S-series, S20424 A6 (unpublished).

GHORI, K. A. R., 1998, Petroleum generating potential and thermal history of the Neoproterozoic Officer Basin, Western Australia, *in* The sedimentary basins of Western Australia 2 *edited by* P. G. and R. R. PURCELL: Petroleum Exploration Society of Australia, Symposium, Perth, W.A., 1998, Proceedings, p. 717–730.

GREEN, P. F., and GLEADOW, A. J. W., 1984, Fission track analysis of samples from Kanpa 1A and Yowalga 3, Officer Basin: Geotrack Report No. 14, November 1984, prepared for Shell Development (Australia) Pty Ltd, University of Melbourne (unpublished).

GREY, K., 1995, Neoproterozoic stromatolites from the Skates Hills Formation, Savory Basin, Western Australia, and a review of the distribution of *Acaciella australica*: Australian Journal of Earth Sciences, v. 42, p. 123–132.

GREY, K., and STEVENS, M. K., 1997, Neoproterozoic palynomorphs of the Savory Sub-basin, Western Australia, and their relevance to petroleum exploration: Western Australia Geological Survey, Annual Review 1996–97, p. 49–54.

HEGARTY, K. A., O'BRIEN, C., and WATSON, P. G. F., 1998, Thermal history reconstruction for the Empress 1A well (Officer Basin) using apatite fission-track analysis and reflectance: Western Australia Geological Survey, S-series, S20424 A2 (unpublished).

HOCKING, R. M., 1994, Subdivisions of Western Australian Neoproterozoic and Phanerozoic sedimentary basins: Western Australia Geological Survey, Record 1994/4, 84p.

JACKSON, M. J., and van de GRAAFF, W. J. E., 1981, Geology of the Officer Basin, Western Australia: Australia BMR, Bulletin 206, 102p.

JACKSON, M. J., van de GRAAFF, W. J. E., and BOEGLI, J. C., 1975, Shallow stratigraphic drilling in the Officer Basin, Western Australia, 1972: Australia BMR, Record 1975/49 (unpublished).

KEMP, E. M., 1976, Palynological observations in the Officer Basin, Western Australia: Australia BMR, Bulletin 160, p. 23–39.

KENNEWELL, P. J., 1977a, Westwood, W.A.: Western Australia Geological Survey, 1:250 000 Geological Series Explanatory Notes, 14p.

KENNEWELL, P. J., 1977b, Yowalga, W.A.: Western Australia Geological Survey, 1:250 000 Geological Series Explanatory Notes, 15p.

LOWRY, D. C., JACKSON, M. J., van de GRAAFF, W. J. E., and KENNEWELL, P. J., 1972, Preliminary result of geological mapping in the Officer Basin, Western Australia: Western Australia Geological Survey, Annual Report 1971, p. 50–56.

MARTIN, K. R., in prep., Empress 1/1A petrological analysis, final report : Western Australia Geological Survey, S-series, S20424 (unpublished).

MORTON, J. G. G., and DREXEL, J. F., 1997, The petroleum geology of South Australia. Volume 3 — Officer Basin: South Australia Department of Mines and Energy Resources, Report Book, 97/19.

NELSON, D. R., in prep., Compilation of SHRIMP U–Pb zircon geochronology data, 1998: Western Australia Geological Survey, Record 1999/2.

PERINCEK, D., 1996a, The age of Neoproterozoic–Palaeozoic sediments within the Officer Basin of the Centralian Superbasin can be constrained by major sequence-bounding unconformities: APPEA Journal, v. 36, pt 1, p. 350–368.

PERINCEK, D., 1996b, The stratigraphic and structural development of the Officer Basin, Western Australia — a review: Western Australia Geological Survey, Annual Review 1995–96, p. 135–148.

PERINCEK, D., 1998, A compilation and review of data pertaining to the hydrocarbon prospectivity of the Officer Basin: Western Australia Geological Survey, Record 1997/6, 209p.

PHILLIPS, B. J., JAMES, A. W., and PHILIP, G. M., 1985, The geology and hydrocarbon potential of the northwestern Officer Basin: APEA Journal, v. 25, pt 1, p. 52–61.

PIRAJNO, F., 1999, Brief petrographic descriptions of mafic igneous rocks intersected by Empress 1A: Western Australia Geological Survey, S-series, S20424 A9 (unpublished).

PREISS, W. V., WALTER, M. R., COATS, R. P., and WELLS, A. T., 1978, Lithological correlations of Adelaidean glaciogenic rocks in parts of the Amadeus, Ngalia, and Georgina Basins: Australian BMR, Journal of Australian Geology and Geophysics, v. 3, p. 43–53.

SHEVCHENKO, S. I., and IASKY, R. P., 1997, Calculating depth to basement from magnetic and gravity data, with an example from the western Officer Basin: Western Australia Geological Survey, Annual Review 1996–97, p. 69–75.

STEVENS, M. K., and GREY, K., 1997, Skates Hill Formation and Tarcunyah Group, Officer Basin — carbonate cycles, stratigraphic position, and hydrocarbon prospectivity: Western Australia Geological Survey, Annual Review 1996–97, p. 55–60.

TOWNSON, W. G., 1985, The subsurface geology of the western Officer Basin — results of Shell's 1980–1984 petroleum exploration campaign: APEA Journal, v. 25, pt 1, p. 34–51.

WALTER, M. R., and GORTER, J., 1994, The Neoproterozoic Centralian Superbasin in Western Australia — the Savory and Officer Basins, *in* The sedimentary basins of Western Australia *edited by* P. G. and R. R. PURCELL: Petroleum Exploration Society of Australia, Symposium, Perth, W.A., 1994, Proceedings, p. 851–864.

WALTER, M. R., GREY, K., WILLIAMS, I. R., and CALVER, C. R., 1994, Stratigraphy of the Neoproterozoic to early Palaeozoic Savory Basin and correlation with the Amadeus and Officer Basins: Australian Journal of Earth Sciences, v. 41, p. 533–546.

WALTER, M. R., and VEEVERS, J. J., 1997, Australian Neoproterozoic palaeogeography, tectonics, and supercontinental connections: Australian Geological Survey Organisation, Journal of Australian Geology and Geophysics, v. 17, p. 73–92.

Appendix 1
Operations report
(by M. K. Stevens)

Drillhole history

Empress 1 and 1A are stratigraphic drillholes drilled in the Officer Basin by the Geological Survey of Western Australia to test the source-rock potential of Neoproterozoic strata. Empress 1 was spudded at 18:00 on Saturday, 21 June 1997 and reached a total depth (TD) of 615 m (drillers depth) at 13:00, 4 July 1997. The base of the recovered core was 612.9 m. The drill rods parted at 374 m while drilling at 615 m and attempts to recover the fish were largely unsuccessful, so Empress 1 was plugged and abandoned at 06:00, 13 July 1997 (Fig. 1.1).

Time to TD for Empress 1 was 12 days, 19 hours, and the total time was 21 days, 12 hours. The drillhole was not geophysically logged.

Empress 1A was spudded 6 m northwest of Empress 1 at 18:00 on Sunday, 13 July 1997 and reached a TD of 1624.6 m (drillers depth) at 19:45, 23 August 1997. The drillhole was plugged and abandoned at 11:15, 28 August 1997.

Time to TD for Empress 1A was 41 days, 1:45 hours, and the total time was 45 days, 17:15 hours.

Empress 1A was geophysically logged by BPB Slimline Services who recorded a TD of 1583 m during the first logging suite on 24 and 25 August 1997. The logging tools were unable to pass through a constriction at 1583 m and went into casing at 651 m. Several attempts were made to recover the PF 4.5" casing but this was only partially successful, resulting in open hole logs of the second suite being acquired from 303 to 211 m on 27 August 1997.

Water for drilling and camp use was pumped from WTDB 1, a waterbore drilled 29 m to the south-southeast of Empress 1A, which was completed from 122.35 to 104.35 m and produced water from the Paterson Formation.

Empress 1 was abandoned at 615 m TD after unsuccessful fishing attempts with good core recoveries in both the PQ and HQ cored intervals. Empress 1A achieved the geological objective of fully penetrating the Officer Basin succession and was terminated in pre-Officer Basin volcanic rocks at 1624.6 m. Excellent core recoveries were obtained in both the PQ and HQ cored intervals. Open-hole wireline logs were acquired between 1580 and 651 and between 303 and 211 m in Empress 1A.

Operations

Drilling shifts: Two 12-hour shifts operated each day (Table 1.1). Shift change was at 06:00 and 18:00 hrs.

Drilling crews: Each crew consisted of the driller and two or three driller's offsiders. The drilling supervisor was Ray O'Brien and the drillers were Rick Armstrong, Kevin Davies, Gary Birkett, and Mark Angelico.

GSWA personnel: Mark Stevens, Peter Havord, and Chris Brooks.

Orientation surveys: Hole orientation was monitored during drilling operations at various intervals with an Eastman Single Shot Camera (Table 1.2 and 1.3).

Core recovery: Empress 1, PQ core recovery was about 178.1 m of the 189.2 m drilled (94%). HQ core recovery was about 297.35 m of the 320.1 m drilled (93%).

Empress 1A, PQ core recovery was about 429.7 m of the 439.3m drilled (98%). HQ core recovery was about 100% of the 974.8 m drilled.

Time-depth curve: The time–depth curve (Fig. 1.2) shows the progress of the drillhole during drilling. The data are tabulated in Table 1.4.

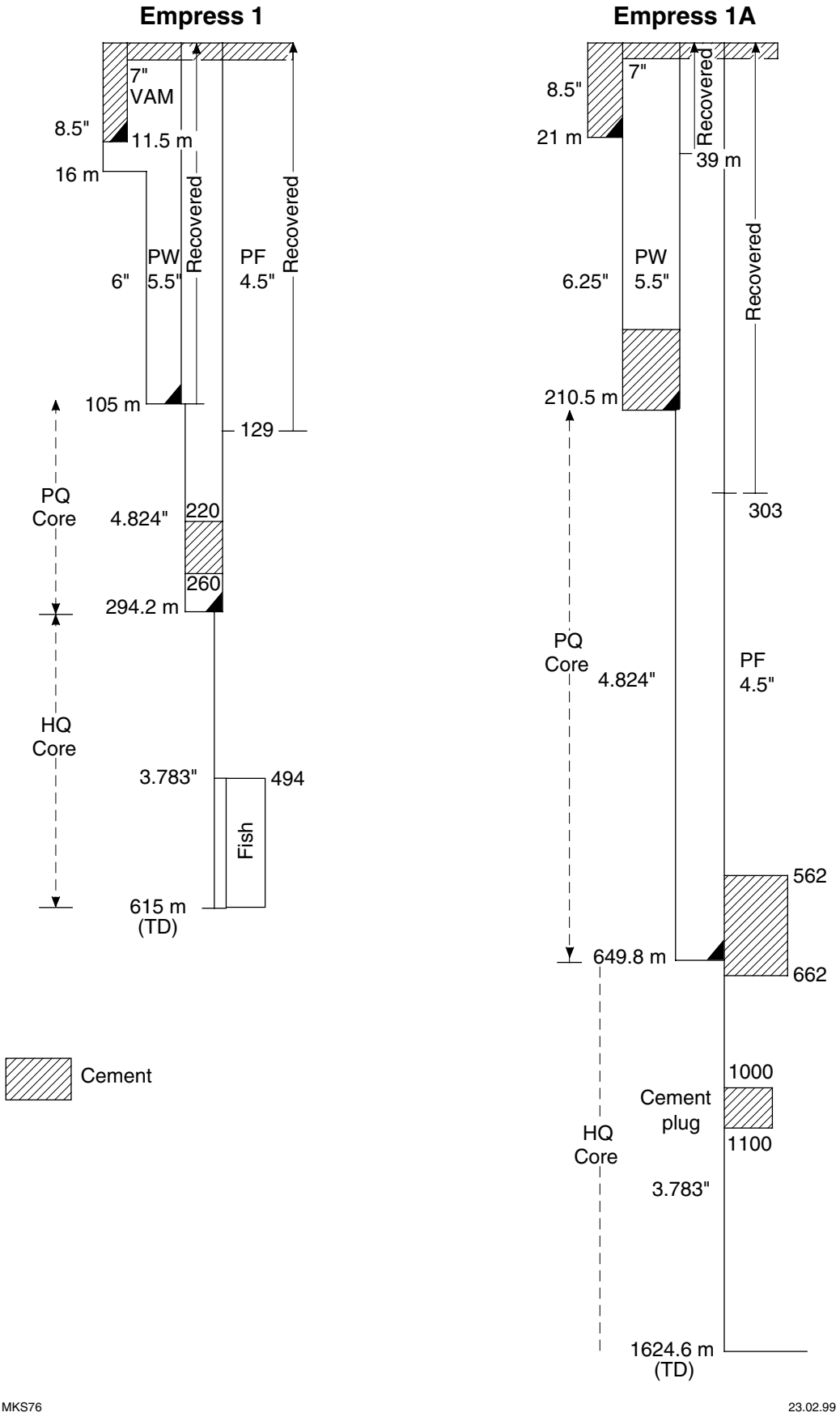

Figure 1.1. Engineering diagram for Empress 1 and 1A

Table 1.1. Daily drilling summary, Empress 1 and 1A

Date	*Shift*	*Time*	*Activity*
21 June 1997	Night	Rotary drilling: 6 hrs	**Spud Empress 1 at 18:00 hrs**, rotary drill with 215.9 mm, 8.5" rock roller bit to 16 m, run 11.5 m of 177.8 mm, 7" casing. Note: No samples 0–16 m (16 m)
		Trip: 0:30 hrs	
		Run casing: 1 hrs	
		Cement casing: 3 hrs	
		Rig repairs: 1:30 hrs	
22 June 1997	Day	Cement casing: 6 hrs	Rotary drill with 152.4 mm, 6" rock roller bit to 24 m (8 m)
		Rig up: 4 hrs	
		Rotary drilling: 2 hrs	
22 June 1997	Night	Rotary drilling: 12 hrs	Rotary drill with 152.4 mm, 6" rock roller bit 24 to 66 m (42 m)
23 June 1997	Day	Rotary drilling: 8:30 hrs	Rotary drill with 152.4 mm, 6" rock roller bit 66 to 105 m (39 m)
		Trip for bit change: 1:30 hrs	
		Trip: 1 hrs	
		Run PW casing: 1 hrs	
23 June 1997	Night	Run PW casing: 3:30 hrs	Run and seat PW casing at 105 m. PQ core 105 to 117 m, two trips due to stuck tube (12 m)
		Run PQ barrel: 1 hrs	
		PQ core: 3 hrs	
		Trip, stuck tubes: 4:30 hrs	
24 June 1997	Day	Stuck tube: 1:00 hrs	Work stuck PQ tube, trip to recover tube, PQ core 117 to 129 m (12 m)
		Trip, stuck tubes: 2 hrs	
		PQ core: 5 hrs	
		Repair PQ barrel: 4 hrs	
24 June 1997	Night	PQ core: 11 hrs	PQ core 129 to 201 m (72 m)
		Trip for bit change: 1 hrs	
25 June 1997	Day	Trip for bit change: 1 hrs	PQ core 201 to 225 m (24 m)
		PQ core: 9:30 hrs	
		Survey: 0:30 hrs	
		Rig repairs: 1 hrs	
25 June 1997	Night	PQ core: 10 hrs	PQ core 225 to 252 m (27 m)
		Survey: 0:30 hrs	
		Trip for bit change: 1 hrs	
26 June 1997	Day	Trip for bit change: 0:30 hrs	PQ core 252 to 279 m (27 m)
		PQ core: 10:30 hrs	
		Survey: 0:30 hrs	
		Rotate: 0:30 hrs	
26 June 1997	Night	PQ core: 3:30 hrs	PQ core 279 to 294.2 m, trip, condition hole, run and seat PF casing at 294.2 m, cement hole, install BOP (15.2 m)
		Consult geologist: 0:30 hrs	
		Survey: 1 hrs	
		Trip, case and condition hole: 4 hrs	
		Cement hole, rig BOP: 3 hrs	
27 June 1997	Day	Cement hole, rig BOP: 10 hrs	Cut 7" casing, rig up BOP and HQ coring equipment
		Rigging up: 2 hrs	
27 June 1997	Night	Trip in: 1:30 hrs	Run in with HQ, install BOP, test and replace leaking bladder, drill out rubber plug and shoe, pressure test, HQ core 294.2 to 342 m (45.8 m)
		Hook up BOP: 1 hrs	
		Replace bladder: 1:30 hrs	
		Drill out plug: 1 hrs	
		Leak off test: 0:30 hrs	
		Survey: 0:30 hrs	
		HQ core: 6 hrs	
28 June 1997	Day	HQ core: 9 hrs	HQ core 342 to 391m, leak off test equivalent mud weight 13.7 pounds per gallon, bit change at 375 m (49 m)
		Leak off test: 0:30 hrs	
		Bit change: 1:30 hrs	
		Service rotation head: 0:30 hrs	
		Survey: 0:30 hrs	
28 June 1997	Night	HQ core: 11:30 hrs	HQ core 391 to 451 m (60 m)
		Survey: 0:30 hrs	
29 June 1997	Day	HQ core: 9 hrs	HQ core 451 to 481 m, safety meeting, bit change (30 m)
		Survey: 0:30 hrs	
		Rotate and circulate: 0:30 hrs	
		Bit change: 2 hrs	
29 June 1997	Night	HQ core: 11:30 hrs	HQ core 481 to 526 m (45 m)
		Survey: 0:30 hrs	
30 June 1997	Day	HQ core: 4:30 hrs	HQ core 526 to 550 m, high torque and rods locking up, flush sumps and add KCl and Aqua Pac, reduce sump volume (24 m)
		Rotate and circulate: 1:30 hrs	
		Flush sumps, add KCl: 6 hrs	
30 June 1997	Night	HQ core: 11 hrs	HQ core 550 to 580 m, bit change (30 m)
		Rotate and circulate: 0:30 hrs	
		Bit change: 0:30 hrs	
1 July 1997	Day	HQ core: 8 hrs	Bit change, HQ core 580 to 598 m (18 m)
		Condition hole: 1:30 hrs	
		Bit change: 2:30 hrs	

Table 1.1. (continued)

Date	*Shift*	*Time*	*Activity*
1 July 1997	Night	HQ core: 3 hrs Fishing: 9 hrs	HQ core 598 to 604.3 m, broken rod at 362.7 m (6.3 m)
2 July 1997	Day	Fishing: 12 hrs	Fishing (0 m)
2 July 1997	Night	Fishing: 5 hrs Trip, core, condition hole: 7 hrs	Fishing, all drillstring recovered, run in, clean and condition hole, HQ core 604.3 to 607.9 m, trip out due to rubbish in hole (3 m)
3 July 1997	Day	Core and condition hole: 12 hrs	Condition hole as rods not turning smoothly, recognize that hole is 3 m shallower than thought and correct core-block markers with error believed to be at 550 m, HQ core 604.9 to 608.4 m (0.5 m)
3 July 1997	Night	Condition hole, trip, ream: 12 hrs	Condition hole, trip, rotary drill with 98.4 mm, 3.875" 608.4 to 608.9 m, reaming from 470 m to bottom of hole (0.5 m)
4 July 1997	Day	Trip: 2 hrs HQ core: 5 hrs Fishing: 5 hrs	Bit change, HQ core 608.9 to 615 m, large sand returns from hole, fishing for broken rod at 374 m (6.1 m)
4 July 1997	Night	Fishing: 12 hrs	Fishing, run HQ bell tap unsuccessfuly, run metzke spear plus shear pins unsuccessfuly, run in with NQ and circulate while awaiting Bowen spear (0 m)
5 July 1997	Day	Fishing: 12 hrs	Fishing, run Bowen spear, latch onto fish but unable to recover, disengage, run in to sit NQ on metzke spear (0 m)
5 July 1997	Night	Fishing: 12 hrs	Fishing, finish running in to sit NQ on metzke spear, run HMQ rods with blank into fish at 374 m, then use NQ as jarring tool to try and free spear, pull out NQ (0 m)
6 July 1997	Day	Fishing: 12 hrs	Fishing, run in NQ barrel and drill over spear, which moves, run in NQ string plus BQ bell tap and chase spear to bottom (0 m)
6 July 1997	Night	Fishing: 12 hrs	Fishing, successfully recover metzke spear plus NQ overshot on third attempt, flush hole around HQ back end (0 m)
7 July 1997	Day	Fishing: 12 hrs	Fishing, run in NQ string with jarring assembly to free tube, run NQ bell tap and try to move tube (0 m)
7 July 1997	Night	Fishing: 12 hrs	Fishing, run new tap unsuccessfully, run NQ and core some of HQ back end, pull out (0 m)
8 July 1997	Day	Fishing: 9 hrs	Fishing, run NQ bell tap to recover tube, run NQ barrel to core tube unsuccessfully, remove BOP, try to recover cemented PF casing unsuccessfully, decision made to abandon hole with base of recovered core at 612.9 m (0 m)
8 July 1997	Night	Fishing: 9 hrs Rig maintenance: 3 hrs	Fishing, run into HMQ string and cut at 605 m, run Bowen spear to recover HMQ unsuccessfully, run NQ to circulate (0 m)
9 July 1997	Day	Fishing: 12 hrs	Fishing, pull out, run NQ to cut HMQ at 495 m, run spear and successfully recover 486 m of useable HMQ rods, cut HMQ string at 555 and 552 m (0 m)
9 July 1997	Night	Fishing: 12 hrs	Fishing, run in to recover more HMQ rods but hole caved at 432 m, fish left in hole is from 615 to 494 m and consists of: core bit, 7 m barrel and tubes, 38 x 3 m HMQ rods, 1 × HMQ back end (0 m)
10 July 1997	Day	Recovering casing: 12 hrs	Run in and cut PF casing at 251 m, unable to recover, cut PF casing at 150 m, casing only moves 1 m, then becomes stuck (0 m)
10 July 1997	Night	Recovering casing: 12 hrs	Run in and cut PF casing at 138, 132, and 126 m, unable to recover (0 m)
11 July 1997	Day	Recovering casing: 12 hrs	Work PF casing, unable to recover, PW casing is able to be moved (0 m)
11 July 1997	Night	Recovering casing: 2 hrs Cementing: 4 hrs Maintenance and standby: 6 hrs	Run in and cut PF casing at 120 m, unable to recover, cement plug from 260 to 220 m, waiting for delivery of cutter blades (0 m)
12 July 1997	Day	Maintenance and standby: 6 hrs Recovering casing: 6 hrs	Waiting for delivery of cutter blades, run in and cut PF casing at 108 and 105 m, unable to recover (0 m)
12 July 1997	Night	Recovering casing and cementing: 12 hrs	Recover 129 m of PF casing and all 105 m of PW, cement top of hole. **Empress 1 plugged and abandoned at 06:00 hrs 13 July 1997** (0 m)
13 July 1997	Day	Rig down, move, rig up: 12 hrs	Rig down Empress 1, move rig 6 m to 300°, rig up Empress 1A
13 July 1997	Night	Spud, ream, and case: 12 hrs	**Spud Empress 1A at 18:00 hrs 13 July 1997**, rotary drill with 159 mm, 6.25" rock roller to 26 m, ream with 215.9 mm, 8.5" rock roller to 21 m, run 177.8 mm, 7" casing to 21 m and cement (26 m)
14 July 1997	Day	Cementing: 8:30 hrs Rotary drill: 3:30 hrs	Wait on cement, rotary drill with 159 mm, 6.25" rock roller to 32 m (6 m)
14 July 1997	Night	Rotary drill: 11 hrs Bit change: 1 hrs	Rotary drill with 159 mm, 6.25" rock roller 32 to 68 m, bit change (36 m)
15 July 1997	Day	Rotary drill: 10 hrs Maintenance: 2 hrs	Rotary drill with 159 mm, 6.25" rock roller 68 to 98 m, bit change (30 m)
15 July 1997	Night	Rotary drill: 12 hrs	Rotary drill with 159 mm, 6.25" rock roller 98 to 188 m (90 m)
16 July 1997	Day	Rotary drill: 9:30 hrs Condition hole and trip: 2:30 hrs	Rotary drill with 159 mm, 6.25" rock roller 188 to 210.5 m, pull out to case (22.5 m)
16 July 1997	Night	Run casing: 5 hrs Cementing: 7 hrs	Run 5.5" PW casing and seat at 210.5 m, cement casing (0 m)
17 July 1997	Day	Cementing: 7 hrs Condition hole and trip: 2:30 hrs Trip in, drill rubber plug: 2:30 hrs Work tube: 0:30 hrs Trip: 1:30 hrs PQ core: 0:30 hrs	Wait on cement, trip in, condition hole, drill out rubber plug, work stuck tube, trip to recover tube, PQ core 210.5 to 214 m (3.5 m)
17 July 1997	Night	PQ core: 10 hrs Seating tubes: 2 hrs	PQ core 214 to 232 m, problem seating tubes due to new PF rods (18 m)

Table 1.1. (continued)

Date	*Shift*	*Time*	*Activity*
18 July 1997	Day	PQ core: 8 hrs Rotate and circulate: 1 hrs Bit change: 2 hrs Rig repairs: 1 hrs	PQ core 232 to 244 m, bit change due to rock flour blocking water ways on bit (12 m)
18 July 1997	Night	PQ core: 8:30 hrs Rotate and circulate: 1:30 hrs Bit change: 2 hrs	PQ core 244 to 259 m, bit change due to rock flour blocking water ways on bit (15 m)
19 July 1997	Day	PQ core: 9 hrs Rotate and circulate: 1 hrs Bit change: 2 hrs	PQ core 259 to 274 m, bit change (15 m)
19 July 1997	Night	PQ core: 12 hrs	PQ core 274 to 304 m (30 m)
20 July 1997	Day	PQ core: 12 hrs	PQ core 304 to 334 m (30 m)
20 July 1997	Night	PQ core: 6:30 hrs Repair rotation unit: 3 hrs Bit change: 2:30 hrs	PQ core 334 to 343 m, bit change (15 m)
21 July 1997	Day	PQ core: 12 hrs	PQ core 343 to 364 m, slow drilling due to bit balling in mudstone (21 m)
21 July 1997	Night	PQ core: 12 hrs	PQ core 364 to 385 m, slow drilling due to bit balling in mudstone (short runs; 21 m)
22 July 1997	Day	PQ core: 12 hrs	PQ core 385 to 412 m (27 m)
22 July 1997	Night	PQ core: 8:30 hrs Bit change: 3 hrs Survey: 0:30 hrs	PQ core 412 to 430 m, bit change (18 m)
23 July 1997	Day	PQ core: 10:45 hrs Condition mud: 1:15 hrs	PQ core 430 to 451 m (21 m)
23 July 1997	Night	PQ core: 6:15 hrs Bit change: 4 hrs Freeing inner tube: 1 hrs	PQ core 451 to 460 m, bit change, hole filled 6 m with sludge and 1 hr spent getting back to bottom (9 m)
24 July 1997	Day	PQ core: 11:20 hrs Circulate and flush hole: 0:40 hrs	PQ core 460 to 481 m (21 m)
24 July 1997	Night	PQ core: 7:05 hrs Bit change: 3 hrs Circulate and flush hole: 0:40 hrs Change rods: 1:15 hrs	PQ core 481 to 493 m, bit change at 483 m, change old PF rods for new ones (12 m)
25 July 1997	Day	PQ core: 12 hrs	PQ core 493 to 514 m (21 m)
25 July 1997	Night	PQ core: 12 hrs	PQ core 514 to 535 m (21 m)
26 July 1997	Day	PQ core: 12 hrs	PQ core 535 to 556 m (21 m)
26 July 1997	Night	PQ core: 7:20 hrs Circulate and flush hole: 1:10 hrs Bit change: 3:30 hrs	PQ core 556 to 568 m, bit change (12 m)
27 July 1997	Day	PQ core: 8:45 hrs Rods stuck: 3:15 hrs	PQ core 568 to 583 m, rods stuck due to shale formation, condition mud with KCl (15 m)
27 July 1997	Night	Work stuck tube: 0:45 hrs Trip: 3 hrs Wash to bottom, trip: 8:15 hrs	Trip out to retrieve tube, run in, bottom 45 m filled with sludge, wash to bottom, tube silted up, trip (0 m)
28 July 1997	Day	Trip, wash to bottom: 5:30 hrs PQ core: 6:30 hrs	Trip in, wash 45 m to bottom of hole, PQ core 583 to 590.9 m, slow drilling through shale formation (7.9 m)
28 July 1997	Night	PQ core: 3:20 hrs Rotate and circulate: 0:40 hrs Retrieve core and trip: 7:30 hrs	PQ core 590.9 to 598 m, retrieve core out of barrel due to core lifter failure, trip to remove last of core from barrel (7.1 m)
29 July 1997	Day	PQ core: 12 hrs	PQ core 598 to 610 m, slow drilling through shale formation (12 m)
29 July 1997	Night	PQ core: 12 hrs	PQ core 610 to 625 m, slow drilling through shale formation (15 m)
30 July 1997	Day	PQ core: 12 hrs	PQ core 625 to 643 m (18 m)
30 July 1997	Night	PQ core: 4:10 hrs Rotate and circulate: 0:40 hrs Run PF casing: 2:30 hrs Rotate and circulate: 0:40 hrs Pump casing-pack: 1:30 hrs	PQ core 643 to 649.8 m, condition hole, trip out, run PF casing to 649.8 m, condition hole, pump and displace casing-pack in casing annulus and seat casing (6.8 m)
31 July 1997	Day	Dig cellar, install BOP: 9 hrs Test BOP: 0:15 hrs Trip in: 1:15 hrs	Dig cellar, fit BOP to PW casing, test BOP, trip in with HMQ barrel and rods (0 m)
31 July 1997	Night	Trip in: 1 hrs Drill out plug: 1 hrs Survey: 0:30 hrs Consultation: 0:30 hrs HQ core: 9 hrs	Trip in, drill out rubber plug, HQ core 649.8 to 670 m, consult with geologist as casing-pack is leaking out of hole and onto core (20.2 m)
1 August 1997	Day	Condition mud: 3:30 hrs Mix and spot LCM: 1:15 hrs HQ core: 7:15 hrs	Condition mud due to contamination from casing-pack, spot lost circulation material at PF casing shoe, HQ core 670 to 682 m (12 m)
1 August 1997	Night	HQ core: 12 hrs	HQ core 682 to 706 m (24 m)
2 August 1997	Day	HQ core: 12 hrs	HQ core 706 to 736 m (30 m)

Table 1.1. (continued)

Date	*Shift*	*Time*	*Activity*
2 August 1997	Night	HQ core: 12 hrs	HQ core 736 to766 m (30 m)
3 August 1997	Day	HQ core: 7 hrs	HQ core 766 to 787 m, bit change at 766.4 m (21 m)
		Bit change: 4 hrs	
		Rotate and circulate: 0:30 hrs	
		Survey: 0:30 hrs	
3 August 1997	Night	HQ core: 9:30 hrs	HQ core 787 to 811 m, pull rods due to stuck tube (24 m)
		Rotate and circulate: 0:30 hrs	
		Trip out: 2 hrs	
4 August 1997	Day	Trip in: 2:15 hrs	HQ core 811 to 835 m (24 m)
		Rotate and circulate: 0:40 hrs	
		HQ core: 9:05 hrs	
4 August 1997	Night	HQ core: 6:25 hrs	HQ core 835 to 850 m, bit change (15 m)
		Bit change: 4:30 hrs	
		Freeing stuck tube: 0:35 hrs	
5 August 1997	Day	HQ core: 9:05 hrs	HQ core 850 to 874 m, pull rods (24 m)
		Bit change: 2:15 hrs	
5 August 1997	Night	Trip in: 2:15 hrs	HQ core 874 to 898 m (24 m)
		Survey: 0:30 hrs	
		HQ core: 9:15 hrs	
6 August 1997	Day	HQ core: 12 hrs	HQ core 898 to 928 m (30 m)
6 August 1997	Night	HQ core: 12 hrs	HQ core 928 to 955 m (27 m)
7 August 1997	Day	HQ core: 4:30 hrs	HQ core 955 to 967 m (12 m)
		Rotate and circulate: 0:40 hrs	
		Condition mud: 1:15 hrs	
		Survey: 0:30 hrs	
7 August 1997	Night	HQ core: 12 hrs	HQ core 967 to 991 m (24 m)
8 August 1997	Day	HQ core: 6:20 hrs	HQ core 991 to 1006 m, bit change at 995.7 m (15 m)
		Rotate and circulate: 0:40 hrs	
		Bit change: 5 hrs	
8 August 1997	Night	HQ core: 11:20 hrs	HQ core 1006 to 1036 m (24 m)
		Survey: 0:40 hrs	
9 August 1997	Day	HQ core: 9:30 hrs	HQ core 1036 to 1063 m (27 m)
		Condition mud: 1:30 hrs	
		Beam pump maintenance: 1 hrs	
9 August 1997	Night	HQ core: 5:10 hrs	HQ core 1063 to 1072 m, retrieve stuck tube at 90 m, bit change at 1069 m, make up 9 m HQ barrel and tubes, trip in (9 m)
		Retrieve stuck tube: 0:50 hrs	
		Bit change: 6 hrs	
10 August 1997	Day	HQ core: 11:20 hrs	HQ core 1072 to 1093.5 m, hard broken ground results in short runs (21.5 m)
		Survey: 0:40 hrs	
10 August 1997	Night	HQ core: 12 hrs	HQ core 1093.5 to 1117.5 m, hard broken ground results in short runs (24 m)
11 August 1997	Day	HQ core: 11:15 hrs	HQ core 1117.5 to 1150.5 m (33 m)
		Survey: 0:45 hrs	
11 August 1997	Night	HQ core: 4:55 hrs	HQ core 1150.5 to 1162.5 m, circulate and displace heavy mud, bit change (24 m)
		Circulate bottoms up: 0:40 hrs	
		Displace heavy mud: 0:35 hrs	
		Bit change at 1153 m: 5:50 hrs	
12 August 1997	Day	HQ core: 7 hrs	HQ core 1162.5 to 1180.5 m (18 m)
		Rotate and circulate: 5 hrs	
12 August 1997	Night	HQ core: 11 hrs	HQ core 1180.5 to 1210.5 m (30 m)
		Survey: 1 hrs	
13 August 1997	Day	HQ core: 12 hrs	HQ core 1210.5 to 1237.5 m (27 m)
13 August 1997	Night	HQ core: 6:30 hrs	HQ core 1237.5 to 1255.5 m, stuck tube due to sludge, clean out mud sump and settling tanks (18 m)
		Stuck tube: 2:30 hrs	
		Clean sump and tanks: 3 hrs	
14 August 1997	Day	HQ core: 11 hrs	HQ core 1255.5 to 1276.5 m, add salt to mud at request of geologist (21 m)
		Rotate and circulate: 1 hrs	
14 August 1997	Night	HQ core: 12 hrs	HQ core 1276.5 to 1303.5 m (27 m)
15 August 1997	Day	HQ core: 4:30 hrs	HQ core 1303.5 to 1315.5 m, bit change at 1306 m (12 m)
		Bit change: 5 hrs	
		Rotate and circulate: 1 hrs	
		Rig repairs and service: 1:30 hrs	
15 August 1997	Night	HQ core: 12 hrs	HQ core 1315.5 to 1345.5 m (30 m)
16 August 1997	Day	HQ core: 12 hrs	HQ core 1345.5 to 1381.5 m (27 m)
16 August 1997	Night	HQ core: 12 hrs	HQ core 1381.5 to 1417.5 m (36 m)
17 August 1997	Day	HQ core: 12 hrs	HQ core 1417.5 to 1453.5 m (36 m)
17 August 1997	Night	HQ core: 12 hrs	HQ core 1453.5 to 1486.5 m (33 m)
18 August 1997	Day	HQ core: 10:30 hrs	HQ core 1486.5 to 1513.5 m (27 m)
		Safety meeting: 0:30 hrs	
		Rig repairs: 1 hrs	
18 August 1997	Night	HQ core: 12 hrs	HQ core 1513.5 to 1543.5 m (30 m)
19 August 1997	Day	HQ core: 12 hrs	HQ core 1543.5 to 1570.5 m (27 m)
19 August 1997	Night	HQ core: 12 hrs	HQ core 1570.5 to 1582.5 m, broken ground results in short runs (12 m)
20 August 1997	Day	HQ core: 0:30 hrs	HQ core 1582.5 to 1583 m (0.5 m)
		Freeing stuck tube: 0:30 hrs	
		Standby: 8 hrs	
		Bit change: 3 hrs	

Table 1.1. (continued)

Date	*Shift*	*Time*	*Activity*
20 August 1997	Night	Complete bit change: 4 hrs HQ core: 2:30 hrs Pulling and pumping tubes: 5:30 hrs	HQ core 1583 to 1588.5 m, broken ground results in short runs (5.5 m)
21 August 1997	Day	HQ core: 5:30 hrs Freeing stuck rods: 1:45 hrs Rotate and circulate: 2 hrs Condition mud: 1:30 hrs Ream barrel to bottom: 1:15 hrs	HQ core 1588.5 to 1596.6 m, broken ground results in short runs, rods tight in hole (8.1 m)
21 August 1997	Night	HQ core: 4:25 hrs Ream: 1:20 hrs Rotate and circulate: 0:45 hrs Condition mud: 1 hrs Bit change: 4:30 hrs	HQ core 1596.6 to 1599.6 m, broken ground results in short runs, bit change at 1599.6 m (3 m)
22 August 1997	Day	Complete bit change: 3 hrs Ream back to bottom: 2:15 hrs HQ core: 4:30 hrs Freeing stuck tube: 1:15 hrs Rotate and circulate: 1 hrs	HQ core 1599.6 to 1607.4 m, broken ground results in short runs (7.8 m)
22 August 1997	Night	HQ core: 5:15 hrs Freeing stuck rods: 2:45 hrs Rotate and circulate: 1 hrs Ream through cave in: 1:20 hrs Beam pump maintenance: 1:15 hrs	HQ core 1607.4 to 1615 m, broken ground results in short runs (7.6 m)
23 August 1997	Day	HQ core: 8:25 hrs Ream back to bottom: 2:15 hrs Rotate and circulate: 1:20 hrs	HQ core 1615 to 1621.6 m, broken ground results in short runs (6.6 m)
23 August 1997	Night	HQ core: 1:45 hrs Freeing stuck rods: 1:15 hrs Standby: 1 hrs Pull rods, run in to 1580 m: 8 hrs	HQ core 1621.6 to 1624.6 m, hole coming in on rods, decision to terminate drillhole, **total depth reached about 19:45 hrs 23 August 1997** (3 m)
24 August 1997	Day	Standby: 9 hrs Pull rods to 650 m: 2:30 hrs Logging: 0:30 hrs	Waiting on wireline logger, pull HMQ rods to PF casing shoe at 650 m, logging
24 August 1997	Night	Logging: 12 hrs	Logging
25 August 1997	Day	Logging: 12 hrs	Logging
25 August 1997	Night	Logging: 0:30 hrs Trip in to 1100 m: 2:30 hrs Cementing: 4 hrs Trip out: 2:30 hrs Remove BOP: 0:45 hrs Work casing: 0:45 hrs	Logging, run HMQ to 1100 m and cement hole 1000 to 1100 m, work stuck PF casing
26 August 1997	Night	Run HMQ, cement, pull out: 6:30 hrs Pull PF casing: 2:30 hrs Logging: 3 hrs	Run HMQ to 662 m and cement hole 662 to 652 m, pull 300 m of backed off PF casing, logging
27 August 1997	Day	Logging: 3:30 hrs Work casing: 7:30 hrs Rig down: 1 hrs	Logging, work PW casing
28 August 1997	Day	Cement top of hole: 1 hrs Rig down: 4:15 hrs Packing up: 6:45 hrs	Cement, remove BOP equipment and cellar liner, **plug and abandon hole at 11:15 hrs 28 August 1997**
29 August 1997	Day	Packing up, restore sites: 12 hrs Loader to alternative site: 4:30 hrs	Restore alternative drill site 29 km to east-northeast at YWGB 1 waterbore site

Table 1.2. Hole directional surveys in Empress 1

Depth (m)	*Dip (°)*	*Azimuth (°)*
100	89	–
219	88.8	221
249	89.1	205
279	89.6	235
294.2	89.7	210
328	89.8	230
358	89.3	150
403	89.3	200
463	89.7	180
523	89.4	030
580	89.9	–

Table 1.3. Hole directional surveys in Empress 1A

Depth (m)	*Dip (°)*	*Azimuth (°)*
217	88.1	180
424	88.6	180
661	87.8	182
775	89.0	175
835	88.8	195
898	88.6	170
958	88.9	180
1 018	89.0	175
1 078	89.1	189
1 138.5	88.9	181
1 207.5	89.0	195

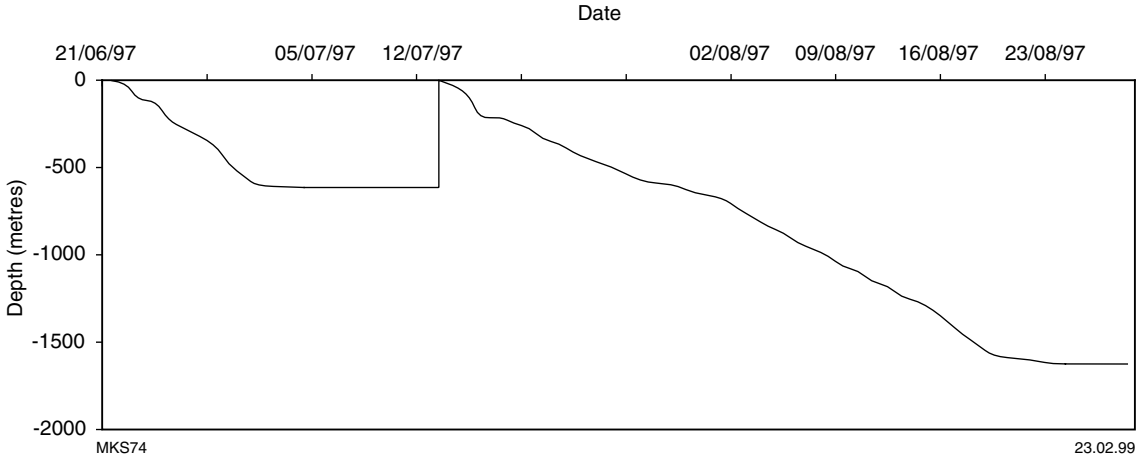

Figure 1.2. Time versus depth curve for Empress 1 and 1A

Table 1.4. Drilling date and depth, Empress 1 and 1A

Date	*Time*	*Depth (m)*
21 Jun 1997	1800	0
22 Jun 1997	0600	-16
22 Jun 1997	1800	-24
23 Jun 1997	0600	-66
23 Jun 1997	1800	-105
24 Jun 1997	0600	-117
24 Jun 1997	1800	-129
25 Jun 1997	0600	-201
25 Jun 1997	1800	-225
26 Jun 1997	0600	-252
26 Jun 1997	1800	-279
27 Jun 1997	0600	-294.2
27 Jun 1997	1800	-294.2
28 Jun 1997	0600	-342
28 Jun 1997	1800	-375
29 Jun 1997	0600	-451
29 Jun 1997	1800	-481
30 Jun 1997	0600	-526
30 Jun 1997	1800	-550
1 Jul 1997	0600	-580
1 Jul 1997	1800	-598
2 Jul 1997	0600	-604.3
2 Jul 1997	1800	-604.3
3 Jul 1997	0600	-607.9
3 Jul 1997	1800	-608.4
4 Jul 1997	0600	-608.9
4 Jul 1997	1800	-615
5 Jul 1997	0600	-615
5 Jul 1997	1800	-615
6 Jul 1997	0600	-615
6 Jul 1997	1800	-615
7 Jul 1997	0600	-615
7 Jul 1997	1800	-615
8 Jul 1997	0600	-615
8 Jul 1997	1800	-615
9 Jul 1997	0600	-615
9 Jul 1997	1800	-615
10 Jul 1997	0600	-615
10 Jul 1997	1800	-615
11 Jul 1997	0600	-615
11 Jul 1997	1800	-615
12 Jul 1997	0600	-615
12 Jul 1997	1800	-615
13 Jul 1997	0600	-615
13 Jul 1997	1800	0
14 Jul 1997	0600	-26
14 Jul 1997	1800	-32
15 Jul 1997	0600	-68
15 Jul 1997	1800	-98
16 Jul 1997	0600	-188
16 Jul 1997	1800	-210.5
17 Jul 1997	0600	-210.5
17 Jul 1997	1800	-214
18 Jul 1997	0600	-232
18 Jul 1997	1800	-244
19 Jul 1997	0600	-259
19 Jul 1997	1800	-274
20 Jul 1997	0600	-304
20 Jul 1997	1800	-334
21 Jul 1997	0600	-343
21 Jul 1997	1800	-364
22 Jul 1997	0600	-385
22 Jul 1997	1800	-412
23 Jul 1997	0600	-430
23 Jul 1997	1800	-451
24 Jul 1997	0600	-460
24 Jul 1997	1800	-481
25 Jul 1997	0600	-493
25 Jul 1997	1800	-514
26 Jul 1997	0600	-535
26 Jul 1997	1800	-556
27 Jul 1997	0600	-568
27 Jul 1997	1800	-583
28 Jul 1997	0600	-583
28 Jul 1997	1800	-590.9
29 Jul 1997	0600	-598
29 Jul 1997	1800	-610
30 Jul 1997	0600	-625
30 Jul 1997	1800	-643
31 Jul 1997	0600	-649.8
31 Jul 1997	1800	-649.8
1 Aug 1997	0600	-670
1 Aug 1997	1800	-682
2 Aug 1997	0600	-706
2 Aug 1997	1800	-736
3 Aug 1997	0600	-766
3 Aug 1997	1800	-787
4 Aug 1997	0600	-811
4 Aug 1997	1800	-835
5 Aug 1997	0600	-850
5 Aug 1997	1800	-874
6 Aug 1997	0600	-898
6 Aug 1997	1800	-928
7 Aug 1997	0600	-955
7 Aug 1997	1800	-967
8 Aug 1997	0600	-991
8 Aug 1997	1800	-1 006
9 Aug 1997	0600	-1 036
9 Aug 1997	1800	-1 063
10 Aug 1997	0600	-1 072
10 Aug 1997	1800	-1 093.5
11 Aug 1997	0600	-1 117.5
11 Aug 1997	1800	-1 150.5
12 Aug 1997	0600	-1 162.5
12 Aug 1997	1800	-1 180.5
13 Aug 1997	0600	-1 210.5
13 Aug 1997	1800	-1 237.5
14 Aug 1997	0600	-1 255.5
14 Aug 1997	1800	-1 267.5
15 Aug 1997	0600	-1 303.5
15 Aug 1997	1800	-1 315.5
16 Aug 1997	0600	-1 345.5
16 Aug 1997	1800	-1 381.5
17 Aug 1997	0600	-1 417.5
17 Aug 1997	1800	-1 453.5
18 Aug 1997	0600	-1 486.5
18 Aug 1997	1800	-1 513.5
19 Aug 1997	0600	-1 543.5
19 Aug 1997	1800	-1 570.5
20 Aug 1997	0600	-1 582.5
20 Aug 1997	1800	-1 583
21 Aug 1997	0600	-1 588.5
21 Aug 1997	1800	-1 596.6
22 Aug 1997	0600	-1 599.6
22 Aug 1997	1800	-1 607.4
23 Aug 1997	0600	-1 615
23 Aug 1997	1800	-1 621.6
24 Aug 1997	0600	-1 624.6
24 Aug 1997	1800	-1 624.6
25 Aug 1997	0600	-1 624.6
25 Aug 1997	1800	-1 624.6
26 Aug 1997	0600	-1 624.6
26 Aug 1997	1800	-1 624.6
27 Aug 1997	0600	-1 624.6
27 Aug 1997	1800	-1 624.6
28 Aug 1997	0600	-1 624.6
28 Aug 1997	1800	-1 624.6

Chemicals consumed

Empress 1

Aqua Pac, 15 kg	:	97
Aus Thin, 25 kg	:	5
Aus Det, 25 L	:	3
Bentonite, 25 kg	:	20
Cement, 40 kg	:	40
Cement, 25 kg	:	6
Teepol, 20 L	:	1
Thinners, 25 kg	:	2
KCl, 25 kg	:	225
Caustic soda, 25 kg	:	6
Aqua Gel, 25 kg	:	13

Empress 1A

Aqua Pac, 15 kg	:	101
Aqua Pac, 25 kg	:	11
Aus Thin, 25 kg	:	23
Aus Det, 25 L	:	151
Casing pack, 200 L	:	4
Cement, 40 kg	:	65
Flossy salt, 25 kg	:	804
Aus Gel, 25 kg	:	70
Barytes, 25 kg	:	8
KCl, 25 kg	:	918
Caustic soda, 25 kg	:	12
Aqua Gel, 25 kg	:	26
Aus Pac, 25 kg	:	4
Truck wash, 5 L	:	4
Hy Seal, bag	:	1
Aus Thin, 15 kg	:	8
Diesel, L	:	370

Note: diesel used only in trying to recover casing after TD was reached.

Drilling problems

Numerous problems were experienced in these drillholes. In approximate order of occurrence these include:

Empress 1

- 7" casing hanging up at 11.5 m.
- 5.5" PW casing hung up at 24 m and had to be reamed down to 105 m.
- Stuck tubes during PQ coring required pulling rods to recover core.
- Leakage of BOP bladder after installation.
- Excess sludge in mud below 500 m resulted in high torque and rod lock-up, requiring flushing of sumps and addition of KCl to mud.
- The HMQ drillstring parted at the tool joint at 362.7 m while drilling at 604.3 m, this was successfully fished.
- Poor condition of hole after fishing resulted in a trip to ream the hole below 470 m with a 3.875" rock roller.
- The HMQ drillstring parted at 374 m while drilling at 615 m. The fish was not completely recovered after numerous attempts, and after establishing that the cemented PF casing string could not be moved, it was decided to abandon the drillhole.
- It is suspected the ?Lupton Formation at about 370 m had washed out when the rods first failed, resulting in rod whip and eventual rod failure. Large amounts of sand were produced from the drillhole during the fishing operations. Unconsolidated sands and large core loss zones occur at about 340 and 390 m.
- After several attempts to recover as much of the HMQ drillstring as possible, all the drillstring above 494 m was recovered.
- Eight attempts to cut and recover the PF casing were made until the section above 129 m was recovered.

Empress 1A

- Rock flour blocked PQ bit waterways between 232 and 259 m (Table Hill Volcanics).
- PQ bit balling in mudstone reduced drilling rate between 342 and 385 m.
- Large volume of fines in the mud system resulted in the hole sludging up and stuck tubes from 451 to 493 m.
- Stuck rods resulting from shale swelling treated by adding KCl to mud.
- Large volume of fines in the mud system resulted in the hole sludging up and stuck tubes from 583 to 591 m.

- Core lifter failure at 591 m.
- Casing pack leaks into mud system from behind PF casing which is seated at 649.8 m, spot lost circulation material at PF casing shoe.
- Stuck tubes while drilling between 787 and 850 m.
- Large volume of fines in mud system results in hole sludging up below 1036 m and a stuck tube.
- Hard and broken formation results in short coring runs from 1072 to 1117 m.
- Large volume of fines in mud system results in hole sludging up below 1237 m, cleaned out sump and tanks.
- Salt was added to mud system below 1255 m to core halite beds (Browne Formation).
- Hard and broken formation results in short coring runs from about 1570 m to TD of 1624.6 m (pre-Officer Basin volcanic rocks).
- Unstable hole below about 1588 m results in stuck rods and having to ream through cavings at bottom on several occasions, leading to a decision to terminate well because of poor drilling conditions.
- Wireline logger unable to get tool below obstruction at 1583 m.
- Uncemented PF casing string could not be recovered and casing cuts at 450, 400, and 350 m did not free casing.
- PF casing backed off and 300 m retrieved.

Core loss zones

Significant zones of core loss (commonly greater than 0.2 m) are in Table 1.5. The top of the core-loss zone (in metres) is listed first and is assumed to be from the base of the core run unless there was evidence to the contrary. The estimated core loss (in metres) follows the top core-loss zone depth. The asterisk at 349.0 m in Empress 1A is to indicate that the 0.7 m is core excess to that drilled.

Table 1.5. Core loss zones

Empress 1		*Empress 1A*	
Core loss zone (m)	*Estimated core loss (m)*	*Core loss zone (m)*	*Estimated core loss (m)*
117.8	0.2	219.8	0.2
118.9	1.1	222.5	0.3
122.4	0.6	291.6	0.2
125.8	0.2	324.7	0.2
134.6	0.4	339.5	0.4
137.7	0.3	341.3	1.3
149.6	0.4	349.0	0.7*
178.4	0.6	396.3	0.2
182.7	0.3	411.6	0.2
185.6	0.2	473.1	1.9
197.7	0.3	482.7	0.3
199.6	1.4	545.8	0.7
285.3	0.8	547.9	0.5
297.5	0.5	549.0	1.0
327.5	0.5	552.1	0.9
335.0	5.0	557.9	1.1
388.6	1.4	560.9	1.1
394.3	2.7	563.9	1.0
402.5	0.5		
474.5	0.5		
479.7	1.3		
481.55	0.55		
543.4	1.6		
548.1	3.9		
581.5	0.2		

Depth matching of core to logs

Five tie points were established between the core and wireline logs and a line of best fit was calculated using the equation:

$$\text{Logger's depth (m)} = \text{driller's depth (m)} + (0.0016 \times \text{driller's depth (m)} + 0.3237).$$

No depth corrections were applied to the lithological column in Plate 1 above 210.5 m as the majority of the descriptions are from the unlogged Empress 1. The depth shift to convert driller's depth to loggers depth below 210.5 m in Plate 1, was always positive and can be approximated by the driller's depth (m) and depth increment (m) (Table 1.6).

Table 1.6. Depth matching of core to logs

Drillers depth (m)	*Increment (m)*
210	0.7
270	0.8
320	0.9
380	1.0
450	1.1
520	1.2
580	1.3
640	1.4
700	1.5
760	1.6
830	1.7
880	1.8
950	1.9
1 020	2.0
1 070	2.1
1 130	2.2
1 200	2.3
1 260	2.4
1 320	2.5
1 380	2.6
1 450	2.7
1 510	2.8
1 570	2.9

Appendix 2
K–Ar dating of two basalts
(by Amdel Limited)

Introduction

Two samples of basalt from drillcores were received from D. R. Nelson, Geological Survey of Western Australia (GSWA), with a request to carry out total rock K–Ar age determinations. These samples (GSWA sample 153903 and 153904) have been examined previously (Amdel Report G708000G/97) and were considered to be of suitable quality for dating.

Procedures

The samples were crushed and screened to produce fractions in the size range -0.710 to +0.420 mm. This material was used for radiogenic-argon analysis by isotope-dilution mass spectrometry. Representative portions of the –0.710 to +0.420 mm fractions were pulverized and used for determination of K in duplicate by AAS.

Results

The K and Ar analyses and calculated K–Ar ages are listed in Table 2.1. In the absence of evidence for thermal metamorphism of the samples, the results are interpreted as indicators of the minimum age of crystallization of the basalts.

Table 2.1. Potassium–argon analyses

Sample	*Unit*	*%K[(a)]*	*$^{40}Ar^{(b)}$ ($\times 10^{-10}$ moles/g)*	*$^{40}Ar^{(b)}/^{40}Ar_{Total}$*	*Age[(c)] (Ma)*
GSWA 153903 Total Rock	pre-Officer Basin sequence	1.29 1.29	32.268	0.978	1058 ± 13
GSWA 153904 Total Rock	Table Hill Volcanics	0.634 0.635	6.1165	0.956	484 ± 4

NOTES: (a) The mean K value is used in the age calculation
(b) Denotes radiogenic ^{40}Ar
(c) Age in Ma with error limits given for the analytical uncertainty at one standard deviation

Constants ^{40}K 0.01167 atom %
λ_B $4.962 \times 10^{-10}y^{-1}$
λ_ε $0.581 \times 10^{-10}y^{-1}$

Appendix 3
Gravity modelling
(by S. Shevchenko)

To assist in locating Empress 1, the gravity response was modelled along section from Westwood 1 in the southeast, to seismic line T81-07/EXT in the northwest. Prior to this modelling, a qualitative interpretation using gravity and magnetic images was conducted. The Bouguer gravity field was compared to the limited seismic control in the centre of the Yowalga Sub-basin. The stratigraphy, as interpreted from seismic lines tied to Yowalga 3 and Kanpa 1A, was extrapolated to Westwood 1 using gravity (to constrain its thickness) and a geological model (to constrain the style of sedimentary thinning onto the basin margin). The first vertical derivative of the gravity was used to locate the wellsite away from possible faults (Fig. 3.1).

Data from the Lennis and Breaden semi-detailed gravity surveys were modelled. The densities from Kanpa 1A and Yowalga 3 well logs were used to define a four-layer density model (Table 3.1).

Table 3.1. Four-layer density model

Layer	*Top*	*Base*	*Density (g/cm^3)*
1	Surface	Base ?Lupton Formation	2.3
2	Base ?Lupton Formation	Top Browne Formation	2.5
3	Top Browne Formation	Base Browne Formation	2.4
4	Mesoproterozoic	–	2.6

An initial gravity model was compared with the interpretation of seismic line T81-7/EXT SP5135. This produced the regional gravity curve over the area of seismic interpretation. In this case, the regional curve depicts the geology below the Browne Formation and allows for the extrapolation of the regional curve to the southwest part of the model. The final gravity model is displayed in Figure 3.2. An important inference from this model is that the Browne Formation pinches out at the Westwood 1 wellsite.

It was recommended that the Empress 1 wellsite be located between the seismic lines to the northeast, where the Browne Formation is too deep to be fully penetrated in a 2000 m drillhole, and Westwood 1, where there is a risk that the Browne Formation is absent. The gravity model predicted that the Top Browne Formation would be 800 m below the surface, and the base Browne Formation 1200 m below the surface at the projected well location.

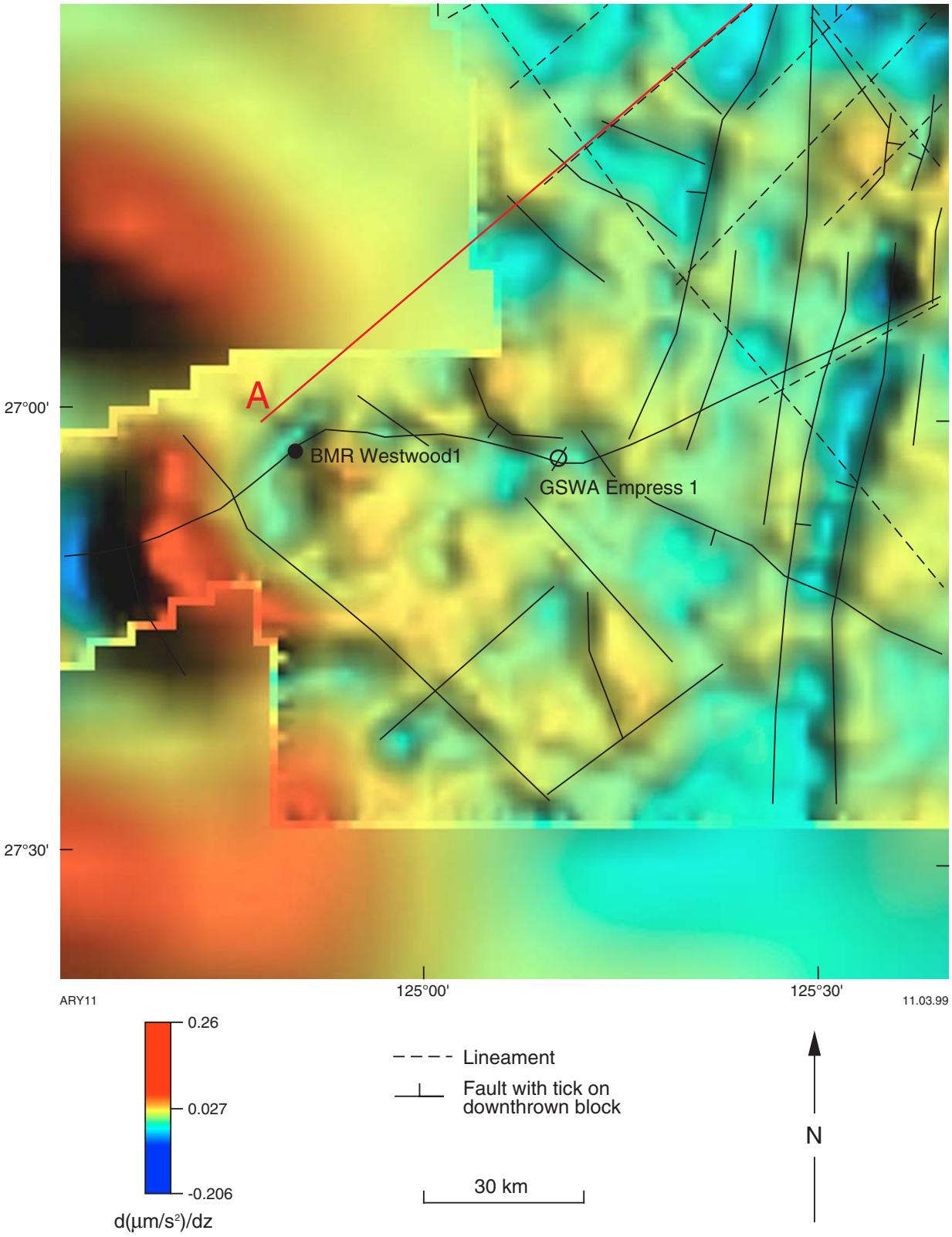

Figure 3.1. First vertical derivative gravity with structures

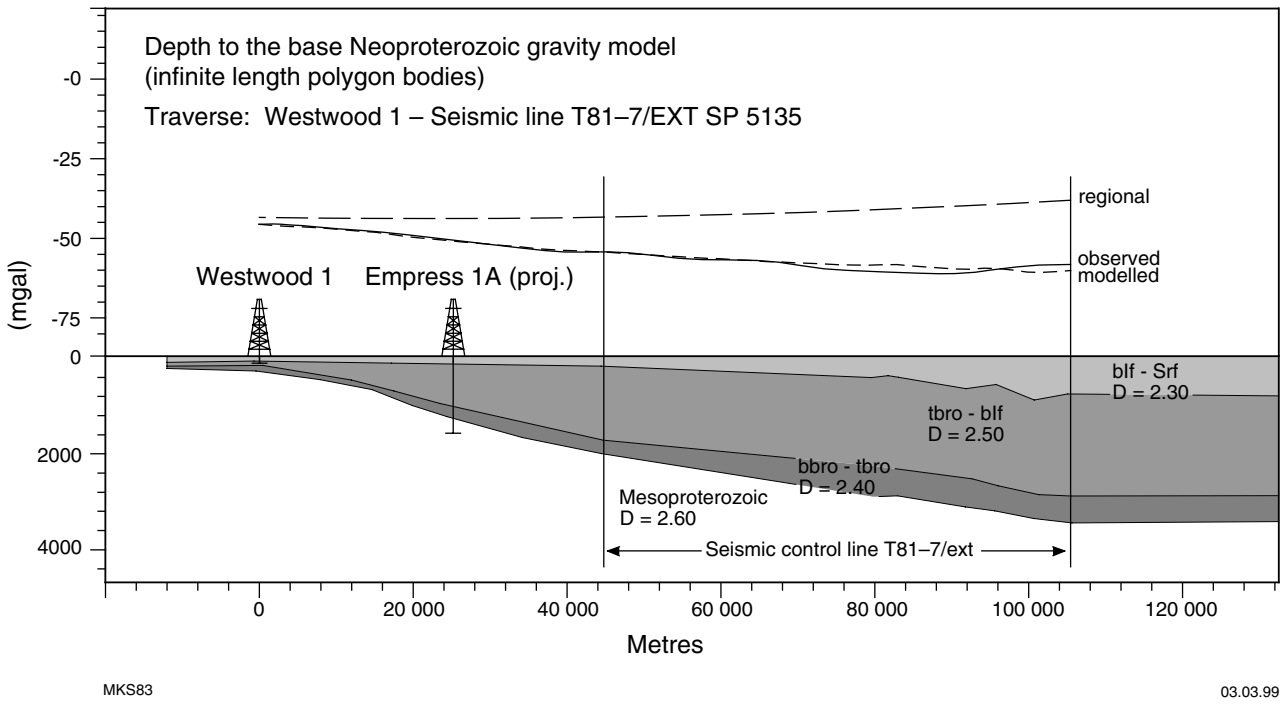

Figure 3.2. Depth to the base Neoproterozoic gravity model

Appendix 4
Petrography of eleven rocks from Empress 1A
(by Amdel Limited)

Eleven rock samples were submitted by the Geological Survey of Western Australia to Amdel Limited for petrographic description and assessment of their suitability for K–Ar dating. This appendix outlines the petrography and the suitability of samples for K–Ar dating.

A thin section was made of each sample and examined by transmitted light microscopy. The thin sections were stained with an alizarin red S solution to distinguish calcite from other carbonates by staining it pink. In the thin-section descriptions, calcite is used only for stained carbonates; any unstained carbonate has been termed carbonate. The offcut chips from the thin-section preparation were stained with sodium cobaltinitrite after a hydrofluoric acid etch to aid in the detection and location of K-feldspar.

Petrographic descriptions

The individual petrographic descriptions are as follows.

GSWA sample : 154111
Location : Empress 1A, 215.8 m
Rock name : Basalt
Thin section : TS C69664

An optical estimate of the constituents is in Table 4.1.

Table 4.1. Optical estimate of constituents in GSWA sample 154111

Mineral	*Percentage*	*Origin*
Plagioclase	45	Igneous
Augite	30	Igneous
Chlorite/clay	15	Alteration
Amphibole	3	Alteration
Sericite/clay	1	Alteration
Opaque and semi-opaque minerals	6	Igneous/alteration

This sample consists of plagioclase laths, ranging up to 0.3 mm in diameter, intergrown with augite crystals commonly 0.1 – 0.4 mm in diameter. The augite crystals have anhedral shapes and some show skeletal shapes containing intergrowths of plagioclase.

The major alteration product in this sample is an interstitial, pale-green phyllosilicate that forms irregular patches up to 0.3 mm in diameter, some of which have irregular shapes and could be vesicles. The plagioclase shows incipient alteration to finely divided sericite. The augite shows some alteration to a fibrous, pale-green amphibole.

Opaque minerals are disseminated through the rock as anhedral grains less than 0.1 mm in diameter. The rock also contains translucent, reddish-brown limonitic material as fine intergrowths with some interstitial fillings.

Overall, this rock is quite fresh and a suitable mineral concentrate of either plagioclase or augite could be made for potassium–argon dating.

GSWA sample : 154110
Location : Empress 1A, 234.5 m
Rock name : Basalt
Thin section : TS C69665

An optical estimate of the constituents is in Table 4.2.

Table 4.2. Optical estimate of constituents in GSWA sample 154110

Mineral	*Percentage*	*Origin*
Augite	25	Igneous
Sericite/clay	25	Alteration
Plagioclase	20	Igneous
Chlorite/clay	15	Alteration
Amphibole	5	Alteration
K-feldspar	5	?Alteration
Opaque and semi-opaque minerals	5	Igneous/alteration

This sample consists of altered plagioclase laths, ranging up to 0.4 mm in diameter, intergrown with an interstitial to intergranular augite, which forms anhedral crystals ranging up to 0.5 mm in diameter. The plagioclase shows pervasive alteration to finely divided sericite/clay. The augite shows some alteration to a fibrous, pale-green amphibole. The augite also locally shows some reddish-brown iron staining.

A green clay mineral, termed chlorite/clay in the above list of minerals, forms irregular patches ranging up to 0.5 mm in diameter, which have vague vesicular to interstitial characters. The interstitial chlorite/clay locally contains intergrowths of K-feldspar. K-feldspar also forms interstitial intergrowths between the altered plagioclase crystals. The K-feldspar was detected by staining the hand specimen, and is commonly difficult to distinguish in thin section.

Opaque minerals are disseminated through the rock as anhedral grains ranging up to 0.2 mm in diameter. The rock also contains some translucent, reddish-brown limonitic material.

This rock shows moderate to pervasive sericitization of plagioclase, along with the development of uralitic amphibole after pyroxene. Much of the pyroxene is relatively fresh, and it may be possible to produce a pyroxene concentrate for potassium–argon dating.

GSWA sample : 154108
Location : Empress 1A, 666.8 m
Rock name : Sandstone
Thin section : TS C69666

An optical estimate of the constituents is in Table 4.3.

Table 4.3. Optical estimate of constituents in GSWA sample 154108

Mineral	*Percentage*	*Origin*
Clay	45	Sedimentary
Quartz	20	Detrital
Carbonate	15	Authigenic/?detrital
Feldspar	15	Detrital
Muscovite	Tr–1	Detrital
Tourmaline	Tr	Detrital
Zircon	Tr	Detrital
Opaque minerals	5	Detrital

This sedimentary rock is composed of detrital particles with a typical grain size between 0.1 and 0.2 mm in an interstitial clay matrix. The detrital particles consist of quartz and feldspar grains as well as a significant proportion of clay pellets. The clay pellets commonly have a very weak birefringence and some are very pale green and could be glauconitic. The detrital quartz and feldspar grains typically show subangular shapes. The feldspar consists of both K-feldspar and polysynthetically twinned plagioclase.

The rock has a banded character produced mainly by the tendency for finely granular carbonate to form as interstitial fillings within bands up to about 1 mm wide. Minor carbonate also forms fine intergrowths with the interstitial matrix or occurs as finely granular bodies up to 0.2 mm in size, which could be detrital carbonate grains. The carbonate is unaffected by the alizarin red S stain and has relatively high relief suggesting that it is siderite.

Opaque minerals form disseminated grains ranging up to 0.3 mm in diameter, which tend to be concentrated in discontinuous bands up to about 0.5 mm wide. Traces of tourmaline and zircon form detrital grains up to 0.1 mm in diameter. Muscovite forms flakes up to 0.2 mm in length and are thought to be detrital.

This is a detrital sedimentary rock with a relatively fine grain size. It is considered unlikely to be suitable for potassium–argon dating.

GSWA sample : 154100
Location : Empress 1A, 1525.2 m
Rock name : Altered basalt
Thin section : TS C69667

An optical estimate of the constituents is in Table 4.4.

Table 4.4. Optical estimate of the constituents in GSWA sample 154100

Mineral	*Percentage*	*Origin*
Plagioclase	35	Igneous
Chlorite	25	Alteration
Quartz	15	Alteration/?igneous
Saussurite	7	Alteration
Carbonate	5	Alteration
Amphibole	3	Alteration
Opaque and semi-opaque minerals	10	Alteration/igneous

This sample consists of plagioclase laths, ranging up to 1.5 mm in diameter, intergrown with interstitial felsic material, including plagioclase and quartz and highly altered mafic minerals. The plagioclase laths have a turbid character due to saussuritization or alteration to a finely granular turbid epidote and possible minor sericite. The original mafic minerals have been completely replaced by a pale-green, weakly pleochroic chlorite with anomalous blue interference colours and minor amounts of a weakly pleochroic green amphibole. The amphibole is probably a late-stage, deuteric alteration product and the remnant pyroxene has subsequently been altered to chlorite. The interstitial felsic minerals include minor quartz but consist mainly of feldspar, which is thought to be plagioclase.

The rock is transected by veins, up to about 1 cm wide, composed of bands containing varying proportions of quartz, carbonate, and opaque to translucent, reddish-brown limonitic material. The quartz includes granular, vein-type quartz and a fibrous chalcedony. Much of the chalcedony is translucent and reddish-brown due to very finely intergrown iron oxides. The carbonate forms a coarsely granular mosaic and is commonly unaffected by the alizarin red S stain; therefore, it is most likely to be dolomite. The opaque to translucent, reddish-brown limonite forms irregular bands within the veins, as well as localized fine intergrowths with quartz.

Opaque minerals are disseminated through the host rock as anhedral to subhedral grains ranging up to 0.5 mm in length, although most of the opaque minerals have a grain size less than 0.2 mm. Opaque to translucent, reddish-brown limonitic material also forms fine intergrowths with the host rock, particularly the interstitial felsic material. Minor translucent, reddish-brown limonite also forms discontinuous vein fillings less than 0.05 mm wide, which transect the basaltic rock.

This is a relatively coarse grained basalt showing moderate alteration of plagioclase to epidote, and pervasive alteration of original mafic minerals to chlorite. The rock is transected by veins filled with quartz/chalcedony, carbonate (probably dolomite), and limonitic material. This rock is too highly altered to be suitable for radiometric dating.

GSWA sample : 154107
Location : Empress 1A, 1539.4 m
Rock name : Sericitic sandstone
Thin section : TS C69668

An optical estimate of the constituents is in Table 4.5.

Table 4.5. Optical estimate of the constituents in GSWA sample 154107

Mineral	*Percentage*	*Origin*
Sericite/clay	60	Sedimentary
Quartz	20	Detrital
Muscovite	10	Detrital
Biotite	5	Detrital
Feldspar	2	Detrital
Tourmaline	Tr	Detrital
Zircon	Tr	Detrital
Opaque and semi-opaque minerals	3	Detrital/alteration

This sample consists of detrital quartz grains, less than 0.1 mm in diameter, and mica flakes, up to 0.2 mm in length, distributed through an argillaceous matrix composed of very finely divided sericite intergrown with a weakly birefringent clay. The mica flakes show a very well developed, preferred orientation defining the foliation. The mica flakes consist mainly of muscovite, but include a small amount of biotite. The biotite typically has a reddish-brown, pleochroic colour and can tend to have a somewhat degraded character. Some biotite has been partially replaced by limonitic iron oxides, producing a translucent, reddish-brown colour.

The detrital quartz grains have angular to subangular shapes. In addition to the quartz, the rock contains a small amount of feldspar as angular detrital grains up to 0.1 mm in size. Traces of tourmaline and zircon were also noted as detrital grains less than 0.1 mm in size.

Opaque minerals are disseminated through the rock as anhedral to subhedral crystals 0.2 – 0.3 mm in diameter. The rock also contains irregular patches of translucent, reddish-brown limonitic material which, in some cases, occurs marginal to opaque grains.

This is a detrital sedimentary rock and is considered unsuitable for radiometric dating, particularly due to the probable presence of detrital mica.

GSWA sample : 154106
Location : Empress 1A, 1542.5 m
Rock name : Fine-grained sandstone
Thin section : TS C69669

An optical estimate of the constituents is in Table 4.6.

Table 4.6. Optical estimate of constituents in GSWA sample 154106

Mineral	*Percentage*	*Origin*
Chert and lithic clasts	45	Detrital
Quartz	25	Detrital
Sericite/clay	18	Authigenic
Chlorite	5	Authigenic
Feldspar	2	Detrital
Muscovite	Tr–1	Detrital
Tourmaline	Tr	Detrital
Zircon	Tr	Detrital
Opaque and semi-opaque minerals	5	Detrital/authigenic

This is a fine-grained, detrital sedimentary rock composed of lithic and chert clasts less than 0.8 mm in diameter and detrital quartz grains. The lithic and chert clasts contain moderate amounts of finely intergrown sericite/clay. Some sericite/clay also forms pellets ranging up to 0.1 mm in diameter. The detrital quartz grains show angular to subangular shapes that, at least locally, appear to have been modified by recrystallization.

Minor feldspar composed mainly of polysynthetically twinned plagioclase is also present as angular, detrital grains up to 0.1 mm in diameter. A small number of muscovite flakes, up to 0.15 mm long, are disseminated through the rock and are probably of detrital origin. Traces of tourmaline and zircon form detrital grains less than 0.1 mm in size.

Chlorite forms pale-green, flaky aggregates which tend to form interstitially between the detrital grains. Opaque minerals are disseminated through the rock as anhedral grains less than 0.1 mm in size. The rock also contains translucent, reddish-brown limonitic material as disseminated grains and aggregates.

This sedimentary rock contains lithic and chert clasts as well as detrital quartz grains. The rock is considered unsuitable for potassium–argon dating.

GSWA sample : 154105
Location : Empress 1A, 1552.5 m
Rock name : Silty shale
Thin section : TS C69670

An optical estimate of the constituents is in Table 4.7.

Table 4.7. Optical estimate of constituents in GSWA sample 154105

Mineral	*Percentage*	*Origin*
Clay/sericite	70	Detrital/authigenic
Quartz	20	Detrital
Muscovite	3	Detrital
Chlorite	2	Authigenic
Biotite	1	Detrital
Calcite	1	Veining
Tourmaline	Tr	Detrital
Opaque minerals	3	Authigenic

This sample consists mainly of clay minerals, including weakly birefringent clay and fibrous sericite, which form a matrix comprising disseminated detrital quartz grains commonly less than 0.05 mm in size. The sericite, in particular, shows a weakly developed, preferred orientation which produces a fine, fissile foliation in hand specimen. The rock also contains some disseminated larger muscovite and biotite flakes that are most likely to be of detrital

origin, although some could be due to recrystallization of clay minerals. Some of the biotite flakes have fibrous, degraded-appearing characters.

The rock is transected by narrow calcite veins that are associated with euhedral opaque crystals, which could be pyrite. Opaque minerals are also disseminated through the host rock as euhedral to subhedral crystals, as well as anhedral grains and granular aggregates.

Although quartz is the major detrital component, it is possible that minor feldspar could also be present. Traces of tourmaline form disseminated grains commonly less than 0.05 mm across.

This is a very fine grained, detrital sedimentary rock composed mainly of clay minerals and silt-sized, quartz-rich detritus. The sample shows mild calcite veining and is thought to contain authigenic pyrite. The rock is considered unsuitable for radiometric dating.

GSWA sample : 154104
Location : Empress 1A, 1589.2 m
Rock name : Basalt
Thin section : TS C69671

An optical estimate of the constituents is in Table 4.8.

Table 4.8. Optical estimate of constituents in GSWA sample 154104

Mineral	*Percentage*	*Origin*
Plagioclase	40	Igneous
Pyroxene	30	Igneous
Sericite/clay	10	Alteration
Amphibole	5	Alteration
Quartz	5	Igneous
Biotite	3	Igneous
Chlorite	1	Veining
K-feldspar	Tr–1	Veining
Opaque minerals	5	Igneous

This sample consists of plagioclase laths intergrown with intergranular pyroxene and has a typical grain size less than 0.2 mm. Minor quartz is also disseminated through the rock as interstitial intergrowths between the plagioclase laths. The plagioclase shows alteration to finely divided sericite/clay, which is generally very minor although within some areas, the plagioclase shows moderate to pervasive replacement by finely divided sericite/clay. The pyroxene tends to have a turbid, degraded character and shows some marginal replacement by a bluish-green, weakly pleochroic amphibole, which is probably a deuteric alteration product of pyroxene. As with the plagioclase alteration, the pyroxene also shows varying degrees of alteration within different areas.

Biotite is disseminated through the rock as pleochroic, brown flakes that are located interstitially between the plagioclase laths. Opaque minerals are disseminated through the rock as anhedral to subhedral crystals less than 0.4 mm across.

The rock is transected by some narrow veins which are filled with a green, moderately birefringent phyllosilicate, termed chlorite in the above list of minerals. Some of these veins contain intergrowths of K-feldspar.

This is a fine-grained, basaltic rock showing varying degrees of alteration with some areas having a moderately altered character and other areas being quite fresh. The sample is considered only marginally suitable for whole rock potassium–argon dating.

GSWA sample : 154103
Location : Empress 1A, 1602.0 m
Rock name : Basalt
Thin section : TS C69672

An optical estimate of the constituents is in Table 4.9.

Table 4.9. Optical estimate of constituents in GSWA sample 154103

Mineral	*Percentage*	*Origin*
Plagioclase	55	Igneous
Pyroxene	35	Igneous
K-feldspar	3	Igneous
Sericite/clay	1	Alteration
Amphibole	1	Alteration
Biotite	1	Alteration
Quartz	Tr	Igneous
Chlorite	Tr	Alteration
Opaque minerals	4	Igneous

This sample consists of randomly oriented plagioclase laths, generally less than 0.2 mm in length, intergrown with granular pyroxene. The pyroxene consists mainly of augite, but includes smaller amounts of hypersthene. The thin section shows some variation in grain size, containing some coarser grained areas with a maximum grain size of 0.4 mm. Some slightly larger plagioclase phenocrysts, up to 1 mm in length, are also disseminated through the finer grained portion of the rock. Small amounts of K-feldspar and traces of quartz form interstitially between the plagioclase laths.

Overall, the rock is very fresh although the plagioclase locally shows mild alteration to finely divided sericite/clay. The pyroxene contains minor amounts of a pale-green amphibole and a pleochroic, brown biotite as marginal intergrowths, which probably represent a deuteric alteration product of pyroxene. Traces of a green phyllosilicate, termed chlorite in the above list of minerals, are also present as interstitial intergrowths less than 0.2 mm across.

Opaque minerals are disseminated through the rock as anhedral to subhedral crystals up to 1 mm across, and tend to have irregular, embayed shapes.

This is a very fresh basaltic rock showing slight variations in the degree of alteration but typically has an unaltered character. This rock is considered suitable for whole rock potassium–argon dating.

GSWA sample : 154102
Location : Empress 1A, 1602.2 m
Rock name : Basalt
Thin section : TS C69673

An optical estimate of the constituents is in Table 4.10.

Table 4.10. Optical estimate of constituents in GSWA sample 154102

Mineral	*Percentage*	*Origin*
Plagioclase	45	Igneous
Pyroxene	30	Igneous
Sericite/clay	7	Alteration
Amphibole	5	Alteration
Biotite	3	Alteration
Quartz	3	Igneous
K-feldspar	1	Igneous
Chlorite	1	Alteration
Carbonate	Tr	Alteration
Opaque minerals	5	Igneous

This sample consists of randomly oriented plagioclase laths intergrown with granular pyroxene. Small amounts of interstitial quartz formed between the plagioclase laths and minor interstitial K-feldspar is locally present. Most of the sample has a relatively fine grain size containing plagioclase laths less than 0.2 mm in length, but some coarser grained patches containing plagioclase laths up to 0.6 mm long are present. A small number of large plagioclase phenocrysts, ranging up to 2 mm in size, are disseminated through the rock.

The rock shows a great variation in the degree of alteration, even within the area of the thin section. Most of the rock shows moderate alteration, although some areas have a higher degree of alteration and at least one area shows very little alteration. The alteration consists of the replacement of plagioclase by finely divided sericite/clay and the marginal alteration of pyroxene to a green amphibole and a pleochroic, brown biotite. Traces of carbonate are intergrown with the altered plagioclase. Minor chlorite forms patches up to 0.2 mm across composed of finely divided, pale-green flakes.

Opaque minerals are disseminated through the rock as anhedral crystals ranging up to 1 mm in size, and tend to have irregular and somewhat embayed to poikilitic shapes due to fine intergrowths of plagioclase.

This is a basaltic rock generally showing moderate alteration to finely divided sericite/clay as well as amphibole and biotite. The rock is considered only marginally suitable for radiometric dating. It is worth noting that this sample, and some of the other samples, show great variations in the degree of alteration over relatively small areas. It is possible that the thin section from the one rock would not be characteristic of the degree of alteration from a much larger sample.

GSWA sample : 154101
Location : Empress 1A, 1620.5 m
Rock name : Basalt
Thin section : TS C69674

An optical estimate of the constituents is in Table 4.11.

Table 4.11. Optical estimate of constituents in GSWA sample 154101

Mineral	*Percentage*	*Origin*
Plagioclase	35	Igneous
Amphibole	35	Alteration
Sericite/clay	10	Alteration
Biotite	5	Alteration
Chlorite	3	Alteration
Carbonate	1	Alteration
Quartz	1	Igneous
Opaque minerals	10	Igneous

This sample consists of randomly oriented plagioclase laths, ranging up to 0.3 mm in length, intergrown with an interstitial, pale-green, weakly pleochroic amphibole. Some larger plagioclase phenocrysts, ranging up to 1 mm in diameter, are disseminated through the rock. The plagioclase shows moderate alteration to finely divided sericite/clay. This alteration is most pronounced in some plagioclase phenocrysts that show pervasive alteration to sericite/clay. Minor carbonate is intergrown with the altered plagioclase phenocrysts and also forms fine disseminations in the altered matrix. The amphibole is probably an alteration product of original mafic minerals and has a very pale green, weakly pleochroic colour. Biotite is intergrown with the amphibole as pleochroic, brown flakes less than 0.05 mm in size. The rock is transected by some veins that are filled with a dark-green, intensely pleochroic mineral with high birefringence, which is thought to be chlorite. Some of these veins also contain minor amounts of biotite.

Minor quartz forms anhedral disseminated grains located interstitially between the plagioclase laths. Opaque minerals are disseminated through the rock as anhedral grains commonly less than 0.3 mm in size.

This is a fine-grained basaltic rock with a moderately altered character. The rock is considered unsuitable for radiometric dating.

Appendix 5
Empress 1 and 1A petrological analysis
Preliminary report
(by K. R. Martin)

Summary of sample characteristics

Approximately half of the thin sections described herein were prepared from trimmed core plugs used for porosity and permeability measurements. The remainder were prepared from core chips. A minimum of 200 points were counted for each thin section. Based on lithologic characteristics and without regard to stratigraphic position, the samples from Empress 1/1A have been grouped into the following four categories:

- clastic samples;
- mixed clastic and carbonate samples;
- dolostones, evaporites, and silicified carbonates; and
- volcanic rocks.

Clastic samples

Samples having framework grains of mainly detrital origin are included in this class. With the exception of two mudrocks (800 m, 804.4 m), the samples are mainly fine- and medium-grained sandstones, but there are also five very fine grained sandstones. Grain size, sorting, and roundness are listed in Table 5.1.

The quartz, feldspar, and rock fragment (QFR) compositions of the samples are given in Table 5.2 and plotted in Figure 5.1. The deepest sample (1542.7 m) differs from all others due to its high content of mica and micaceous rock fragments; the sample falls in the litharenite field. All other samples are essentially quartzofeldspathic sands that plot along the quartz–feldspar axis and range from quartz arenite to arkose, with the majority being subarkoses. Feldspar is almost exclusively of potassic composition, and is mainly microcline and microperthite. Feldspar tends to be most concentrated in the very fine to fine sand size-range and its abundance decreases with increasing grain size. The only significant exception is at 741.5 m where the sand is relatively feldspathic, but is also one of the most coarse grained in the suite.

Clay content is highest in the very fine grained sandstones and mudrock.

In the clastic samples, carbonate is entirely dolomite with the exception of a solitary small patch of calcite cement at 294.7 m. Dolomite forms mainly as sparry cement (Dsc) or as microspar (Dmc), which are commonly abundant and collectively reach a maximum of 33% at 724.8 m. Dolomite, as an allochem, is rare with micrite/microspar peloids reaching a maximum of only 3.5%.

Halite cement is found in only one of the clastic samples (1521.2 m).

Visible porosity is variable. It is highest in the top three sandstones, which have little compaction and may possibly have been decemented. In deeper sandstones, visible porosity is present mostly in small amounts but it is locally abundant (up to 11.5%). It is mostly intergranular, but is supplemented by secondary porosity resulting from feldspar dissolution. How much of the intergranular porosity could be secondary due to carbonate dissolution is difficult to determine from thin section alone. In some samples (e.g. 741.5 m), there is sporadic secondary porosity from the partial dissolution of dolomitic peloids. In porous sands where little dolomite is present (e.g. 878.1 m), quartz overgrowth cement may be well developed, but not to the point where it has caused near-complete loss of porosity. In most of the sands, overgrowth development has been inhibited by the presence of pervasive, earlier-formed carbonate.

Mixed clastic and carbonate samples

Samples of this group are characterized by the presence of an important component of dolomitic allochems (up to 34%), as well as clastic grains and dolomite cement/matrix replacement. Allochems are mostly micrite/microspar peloids and intraclasts. Intraclast is used to describe large clasts of carbonate, commonly of heterogeneous

Table 5.1. Clastic grain texture

Depth (drill m)	*Depth (log m)*	*AvGS (mm)*	*Sorting*	*Roundness*
Clastic samples				
159.9		0.24	mod.	rounded
191.1		0.30	mod.	rounded
294.7	295.5	0.15	well	subrounded
639.3	640.6	0.09	mod.–well	subrounded
639.8	641.1	0.08	mod.–well	subrounded
669.1	670.5	0.13	mod.–well	rounded
694.1	695.5	0.30	mod.–well	rounded
696.5	697.9	0.16	well	rounded
724.8	726.3	0.13	mod.–well	subrounded
732.5	734.0	0.15	poor	subrounded
741.5	743.0	0.48	mod.–well	rounded
743.6	745.1	0.40	mod.–well	rounded
800.0	801.6	<0.03		
804.4	806.0	<0.03		
864.3	866.0	0.45	mod.	rounded
878.1	879.8	0.18	well	subrounded
937.8	939.6	0.23	poor	rounded
957.8	959.7	0.30	well	rounded
958.4	960.3	0.27	well	rounded
980.9	982.8	0.08	mod.	subrounded–rounded
997.2	999.1	0.20	mod.	rounded
1 521.2	1 524.0	0.30	poor	rounded
1 542.7	1 545.5	0.09	mod.–well	subrounded
Mixed clastic and carbonate samples				
644.3	645.7	0.40	mod.–well	rounded
667.8	669.2	0.48	mod.	rounded
691.3	692.7	0.20	poor	rounded
739.8	741.3	0.35	mod.–well	rounded
752.8	754.3	0.35	mod.–well	rounded
931.5	933.3	0.08	mod.–well	rounded
932.7	934.5	0.30	mod.–well	rounded
934.4	936.2	0.28	mod.–well	rounded

NOTES: AvGS: Average grain size
Average grain size (AvGS) is based on thin-section estimates only as no systematic grain size analysis was undertaken on any of the samples. Reliability of the grain size estimates decreases with deteriorating sorting. Roundness refers to the most common roundness class apparent in the sample
mod.: moderately sorted

composition, which represent reworked carbonate sediment. However, in some cases the distinction between some peloids and intraclasts is uncertain. Characteristics of these samples are listed in Tables 5.1 and 5.3.

Detrital grains in this sample group are similar to those in the clastic sample group. In their QFR composition, the samples are either subarkoses or quartz arenites (Fig. 5.1). The clastic grain component is mostly medium grained, with only one fine and one very fine grained sample in the eight sample suite.

All the samples in this group contain pervasive, intergranular, dolomite pore-filling cement or recrystallized matrix. Visible porosity is rare.

Dolostones, evaporites, and silicified carbonates

This group of 40 samples is diverse and compositionally and texturally complex. Most are composed of dolomite, but some evaporitic samples containing anhydrite and/or halite are included in the group. There is also a variable, but mostly small (<20%), clastic component in many samples. The group also includes samples that have been variably replaced by authigenic silica. The overall impression from the sample suite is that they were deposited in mostly shallow-water environments including shallow-marine, estuarine, tidal-flat, and hypersaline-basin environments. Characteristics of these samples are listed in Table 5.4.

Table 5.2. Clastic samples

Depth (drill m)	Depth (log m)	Thin-section composition																QFR composition		
		Qtz	Cher	Kfs	Pl	Irf	Mrf	Srf	Mi	HM	Opq	Dpl	Dmc	Dsc	Hl	Cpl	Clay	Vpor	Q% Quartz + chert	F% Feldspar	R% Rock frags
159.9	–	66.0	0.5	9.0	–	–	–	–	–	–	–	–	–	–	–	0.5	1.5	22.5	88.1	11.9	0.0
191.1	–	60.0	–	11.5	–	1.5	1.5	–	1.0	–	4.0	–	–	–	–	0.5	6.5	13.5	80.5	15.4	4.0
294.7	295.5	43.5	–	20.0	0.5	2.0	–	3.5	–	–	1.0	–	–	5.5	–	–	3.0	21.0	62.6	29.5	7.9
639.3	640.6	31.5	–	11.0	–	–	–	1.5	4.0	0.5	13.0	–	–	5.5	–	1.0	31.5	0.5	71.6	25.0	3.4
639.8	641.1	38.5	–	8.0	–	–	–	1.0	1.5	0.5	8.5	–	–	–	–	–	36.5	5.5	81.1	16.8	2.1
669.1	670.5	19.0	–	2.5	1.0	1.5	–	1.0	0.5	–	9.5	–	1.5	2.0	–	24.0	37.0	0.5	76.0	14.0	10.0
694.1	695.5	57.0	1.0	2.0	–	–	–	–	–	–	0.5	1.5	26.5	–	–	–	0.5	11.0	96.7	3.3	0.0
696.5	697.9	54.0	–	7.5	1.0	–	–	–	–	0.5	–	1.0	14.0	12.5	–	1.5	8.0	–	86.4	13.6	0.0
724.8	726.3	41.0	–	17.0	–	–	–	–	–	–	–	3.5	19.0	14.0	–	–	0.5	5.0	70.7	29.3	0.0
732.5	734.0	43.0	–	13.5	–	0.5	–	–	1.5	–	1.0	–	28.5	4.0	–	–	5.0	3.0	75.4	23.7	0.9
741.5	743.0	46.0	–	12.0	1.5	1.0	–	–	0.5	–	–	3.5	18.5	11.0	–	–	1.0	5.0	76.0	22.3	1.7
743.6	745.1	54.5	–	7.5	0.5	–	–	–	–	–	–	3.5	26.0	4.5	–	–	–	3.5	87.2	12.8	0.0
800.0	801.6	11.0	–	2.0	–	–	–	–	17.5	–	5.5	–	–	0.5	–	–	63.5	–	84.6	15.4	0.0
804.4	806.0	18.5	–	1.5	–	–	–	–	10.0	–	5.0	–	–	–	–	–	65.0	–	92.5	7.5	0.0
864.3	866.0	74.0	0.5	3.0	–	1.0	–	1.0	–	–	–	–	–	–	–	–	11.5	9.0	93.7	3.8	2.5
878.1	879.8	70.5	0.5	11.5	–	–	0.5	–	–	–	0.5	–	–	1.0	–	–	4.0	11.5	85.5	13.9	0.6
937.8	939.6	67.5	–	7.5	–	–	–	–	–	–	–	–	–	20.5	–	–	3.0	1.5	90.0	10.0	0.0
957.8	959.7	75.5	–	0.5	–	–	–	–	–	–	–	–	13.0	–	–	–	0.5	10.5	99.3	0.7	0.0
958.4	960.3	78.0	0.5	0.5	–	–	–	–	–	–	–	–	13.5	–	–	–	–	7.5	99.4	0.6	0.0
980.9	982.8	41.5	1.0	10.0	–	1.5	0.5	0.5	1.5	–	5.5	–	–	1.5	–	–	28.5	8.0	77.3	18.2	4.5
997.2	999.1	68.5	–	2.5	–	–	–	–	–	–	–	–	–	27.0	–	–	0.5	1.5	96.5	3.5	0.0
1 521.2	1 524.0	54.0	–	6.5	–	–	0.5	3.0	–	–	–	1.0	10.0	–	25.0	–	–	–	84.4	10.2	5.5
1 542.7	1 545.5	32.5	0.5	3.5	–	1.0	23.0	5.0	10.0	0.5	5.0	–	–	–	–	–	19.0	–	50.4	5.3	44.3

NOTES:
Qtz: quartz
Cher: chert
Kfs: K-feldspar
Pl: plagioclase
Irf: igneous rock fragments
Mrf: metamorphic rock fragments
Srf: sedimentary rock fragments
Mi: mica
HM: heavy minerals
Opq: opaque minerals
Dpl: dolomitic peloids typically composed of dolomicrite and/or microspar
frags: fragments
Dmc: dolomicrite — dense, uniform, structureless
Dsc: dolomitic spar interpreted to be a pore-filling cement
Hl: halite
Cpl: peloidal clay
Vpor: visible macroporosity

Opaque minerals (Opq) most commonly consist of authigenic pyrite but detrital opaque minerals are particularly common in several samples (639.3 m, 639.8 m, 669.1 m)

Staining with alizarin red S and potassium ferricyanide indicates that the carbonate mineral is dolomite except for an isolated patch of calcite at 294.7 m. Where possible, dolomite has been recorded under several categories of grains (allochems) and matrix/cement depending on the ease of recognition of original textural features. Adopted crystal size divisions were selected to best represent the variation within the sample suite and are as follows :
Dolomicrite (<5 μm); Dolomitic microspar (5–40 μm); Dolomitic spar (>40 μm)

Matrix/cement
Dolomicrite and microspar probably represent dolomitized and variably recrystallized original micritic carbonate mud. Dolomitic spar has probably originated both as an intergranular pore and vug-filling cement, but much of the spar is likely to be neomorphic and has formed by aggrading recrystallization of finer grained micrite and also allochems

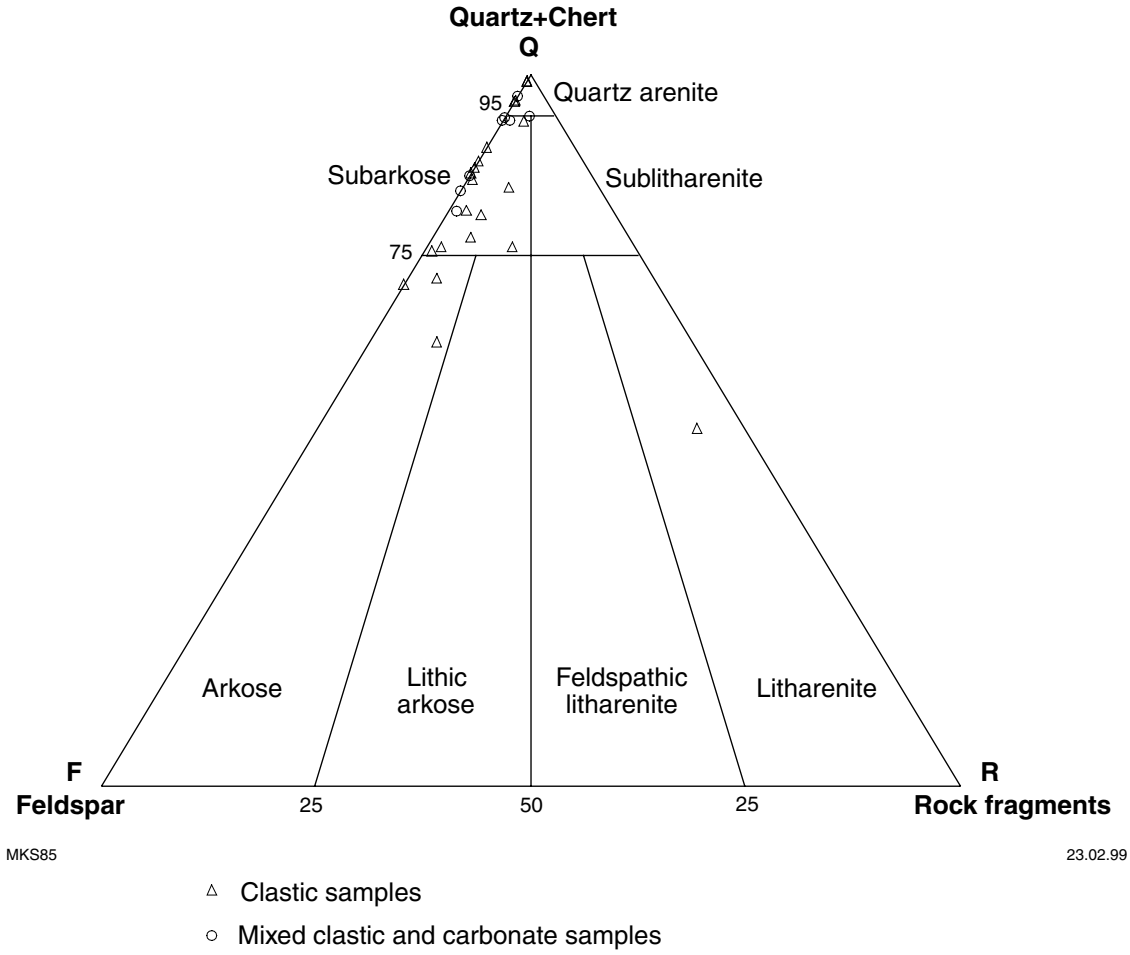

Figure 5.1. QFR compositions of Empress 1 and 1A samples

Many of the carbonates are microbialites that have been modified to different degrees by diagenetic changes. Systematic description of the samples is complicated by the variation in diagenetic alteration that has taken place. Thus, in some samples original allochems are clearly identifiable, whereas in other cases, only local ghost relics of original texture are recognizable. In extreme cases, total recrystallization of carbonate, either before or during dolomitization (aggrading neomorphism), has eliminated all original texture.

Most commonly the microbialites consist of laminated micrite and microspar, within which ghosts of peloidal texture are recognizable. Some of the microspar is interbedded with thin clastic lenses and laminae and patches of coarser, sparry dolomite locally infill inter-peloidal pore spaces or occupy isolated larger vugs within the layered microbialites. More extreme recrystallization to neomorphic spar has occurred in places, but peloidal ghosts are still recognizable within the coarser grained dolomite in places.

Secondary silica replacement is common and original oolitic and peloidal allochems are well preserved within some silicified samples (e.g. 642.3 m). Oolitic rocks are the most prone to replacement by silica.

Anhydrite occurs in many samples below 1070 m and halite is prominent below 1298 m. Samples between 1298.3 and 1302.3 m, which were originally interpreted to be porous, were found instead to be extensively cemented by halite. Most of the samples in this group contain no visible porosity, or where porosity is present, it is sporadically distributed and does not make up more than 1.5% of the rock.

Volcanic rocks

Volcanic rocks occur within the sequence at 231.6, 282.3, 1524.9, and 1593.3 m. Their composition, as determined by point counting, is listed in Table 5.5 and brief descriptions are below:

Table 5.3. Mixed clastic and carbonate samples

Depth (drill m)	Depth (log m)	Clastic grains: Qtz	Cher	Kfs	Pl	Irf	Mrf	Srf	Mi	HM	Opq	Dolomite allochems: Dic	Dpl	Dod	Dmc	Dsc	Cpl	Clay	Vpor	QFR composition: Q% Quartz + chert	F% Feldspar	R% Rock frags
644.3	645.7	34.5	–	1.0	–	–	–	–	–	–	–	32.5	–	1.5	13.5	16.0	1.0	–	–	97.2	2.8	0.0
667.8	669.2	33.5	–	1.0	–	0.5	–	0.5	–	0.5	7.5	30.5	–	–	4.0	5.0	0.5	16.5	–	94.4	2.8	2.8
691.3	692.7	30.0	–	2.0	–	–	–	–	0.5	–	3.5	17.0	–	–	32.5	0.5	–	14.0	–	93.8	6.3	0.0
739.8	741.3	40.0	–	6.0	0.5	–	–	–	–	0.5	–	11.5	6.0	–	11.0	24.5	–	–	–	86.0	14.0	0.0
752.8	754.3	40.5	–	8.5	0.5	0.5	–	–	–	–	–	8.0	4.5	2.0	26.5	8.0	–	–	1.0	81.0	18.0	1.0
931.5	933.3	13.0	–	2.5	–	–	–	–	–	–	5.0	–	2.5	–	69.0	7.0	0.5	0.5	–	83.9	16.1	0.0
932.7	934.5	38.7	–	2.4	–	–	–	–	–	–	2.0	2.9	1.0	–	2.0	49.0	–	–	2.0	94.2	5.8	0.0
934.4	936.2	61.0	–	3.5	–	0.5	–	–	–	–	–	6.0	3.5	–	3.0	21.5	–	1.0	–	93.8	5.4	0.8

NOTES:
Qtz: quartz
Cher: chert
Kfs: K-feldspar
Pl: plagioclase
Irf: igneous rock fragments
Mrf: metamorphic rock fragments
Srf: sedimentary rock fragments
Mi: mica
HM: heavy minerals
Opq: opaque minerals
Dmc: dolomicrite — dense, uniform, structureless
Dsc: dolomitic spar interpreted to a pore-filling cement
Cpl: peloidal clay
Vpor: visible macroporosity
frags: fragments

Opaque minerals (Opq) most commonly consist of authigenic pyrite but detrital opaque minerals are particularly common in several samples (639.3 m, 639.8 m, 669.1 m).

Staining with alizarin red S and potassium ferricyanide indicates that the carbonate mineral in all samples is invariably dolomite. Where possible, dolomite has been recorded under several categories of grains (allochems) and matrix/cement depending on the ease of recognition of original textural features. Adopted crystal size divisions were selected to best represent the variation within the sample suite and are as follows :
Dolomicrite (<5 μm); Dolomitic microspar (5–40 μm); Dolomitic spar (>40 μm)

Dolomite allochems
Dod: Dolomitic ooids
Dpl: Dolomitic peloids typically composed of dolomicrite and/or microspar
Dic: Dolomitic intraclasts mostly composed of micrite/microspar but locally spar

Matrix/cement
Dolomicrite and microspar probably represent dolomitized and variably recrystallized original micritic carbonate mud. Dolomitic spar has probably originated both as an intergranular pore and vug-filling cement, but much of the spar is likely to be neomorphic and has formed by aggrading recrystallization of finer grained micrite and also allochems

Table 5.4. Dolostones, evaporites, and silicified carbonates

Depth (drill m)	Depth (log m)	Dolomitic allochems % Dod	Dpl	Dic	Dolomicrite and microspar % Dmc	Dmr	Dms	Dmsr	Dolomitic spar % Dsc	Dsv	Dsn	Authigenic silica % Sip	Sir	Anh	Hl	Clastic grains % Qtz	Fel	Rock frags	Mica	Opq	Clay	Vpor
520.6	521.8	–	–	–	–	–	40.5	51.5	1.0	0.5	–	–	–	–	–	1.0	–	–	–	1.5	4.0	–
628.5	629.9	–	–	–	–	–	–	–	60.5	–	–	–	–	–	–	11.0	0.5	–	–	9.5	17.5	1.0
629.0	630.3	–	–	–	64.0	2.0	24.0	–	–	–	–	–	–	–	–	2.5	–	–	0.5	6.0	1.0	–
631.2	632.5	–	–	–	2.0	–	67.5	–	1.0	–	–	–	–	–	–	7.0	1.0	–	0.5	9.5	10.0	1.5
642.1	643.5	–	–	–	–	–	–	92.0	2.5	–	–	–	–	–	–	–	–	–	–	–	5.5	–
642.3	643.7	4.5	8.5	–	–	1.0	18.5	17.0	20.0	–	6.0	0.5	8.0	–	–	16.0	–	–	–	–	–	–
646.5	647.9	–	–	–	–	3.0	9.0	19.0	–	–	69.0	–	–	–	–	–	–	–	–	–	–	–
685.8	687.2	–	–	–	74.4	–	–	–	24.6	–	0.5	–	–	–	–	–	–	–	–	0.5	–	–
722.4	723.9	–	1.0	2.5	–	5.5	3.5	64.0	15.5	1.0	2.0	–	–	–	–	–	–	–	–	0.5	4.5	–
736.0	737.5	–	–	–	–	–	25.5	1.0	20.0	2.5	0.5	46.5	1.0	–	–	1.0	–	–	–	0.5	1.5	–
782.5	784.1	–	–	–	–	4.0	–	76.5	0.5	9.5	9.5	–	–	–	–	–	–	–	–	–	–	–
939.3	941.1	–	7.5	4.5	–	–	5.5	23.5	1.5	2.5	0.5	37.0	12.5	–	–	4.5	–	–	–	–	0.5	–
941.1	942.9	–	–	1.0	–	–	–	–	4.0	–	87.5	3.0	–	–	–	0.5	–	–	0.5	3.0	–	0.5
941.2	943.0	–	–	–	–	–	2.5	–	41.0	–	–	22.0	32.5	–	–	1.0	–	–	–	–	1.0	–
967.1	969.0	12.5	3.0	5.0	–	1.5	–	10.5	2.0	2.0	–	15.5	31.0	–	–	17.0	–	–	–	–	–	–
1 069.0	1 071.0	–	–	–	–	–	13.5	–	20.0	–	–	57.0	9.5	–	–	–	–	–	–	–	–	–
1 070.8	1 072.8	–	–	–	–	–	2.0	–	–	–	–	–	–	98.0	–	–	–	–	–	–	–	–
1 077.0	1 079.0	–	–	–	–	–	49.5	1.5	40.0	–	–	–	–	6.5	–	–	–	–	–	1.5	1.0	–
1 102.7	1 104.8	–	–	–	–	–	–	68.5	–	6.5	–	–	–	–	–	–	–	–	–	24.5	–	0.5
1 110.3	1 112.4	8.5	19.0	5.0	–	2.5	4.0	38.5	4.5	0.5	1.0	–	–	–	–	14.5	1.5	–	–	0.5	–	–
1 126.0	1 128.1	–	1.5	–	–	–	53.5	–	0.5	–	–	–	–	–	–	16.5	4.0	–	5.0	14.5	4.5	–
1 137.2	1 139.3	54.5	–	–	–	–	–	–	36.5	–	–	–	–	9.0	–	–	–	–	–	–	–	–
1 232.4	1 234.7	–	–	–	–	–	–	–	22.0	–	–	–	–	4.5	–	18.5	9.5	–	8.0	1.0	35.5	1.0
1 247.8	1 250.1	–	–	–	–	–	65.0	11.5	–	–	–	14.0	–	5.5	–	–	–	–	–	4.0	–	–
1 251.0	1 253.3	–	–	–	–	–	–	–	24.5	–	–	–	–	–	–	13.5	5.0	–	13.5	1.5	42.0	–
1 298.0	1 301.3	–	–	–	–	–	66.0	–	–	–	–	–	–	4.0	–	2.5	–	–	–	5.0	22.5	–
1 298.3	1 300.7	–	–	–	–	–	–	–	59.5	–	–	24.0	–	–	16.5	–	–	–	–	–	–	–
1 298.9	1 301.3	–	–	–	–	–	–	–	27.0	–	–	21.5	–	41.0	10.5	–	–	–	–	–	–	–
1 299.6	1 302.0	–	–	–	–	–	–	–	11.0	–	–	–	82.0	–	7.0	–	–	–	–	–	–	–
1 299.8	1 302.2	–	–	–	–	–	–	–	22.0	–	–	–	67.0	1.0	10.0	–	–	–	–	–	–	–
1 300.2	1 302.6	–	–	–	–	–	–	–	42.0	–	–	53.5	–	–	4.5	–	–	–	–	–	–	–
1 301.4	1 303.8	–	–	–	–	–	10.5	–	69.5	–	–	–	–	–	20.0	–	–	–	–	–	–	–
1 302.3	1 304.7	–	–	–	–	–	1.5	–	56.0	–	–	31.5	–	0.5	9.0	–	–	–	–	–	–	1.5
1 303.4	1 305.8	–	–	–	–	–	64.5	–	–	–	–	–	–	15.0	–	5.0	–	–	–	3.5	12.0	–
1 358.2	1 360.7	–	–	–	–	–	23.0	–	–	–	–	–	–	63.5	–	8.5	2.5	–	–	0.5	1.5	0.5
1 365.0	1 367.5	1.0	12.5	0.5	–	–	–	55.0	12.0	–	–	–	–	–	11.5	–	–	–	–	7.5	–	–
1 498.1	1 500.8	–	–	–	–	–	–	50.5	–	–	25.0	–	–	8.0	13.0	3.5	–	–	–	–	–	–
1 503.0	1 505.7	–	–	–	32.5	–	37.0	–	–	–	–	–	–	3.0	–	5.0	–	–	13.0	6.5	3.0	–
1 506.0	1 508.7	–	20.5	37.5	4.0	–	–	2.5	4.0	–	–	–	–	2.5	19.5	7.0	2.0	–	–	–	0.5	–

NOTES:
Qtz: quartz
Fel: feldspar
Vpor: visible macroporosity
Opq: opaque minerals
Dmc: Dolomicrite — dense, uniform, structureless
Dmr: Dolomicrite as grain envelopes, discontinuous laminae and patches, or where relict allochem (usually peloidal) ghosts are recognizable
Dms: Dolomitic microspar — dense, uniform, structureless
Dmsr: Dolomitic microspar as grain envelopes, discontinuous laminae and patches, or where relict allochem (usually peloidal) ghosts are recognizable
Dsc: Dolomitic spar interpreted to be a pore-filling cement
Dsv: Dolomitic spar as vein and vug fillings
Dsn: Dolomitic spar of obvious neomorphic origin with recognizable allochem ghosts
Sip: Authigenic silica replacing inter-allochem carbonate cement/matrix or porosity (mostly as microcrystalline quartz but locally coarser grained, and including chalcedony in places)
Sir: Authigenic silica as above, but replacing allochems such as ooids and peloids
Anh: Anhydrite
frags: fragments
Hl: halite

Opaque minerals (Opq) most commonly consist of authigenic pyrite but detrital opaque minerals are particularly common in several samples (639.3 m, 639.8 m, 669.1 m)

Staining with alizarin red S and potassium ferricyanide indicates that the carbonate mineral in all samples is invariably dolomite. Where possible, dolomite has been recorded under several categories of grains (allochems) and matrix/cement depending on the ease of recognition of original textural features. Adopted crystal size divisions were selected to best represent the variation within the sample suite and are as follows :
Dolomicrite (<5 μm); Dolomitic microspar (5–40 μm); Dolomitic spar (>40 μm)

Dolomite allochems
Dod: Dolomitic ooids
Dpl: Dolomitic peloids typically composed of dolomicrite and/or microspar
Dic: Dolomitic intraclasts mostly composed of micrite/microspar but locally spar

Matrix/cement
Dolomicrite and microspar probably represent dolomitized and variably recrystallized original micritic carbonate mud.
Dolomitic spar has probably originated both as an intergranular pore and vug-filling cement, but much of the spar is likely to be neomorphic and has formed by aggrading recrystallization of finer grained micrite and also allochems

Table 5.5. Volcanic rocks

Depth (m)	*Pl*	*Kfs*	*Cpx*	*Opq*	*Gmass*	*Chl/Non*	*Zeo*	*?Mica*
231.6	40.5	–	32.0	5.5	8.5	13.0	0.5	–
282.3	19.5	–	–	49.0	–	17.0	–	14.5
1 524.9	56.0	–	–	24.5	19.5	–	–	–
1 593.3	55.0	1.5	38.0	4.5	–	1.0	–	–

NOTES: Pl: plagioclase
Kfs: K-feldspar
Cpx: clinopyroxene
Opq: opaque minerals
Gmass: groundmass
Chl/Non: amygdale filled by chlorite or nontronite
Zeo: secondary zeolite
?Mica: secondary ?mica after ferromagnesians and/or plagioclase

231.6 m This is an amygdaloidal basalt/dolerite with an intergranular texture and is composed mainly of clinopyroxene and cloudy plagioclase with interstitial opaque minerals and small areas of turbid interstitial groundmass, as well as numerous large, irregular-shaped amygdales up to 4 mm across, which are filled by secondary green clays (probably chlorite and/or nontronite) and rare zeolite.

282.3 m This altered, amygdaloidal basalt is composed of plagioclase microlites and secondary ?mica, which is an alteration product of ferromagnesians and/or plagioclase, together with abundant interstitial opaque iron oxide and numerous irregular-shaped amygdales up to 1.5 mm long, which are occupied by green secondary clays (probably chlorite and/or nontronite).

1524.5 m This a highly altered and turbid volcanic rock with a trachytic-textured groundmass of flow-aligned, highly elongated plagioclase microlites, which are typically around 1 mm long and are clouded by alteration, together with interstitial fine-grained opaque minerals. In some places, the groundmass feldspars show a radiating, fibrous habit. Tabular, euhedral phenocrysts of plagioclase up to 1 mm long, are sporadically distributed through the groundmass. Because of the degree of alteration, the composition of the rock remains uncertain, but it is probably an intermediate lava.

1593.3 m This is a fresh basalt or dolerite with an intergranular texture and is composed of pale-brown clinopyroxene and fresh plagioclase. Opaque minerals are not uniformly distributed through the interstices but tend to be concentrated into larger, irregular-shaped anhedra or anhedral aggregates up to 0.8 mm in size. Small patches of green interstitial clay (chlorite and/or nontronite) are sporadically distributed through the rock and the same clays occur as partial alterations of one or two large (up to 1.2 mm across) tabular plagioclase phenocrysts.

Appendix 6
Palynology of samples from the top of Empress 1 and from nearby waterbores
(by J. Backhouse)

Introduction

This report covers palynological results from the uppermost interval in Empress 1 (105 – 118.7 m) and from two nearby shallow waterbores. Yowalga Bore 4 (YWGB 4) is located 33.1 km at 67° ENE from Empress 1 (AMG 744682E, 7018007N), and Westwood Bore 1 (WTDB 1) is just 29 m south of Empress 1. Samples from YWGB 4 and WTDB 1 are cuttings; all samples from Empress 1 are from conventional core (Table 6.1). Samples were processed by Laola Pty Ltd, and all slides and residues have been placed in the Geological Survey of Western Australia's Petroleum Relinquishment Fossil Collection.

The lowest core sample from Empress 1 (118.9 m) was barren. All the other samples, except the 74–75 m sample from WTDB 1, produced reasonable yields of palynomorphs. The results are summarized in Table 6.2. The distribution of palynomorphs in the productive samples is shown in Figure 6.1.

Table 6.1. Description of palynological samples from WTDB 1, Empress 1, and YWGB 4

Well/bore	*Depth (m)*	*Sample type*	*Organic yield (cc/gm)*	*Lithology*
WTDB 1	74–75	Cuttings	–	Claystone, grey
WTDB 1	105–106	Cuttings	–	Claystone, grey
Empress 1	105	Core	0.007	Sandstone, poorly sorted, medium grey
Empress 1	105.9	Core	0.007	Sandstone, fine grained, medium grey
Empress 1	106.2	Core	0.002	Sandstone, fine grained, medium grey
Empress 1	107.3	Core	0.002	Sandstone, fine grained, medium grey
Empress 1	118.7	Core	0.0	Claystone, cream with dark grey streaks
YWGB 4	63–67	Cuttings	–	
YWGB 4	76–79	Cuttings	–	

Table 6.2. Palynological summary of samples from WTDB 1, Empress 1, and YWGB 4

Well/bore	*Depth (m)*	*Yield*	*Thermal maturity*	*Environment*	*Zone*	*Estimated age*
WTDB 1	74–75		2- to 2+	?Non-marine	*D. tenuistriatum*	?Stephanian
WTDB 1	105–106		2- to 2+	?Non-marine	*D. tenuistriatum*	?Stephanian
Empress 1	105	moderate	2- to 2+	?Non-marine	*D. tenuistriatum*	?Stephanian
Empress 1	105.9	moderate	2- to 2+	?Non-marine	*D. tenuistriatum*	?Stephanian
Empress 1	106.2	moderate	2- to 2+	?Non-marine	*D. tenuistriatum*	?Stephanian
Empress 1	107.3	moderate	2- to 2+	?Non-marine	*D. tenuistriatum*	?Stephanian
Empress 1	118.7	barren				
YWGB 4	63–67	moderate	2- to 2+	?Non-marine	Indeterminate	Late Carboniferous
YWGB 4	76–79	moderate	2- to 2+	?Non-marine	Indeterminate	Late Carboniferous

YWG B4	YWG B4	EMPRESS 1	EMPRESS 1	EMPRESS 1	EMPRESS 1	WTD B1	WTD B1	Well/Borehole
76-79	63-67	107.30	106.20	105.90	105.00	105-106	74-75	Depth (m)
				X		X		*Anapiculatisporites concinnus*
X	X	X	X	X	X	X		*Botryococcus* sp.
X	X	X		X	X	X		*Brevitriletes parmatus*
X	X	X	X	X	X		X	*Caheniasporites elephas*
			X		X			*Cyclogranisporites infirmus*
X								*Cymatiosphaera* sp.
X		X			X	X		*Densoisporites* sp. aff. *D. rotundidentatus*
X	X							*Dentatispora* sp.
		X	X	X	X	X		*Deusilites tenuistriatus*
X	X				X	X		*Dibolisporites disfacies*
	X					X		*Indotriradites* sp.
X	X	X	X	X	X	X		*Jayantisporites pseudozonatus*
	X			X	X			*Maculatisporites* sp.
X	X	X		X	X	X	X	*Plicatipollenites* spp.
X	X	X		X	X	X		*Potonieisporites novicus*
X								*Psomospora detecta*
X			X			X	X	*Punctatisporites gretensis*
X	X	X	X	X	X	X	X	*Punctatisporites* spp.
X			X					*Reticulatisporites* sp. cf. *R. bifrons*
X								*Rugospora australiensis*
			X					*Spelaeotriletes queenslandensis*
X	X				X			*Tetraporina* sp.
X	X	X	X	X	X		X	*Verrucosisporites andersonii*
Indet.		*D. tenuistriatus*						Zone

MKS86 23.02.99

Figure 6.1. Distribution of palynomorphs from productive samples in Empress 1 and nearby waterbores

Palynological observations

WTDB 1, 74–75 to 105–106 m and Empress 1, 105–107.3 m

The six samples over this interval yielded essentially similar assemblages, as shown in Table 6.1. The presence of monosaccate pollen, *Potonieisporites*, and the acritarch *Deusilites tenuistriatus*, and the absence of *Pseudoreticulatispora confluens* indicates a strong correlation with the *D. tenuistriatus* Assemblage. The *D. tenuistriatus* Assemblage was introduced by Apak and Backhouse (1998, in prep.) for the uppermost interval of the Reeves Formation in the Canning Basin. The unit is considered to be Late Carboniferous in age, possibly Stephanian. It is the palynostratigraphic unit that immediately underlies the *P. confluens* Zone and, or, Stage 2 in the Canning Basin. This is the first record of the unit from the Officer Basin. Other Late Carboniferous to Permian strata in the Officer Basin have been assigned to the Paterson Formation and are correlated with Stage 2 (Kemp, 1976; Backhouse, 1993).

YWGB 4, 63–64 m to 76–79 m

The assemblages from YWGB 4 are essentially similar to those from WTDB 1 and Empress 1, but they lack *D. tenuistriatus*. They also contain *Dentatispora* sp., and the lower sample contains a number of species that do not seem to be present in other samples covered in this report. These differences, though minor, suggest that the

intervals sampled in YWGB 4 are slightly older than the highest sampled interval in Empress 1, and may correlate with the *Diatomozonotriletes birkheadensis* Assemblage of Powis (1984).

Maturity

Palynomorphs on the kerogen slides fall within the maturity range 2- to 2+, with possibly rare grains just within the oil mature range at 2+. Overall, the samples appear to be immature for petroleum generation.

References

APAK, S. N., and BACKHOUSE, J., 1998, Re-interpretation of the Permo-Carboniferous succession, Canning Basin, Western Australia, *in* The sedimentary basins of Western Australia 2 *edited by* P. G. and R. R. PURCELL: Proceedings of Petroleum Exploration Society of Australia Symposium, Perth, W.A., 1998, Proceedings,
p. 683–694.

APAK, S. N., and BACKHOUSE, J., in prep., Stratigraphy and petroleum exploration objectives of the Permo-Carboniferous on the Barbwire Terrace and adjacent areas, northeast Canning Basin, Western Australia: Western Australia Geological Survey, Report 68.

BACKHOUSE, J., 1993, Palynology and correlation of Permian sediments in the Perth, Collie, and Officer Basins, Western Australia: Western Australia Geological Survey, Report 34, p. 111–128.

KEMP, E. M., 1976, Palynological observations in the Officer Basin, Western Australia: Australia BMR, Bulletin 160, p. 23–39.

POWIS, G. D., 1984, Palynostratigraphy of the Late Carboniferous sequence, Canning Basin, W.A., *in* The Canning Basin, W.A. *edited by* P.G. PURCELL: Geological Society of Australia and Petroleum Exploration Society of Australia, Canning Basin Symposium, Perth, W.A., 1984, Proceedings, p. 429–438.

Appendix 7
Proterozoic palynology of samples from Empress 1A
(by K. Grey)

Introduction

The palynological results from Empress 1A are based on 61 conventional core samples (Plate 3). Samples were processed by Laola Pty Ltd using a modified preparation technique for Proterozoic samples that eliminates harsh and vigorous treatments that might fragment large or delicate specimens (Grey, 1998). Most samples between 494.9 and 843.9 m yielded palynomorphs; however, with rare exceptions, nearly all samples from below 843.9 m were barren. The high recovery rates observed in the Kanpa Formation are generally higher than for most previously examined Proterozoic intervals, and several samples, especially those at 600.2, 728.7, 733.9, 745.5, and 799.4 m, showed exceptionally good preservation. The assemblage is similar to that observed in other drillholes in the Officer Basin (Grey, 1995; Zang, 1995; Grey and Cotter, 1996; Cotter, 1997, in press; Grey and Stevens, 1997). However, subdivision of the assemblage has not been possible because of the long ranging and conservative nature of many of the taxa. The slides have been placed in the GSWA relinquishment collection.

Palynological observations

203.0 – 483 m, unsampled interval

The interval from the top of the Table Hill Volcanics to the top of the Kanpa Formation, which includes an unnamed sandstone unit, 'cap dolomite', and ?Lupton Formation, was not sampled because it contained no lithologies suitable for palynological examination.

483 – 860.8 m, Kanpa Formation

Samples from the Kanpa Formation contained a similar suite of palynomorphs throughout, although the numbers of certain taxa varied. The most noticeable taxa in the assemblage are two species of large wrinkled acritarch, *Cerebrosphaera buickii* Butterfield 1994 and a new species (here referred to as *Cerebrosphaera* sp. nov. pending publication by Cotter, in press). The surface wrinkling was considered to be of taxonomic significance by Butterfield et al. (1994) and forms a distinctive pattern. However, the wrinkles in the Officer Basin specimens of *C. buickii* show a slightly different pattern to those of the Svanbergfjellet Formation in Spitsbergen, in that they are not as tightly interfingering. The new species is differentiated from *C. buickii* by a thicker wall and larger wrinkles (Cotter, K. L., 1997, written comm.).

The large, thick-walled, smooth-surfaced acritarch *Chuaria circularis* Walcott 1899 is common in some samples. *Simia annulare* and simple leiospheres, *Leiosphaeridia crass, L. jacutica, L. minutissima,* and *L. tenuissima*, are present in most samples. Colonial clusters of *Synsphaeridium* sp. and a species of *Satka* are abundant in certain samples. Samples between 842.6 and 843.9 m contain well-preserved colonies of *Myxococcoides cantabrigiensis* Knoll 1982 and *Ostiana microcystis* Hermann 1976. Most samples contain a variety of filaments, including several species of *Siphonophycus* and *Oscillatoriopsis amadeus* Schopf and Blacic 1971; Butterfield 1994. Other components are rare.

860.8 – 1247.1 m, Hussar Formation

Lithologies in the Hussar Formation are generally unsuitable for palynological sampling. Two samples, from 971.6 and 973.6 m, were barren of identifiable palynomorphs and contained only severely degraded organic debris. A small cluster of samples between 1074.7 and 1095.7 m was more productive and contained an assemblage similar to that observed in the Kanpa Formation, although preservation is much poorer. Samples from 1102.1 m to the base of the formation were barren.

1247.1 – 1540.2 m, Browne and ?Lefroy Formations

Few samples in this interval were lithologically suitable for palynology and the few samples processed were barren, apart from containing finely disseminated organic material.

1540.2 m to TD at 1624.6 m, pre-Officer Basin succession

Lithologies in this interval were highly unsuitable for palynology. Three samples were processed, but only the sample from 1602.3 m contained palynomorphs. This sample contained large, grainy looking acritarchs that were too badly degraded to be identified.

Discussion

Palynomorphs present in the Kanpa Formation, and to a lesser extent the Hussar Formation, are consistent with those found at the same level elsewhere in the basin (Grey, 1995; Grey and Cotter, 1996; Cotter, K. L., 1997, written comm., in press; Grey and Stevens, 1997). They are characterized by the presence of *Cerebrosphaera buickii* and a new species of *Cerebrosphaera.* Neither of these taxa were recorded from the Alinya Formation of the South Australian Officer Basin (Zang, 1995), or from the Browne Formation, or its lateral equivalents, elsewhere in the Officer Basin. From the available data, these acritarchs appear to be restricted to the younger part of Supersequence 1. Assemblages in the Browne Formation seem similar, but lack the large, wrinkled species.

Maturity

Maturity was determined using thermal alteration index (TAI; see Traverse, 1988, p. 431–435, Pl.1). The index was devised for Phanerozoic spores and pollen and needs to be applied with caution to Proterozoic samples, since the colour variation shown by Proterozoic acritarchs and other biogenic material may be slightly different and is not well calibrated. In spite of the constraints, the colour of Proterozoic biogenic matter is still a useful guide to maturity, and is generally consistent with results obtained using organic geochemistry. Most samples from the Kanpa Formation show a thermal alteration index (TAI) of 2+ to 3– and lie within the oil generation window. Samples below 842.6 m show a slight increase in maturity to 4– and lie within the dry gas window. A few samples at lower depths appear somewhat lighter in colour, but this is probably a result of degradation and lack of suitable palynomorphs to provide an accurate measurement.

Conclusions

Extremely well preserved palynomorphs in Empress 1A demonstrate correlation with assemblages at the same level in drillholes throughout the Officer Basin. Organic material is abundant and consists of a mixture of acritarchs and filamentous and coccoid mat fragments, most probably derived from benthic mats developed in the photic zone.

References

BUTTERFIELD, N. J., KNOLL, A. H., and SWETT, K., 1994, Paleobiology of the Neoproterozoic Svanbergfjellet Formation, Spitsbergen: Fossils and Strata, no. 34, 84p.

COTTER, K. L., 1997, Neoproterozoic microfossils from the Officer Basin, Western Australia: *Alcheringa,* v. 21, p. 247–270.

COTTER, K. L., in press, Palaeobiology of Neoproterozoic chert and siliciclastics of Supersequence 1, from the western Officer Basin, Western Australia: *Alcheringa*.

GREY, K., 1995, Officer Basin drillholes — review of Neoproterozoic palynological data: Western Australia Geological Survey, Palaeontology Report No. 1995/11 (unpublished).

GREY, K., 1998, Ediacarian palynology of Australia: Macquarie University, PhD thesis (unpublished).

GREY, K., and COTTER, K. L., 1996, Palynology in the search for Proterozoic hydrocarbons: Western Australia Geological Survey, Annual Review 1995–96, p. 70–80.

GREY, K., and STEVENS, M. K., 1997, Neoproterozoic palynomorphs of the Savory Sub-basin, Western Australia, and their relevance to petroleum exploration: Western Australia Geological Survey, Annual Review 1996–97, p. 49–54.

TRAVERSE, A., 1988, Palaeopalynology: Boston, Unwin Hyman, 600p.

ZANG, W., 1995, Early Neoproterozoic sequence stratigraphy and acritarch biostratigraphy, eastern Officer Basin, South Australia: Precambrian Research, v. 74, p. 119–175.

Appendix 8
Proterozoic stromatolite biostratigraphy of Empress 1A
(by K. Grey)

Introduction

Stromatolites are abundant in Empress 1A and the core contains more than 70 stromatolitic horizons, nearly all of which belong to previously identified taxa (Preiss, 1972, 1973, 1974, 1976, 1985, 1987; Walter, 1972; Griffin and Preiss, 1976; Walter et al., 1979; Grey, 1995). Stromatolites were identified directly from the core, mostly on cut faces, and selected examples were photographed for a more comprehensive publication (Grey, in prep.). Three significant biostratigraphic assemblages were recognized: the *Acaciella australica* Assemblage, the *Baicalia burra* Assemblage, and the ?*Elleria minuta* horizon near the top of the 'cap dolomite'. The presence of these stromatolite assemblages allows correlation with outcrop and other drillholes in the Western Australian Officer Basin, with successions in other parts of the Centralian Superbasin (the Amadeus and Georgina Basins), the Adelaide Rift Complex, and indirectly with Neoproterozoic successions in Tasmania. Identified specimens have been left in situ in the core.

Stromatolite assemblages

317.79 – 317.99 m, ?Elleria minuta horizon

A 50 cm-thick unit at the top of the ?Lupton Formation has been identified as corresponding lithologically to the 'cap dolomite' associated elsewhere in the Centralian Superbasin and Adelaide Rift Complex with the basal Marinoan glaciation (Preiss, W. V., 1998, written comm.; Walter, M. R., 1998, written comm.). Three thin horizons of silicified dolomite near the top of the cap dolomite consist of incipient stromatolite columns. Microscopic examination shows some of the columns to have a similar shape and lamination pattern to that of *Elleria minuta* Walter and Krylov *in* Walter et al. 1979. The columns are not sufficiently developed for the branching pattern to be observed, so assignment to *E. minuta* remains tentative. The presence of ?*E. minuta* is a good indicator that the cap dolomite is a probable correlative of the one occurring above the Pioneer Sandstone in the Amadeus Basin.

483 – 974.5 m, Baicalia burra Assemblage

The Kanpa Formation consists of cyclic units where stromatolitic carbonate horizons are dominated by *Baicalia burra* Preiss 1972; other stromatolites occur less commonly. These include *Tungussia wilkatanna* Preiss 1974, *Conophyton* form. nov., and a small, dominantly pseudocolumnar form with short columns. All four forms have previously been recorded from outcrop in the Officer Basin.

Baicalia burra occurs at about 60 horizons in the core in the Kanpa Formation (Plate 3). It has a distinctive form characterized by tuberous pinching and swelling columns, and by branching ranging from subparallel to markedly divergent. Lamina shapes are variable, ranging from flat to steeply convex, and they are banded and micro-crosslaminated in places. In many fascicles, the basal part is compacted and is compressed into the surrounding black siltstone, indicating that lithification of the columns was differential and formed earlier than lithification of the interspaces, which were filled with soft sediment. The upper parts of most of these fascicles are not compacted and remain in their growth position. However, several horizons are brecciated and consist of column fragments in a random orientation. *Baicalia burra* was seen in outcrops along the Eagle Highway near the western margin of the Officer Basin, in the Neale Formation near Neale Junction, at Constance Headland, and in Kanpa 1A (Stevens and Grey, 1997). It is widespread in the Burra Group and lateral equivalents in South Australia (Preiss, 1972, 1987, p. 294), and it has been recorded as an erratic in diamictite (Griffin and Preiss, 1976) in what is now the Julius River Member of the Black River Dolomite in northwestern Tasmania.

Baicalia burra is present in dolomite at 483.1 m in the Empress 1A core, immediately below the diamictite. The stromatolite is in situ and this part of the succession is therefore considered to be part of the underlying Kanpa Formation. A stromatolite at 490.7 m is also *B. burra*, but seems to have been exhumed and infilled with diamictite matrix. Interpretation of this interval as a karst surface (Preiss, W. V., 1988, written comm.) is supported by the

stromatolite evidence. The lower specimen of *B. burra* probably represents a weathered cave floor. The upper specimen is in the cave roof. The identification of *B. burra* at both depths is consistent with the whole interval being part of a single stratigraphic unit.

Tungussia wilkatanna Preiss 1974 occurs at 510.5, 512.5, and between 630 and 630.3 m. This form is known from the lower member of the Skillogalee Dolomite (Preiss, 1987, p. 294). It has multiple, markedly divergent branches with numerous horizontal columns or columns that are initially horizontal, which then become vertical once they reach the margin of the bioherm. Laminae are smooth, thin, and moderately convex. *T. wilkatanna* has not been observed in outcrop in Western Australia.

A new species of *Conophyton*, previously observed in outcrop near the Eagle Highway and at Constance Headland (Stevens and Grey, 1997), may be present at 651.7, 687.81, 709.8, 773.0, 775.8, and 779.0 m. Identification of this form is difficult because, although the core specimens show the smooth, steeply convex laminae typical of the form, the diagnostic axial zone was not cut by the core. In outcrop, conical stromatolites are generally found surrounded by rims of *B. burra* (see below).

A small, as yet unnamed, pseudocolumnar type occurs between 520.6 and 522.9 m and at 534.2 m. This form also occurs at the Eagle Highway localities (Stevens and Grey, 1997). It may also be similar to 'Specimen S6' of Preiss (1976) from the Ida Range on central ROBERT, although further work is needed for this to be confirmed.

Stromatolites are rare below about 845 m, where carbonate forms a much smaller proportion of the core. An isolated specimen of *B. burra* occurs in the Hussar Formation at 974.5 m, more than 100 m below the base of the main stromatolite interval. This form is very poorly preserved as a result of recrystallization.

1077.4 m, Unnamed stromatolite, Hussar Formation

A single, unnamed stromatolite formed in greenish-grey, silty dolomite in the Hussar Formation at 1077.4 m. This stromatolite has not been observed in outcrop. The stromatolite has semi-horizontal columns with irregular margins and highly irregular, wispy laminae. The growth habit is similar to that of *Tungussia*, but it cannot be identified with confidence without the details of the overall growth patterns being known.

1368.3 – 1383.5 m, Acaciella australica Assemblage, Browne Formation

A pink dolomite, 18 m thick, contains two stromatolite forms found in the *Acaciella australica* Assemblage. The dominant form in the interval is *Acaciella australica* (Howchin 1914) Walter 1972, which occurs in a series of stacked bioherms. Both the basal domical sections of fascicles and vertical narrow columns typical of *A. australica* are represented in the core, and are consistent with features observed at numerous outcrops in the Officer Basin (Grey, 1995; Stevens and Grey, 1997). A second stromatolite, *Basisphaera irregularis* Walter 1972, dominates in the upper part of the interval, down to about 1375 m. This stromatolite is interbedded with clastic grainstones and, as observed in outcrop (Stevens and Grey, 1997), generally associated with an input of more clastic material. *A. australica* was previously recorded from a series of outcrops in the Skates Hills Formation of the Savory Sub-basin and in Yowalga 3 at 2390 m (Grey, 1995), and has subsequently been identified in outcrop at Woolnough Hills (Stevens and Grey, 1997). The distribution of *A. australica* in other areas of Australian Neoproterozoic sedimentation has been discussed in Grey (1995) and, together with associated forms, it forms a significant marker horizon Australia wide.

Palaeoenvironment

In addition to being useful biostratigraphic markers, the stromatolites provide useful information about palaeoenvironments. The association between *A. australica* and *Bas. irregularis* has been described from outcrop (Stevens and Grey, 1997), and relationships in the core are similar. Southgate (1989) recognized upward-shallowing cycles associated with *A. australica* bioherms in the Bitter Springs Formation, and similar patterns are observed here. The tops of individual fascicles were probably emergent, a feature observed in the Skates Hills Formation outcrops (Grey, 1995). *A. australica* preferred moderately quiet water with low clastic input, probably slightly below wave base to occasionally emergent. As clastic sediment input increased, *A. australica* was replaced by *Basisphaera irregularis.* In outcrop in the Skates Hills Formation, *Bas. irregularis* forms tabular and pedestal biostromes only a few centimetres high, indicating extremely shallow water depths (Stevens and Grey, 1997). The specimens in the core are more club-shaped, indicating slightly deeper water, although conditions were probably still very shallow.

The *B. burra* Assemblage is a more cyclic succession containing fringing or patch reefs of stromatolitic carbonate developed at, or near, wave base. Observations from outcrop indicate that the conical stromatolites are generally found in clusters in the centre of bioherms that have a rim of *B. burra* (Stevens and Grey, 1997). The *B. burra* forms a

protective wall (creating a mini-atoll) that produces quieter conditions in the core of the bioherm. Quiet-water conditions favour the growth of conical stromatolites. The tops of many of the *B. burra* fascicles are eroded suggesting growth near wave base.

As observed in outcrop in the Amadeus Basin (Walter et al., 1979), ?*Elleria minuta* grows as a veneer on erosional horizons.

Conclusions

Stromatolites in the Empress 1A core are useful both for biostratigraphical and palaeoenvironmental interpretations. The thin stromatolite layers in the 'cap dolomite' suggest a correlation with the Pioneer Sandstone (Marinoan glacial) of the Amadeus Basin. The presence of *Baicalia burra* and *Tungussia wilkatanna* indicate correlation of the Kanpa Formation with the Neale Formation and Tarcunyah Group elsewhere in the Officer Basin, and with the Skillogalee Dolomite of the Burra Group in South Australia. *Acaciella australica* and *Basisphaera irregularis* support correlation of the Browne Formation with the Woolnough and Skates Hills Formations elsewhere in the Officer Basin, with the Bitter Springs Formation, the Yackah Beds in other parts of the Centralian Superbasin, and with the Coominaree Dolomite of the Adelaide Rift Complex.

References

GREY, K., 1995, Neoproterozoic stromatolites from the Skates Hills Formation, Savory Basin, Western Australia, and a review of the distribution of *Acaciella australica*: Australian Journal of Earth Sciences, v. 42, p. 123–132.

GREY, K., in prep., Stromatolites of the Officer Basin, Western Australia: Western Australia Geological Survey, Report.

GRIFFIN, B. J., and PREISS, W. V., 1976, The significance and provenance of stromatolitic clasts in a probable late Precambrian diamictite in north-western Tasmania: Papers and Proceedings of the Royal Society of Tasmania, v. 110, p. 111–127.

PREISS, W. V., 1972, The systematics of South Australian Precambrian and Cambrian stromatolites, Part I: Transactions of the Royal Society of South Australia, v. 96, p. 67–100.

PREISS, W. V., 1973, Early Willouran stromatolites from the Peake and Denison Ranges and their stratigraphic significance: South Australia Department of Mines Report Book, 73/208, 27p.

PREISS, W. V., 1974, The systematics of South Australian Precambrian and Cambrian stromatolites, Part III: Transactions of the Royal Society of South Australia, v. 98, p. 185–208.

PREISS, W. V., 1976, Proterozoic stromatolites from the Nabberu and Officer Basins, Western Australia, and their biostratigraphic significance: South Australia Geological Survey, Report of Investigations 47, 51p.

PREISS, W. V., 1985, Stratigraphy and tectonics of the Worumba Anticline and associated intrusive breccias: Geological Survey of South Australia, Bulletin 52, 85p.

PREISS, W. V., (compiler), 1987, The Adelaide Geosyncline: late Proterozoic stratigraphy, sedimentation, palaeontology and tectonics: Geological Survey of South Australia, Bulletin 53, 438p.

STEVENS, M. K., and GREY, K., 1997, Skates Hills Formation and Tarcunyah Group, Officer Basin — carbonate cycles, stratigraphic position, and hydrocarbon prospectivity: Western Australia Geological Survey, Annual Review 1996–97, p. 55–60.

SOUTHGATE, P. N., 1989, Relationships between cyclicity and stromatolite form in Late Proterozoic Bitter Springs Formation, Australia: Sedimentology, v. 36, p. 323–339.

WALTER, M. R., 1972, Stromatolites and the biostratigraphy of the Australian Precambrian and Cambrian: Palaeontological Association, London, Special Papers in Palaeontology, v. 11, 190p.

WALTER, M. R., KRYLOV, I. N., and PREISS, W. V., 1979, Stromatolites from Adelaidean (Late Proterozoic) sequences in central and South Australia: *Alcheringa*, v. 3, p. 287–305.

Appendix 9
Geochemistry
(by K. A. R. Ghori)

Introduction

Eighty-nine core samples from all likely source-rock lithologies and three samples from sandstone for apatite fission-track analysis (AFTA) were collected from stratigraphic drillholes Empress 1 and 1A; 7 samples from Empress 1 and 85 samples from Empress 1A. Of these, one was from the Permian Paterson Formation and 91 were from the Neoproterozoic successions. The numbers of samples analysed from different formations are summarized in Table 9.1.

Table 9.1. Number of core samples analysed

Well	*Formation*	*Samples*
Empress 1	?Lupton Formation	1
	Kanpa Formation	6
	Total	**7**
Empress 1A	Paterson Formation	1
	?Lupton Formation	2
	Kanpa Formation	57
	Hussar Formation	16
	Browne Formation	2
	?Lefroy Formation	2
	Pre-Browne Formation	5
	Total	**85**

Analytical work was carried out by Geotechnical Services to evaluate source potential, Keiraville Konsultants to evaluate thermal maturity, and Geotrack International to evaluate maximum palaeotemperatures and their timing. The number and type of geochemical analyses carried out are summarized in Table 9.2.

Hydrocarbon-generating potential

The total organic carbon (TOC) content is used to measure organic richness and to select samples for Rock-Eval analysis. Genetic potential yields ($S_1 + S_2$) from the Rock-Eval pyrolysis are used to quantify the hydrocarbon-

Table 9.2. Geochemical analyses carried out on core samples from Empress 1 and 1A

Well	*Analysis type*	*Samples*	*Purpose*	*Analyst*
Empress 1	Total organic carbon (TOC)	7	Source potential	Geotech
	Rock-Eval pyrolysis	2	Source potential	Geotech
	Organic petrology	2	Source maturity	KK
Empress 1A	Total organic carbon (TOC)	81	Source potential	Geotech
	Rock-Eval pyrolysis	18	Source potential	Geotech
	Pyrolysis-gas chromatography	3	Source potential	Geotech
	Extract liquid and gas chromatography	3	Source potential	Geotech
	Organic petrology	11	Source maturity	KK
	Apatite fission-track analysis (AFTA)	3	Source maturity	Geotrack

NOTES: Geotech: Geotechnical Services
Geotrack: Geotrack International
KK: Keiraville Konsultants

Table 9.3. TOC and Rock-Eval data of core samples from Empress 1 and 1A

Well	*GSWA number*	*Depth 1 (m)*	*Depth 2 (m)*	*TOC (%)*	T_{max} *(°C)*	S_1	S_2	S_3	$S_1 + S_2$	*PI*	*HI*	*OI*
Empress 1	106420	419.55	–	0.02	–	–	–	–	–	–	–	–
Empress 1	106425	494.65	–	0.02	–	0.00	0.05	0.02	0.05	0.00	250	100
Empress 1A	154071	494.90	–	0.02	–	–	–	–	–	–	–	–
Empress 1	106424	501.60	–	0.10	–	–	–	–	–	–	–	–
Empress 1	106423	516.60	–	0.15	–	0.03	0.10	0.03	0.13	0.23	67	20
Empress 1A	154070	517.00	–	0.11	–	–	–	–	–	–	–	–
Empress 1A	154601	520.60	–	0.03	–	–	–	–	–	–	–	–
Empress 1	106422	524.20	–	0.02	–	–	–	–	–	–	–	–
Empress 1A	154067	555.00	–	0.12	–	–	–	–	–	–	–	–
Empress 1A	154610	587.85	–	1.38	418	0.43	6.20	0.11	6.63	0.06	449	8
Empress 1A	154600	588.35	–	1.52	413	0.46	6.44	0.15	6.90	0.07	424	10
Empress 1A	154066	591.40	–	0.06	–	–	–	–	–	–	–	–
Empress 1	106427	598.10	–	0.08	–	–	–	–	–	–	–	–
Empress 1	106429	608.90	–	0.06	–	–	–	–	–	–	–	–
Empress 1A	106433	620.89	620.98	0.05	–	–	–	–	–	–	–	–
Empress 1A	106434	623.08	623.14	0.07	–	–	–	–	–	–	–	–
Empress 1A	154063	629.40	–	0.57	417	0.05	0.51	0.24	0.56	0.09	89	42
Empress 1A	106435	641.87	642.00	0.41	420	0.03	0.36	0.34	0.39	0.08	88	83
Empress 1A	154061	644.50	–	0.05	–	–	–	–	–	–	–	–
Empress 1A	154060	651.90	–	0.06	–	–	–	–	–	–	–	–
Empress 1A	154059	662.30	–	0.05	–	–	–	–	–	–	–	–
Empress 1A	154602	665.10	–	0.17	–	–	–	–	–	–	–	–
Empress 1A	106436	681.60	–	0.08	–	–	–	–	–	–	–	–
Empress 1A	154058	685.10	–	0.13	–	–	–	–	–	–	–	–
Empress 1A	154057	697.10	–	0.05	–	–	–	–	–	–	–	–
Empress 1A	154056	704.60	–	0.07	–	–	–	–	–	–	–	–
Empress 1A	154055	707.90	–	0.07	–	–	–	–	–	–	–	–
Empress 1A	154054	712.40	–	0.07	–	–	–	–	–	–	–	–
Empress 1A	154053	728.70	–	0.15	–	–	–	–	–	–	–	–
Empress 1A	154052	733.90	–	0.51	423	0.07	0.65	0.31	0.72	0.10	127	61
Empress 1A	154599	737.00	–	0.09	–	–	–	–	–	–	–	–
Empress 1A	154051	737.40	–	0.84	426	0.18	2.33	0.29	2.51	0.07	277	35
Empress 1A	154598	738.80	–	0.16	–	–	–	–	–	–	–	–
Empress 1A	154603	739.20	–	0.02	–	–	–	–	–	–	–	–
Empress 1A	154597	740.40	–	1.10	–	0.05	0.18	0.13	0.23	0.22	16	12
Empress 1A	106437	745.70	–	0.12	–	–	–	–	–	–	–	–
Empress 1A	154604	747.30	–	0.21	–	–	–	–	–	–	–	–
Empress 1A	154596	750.20	–	0.16	–	–	–	–	–	–	–	–
Empress 1A	154595	756.70	–	0.51	411	0.06	1.82	0.12	1.88	0.03	357	24
Empress 1A	154605	757.60	–	0.70	428	0.05	1.62	0.18	1.67	0.03	231	26
Empress 1A	154594	757.80	–	0.38	423	0.05	0.61	0.09	0.66	0.08	161	24
Empress 1A	154593	758.10	–	0.27	414	0.04	0.40	0.03	0.44	0.09	148	11
Empress 1A	154592	760.80	–	0.45	432	0.05	0.59	0.03	0.64	0.08	131	7
Empress 1A	154047	765.40	–	0.14	–	–	–	–	–	–	–	–
Empress 1A	154606	765.80	–	0.43	415	0.12	0.78	0.15	0.90	0.13	181	35
Empress 1A	154591	766.20	–	0.38	411	0.12	0.65	0.03	0.77	0.16	171	8
Empress 1A	154607	768.20	–	0.93	421	0.66	4.02	0.44	4.68	0.14	432	47
Empress 1A	154590	768.70	–	0.10	–	–	–	–	–	–	–	–
Empress 1A	154046	768.90	–	0.27	–	–	–	–	–	–	–	–
Empress 1A	154045	772.30	–	0.25	–	–	–	–	–	–	–	–
Empress 1A	154044	786.10	–	0.05	–	–	–	–	–	–	–	–
Empress 1A	106438	792.20	–	0.18	–	–	–	–	–	–	–	–
Empress 1A	154042	799.40	–	0.16	–	–	–	–	–	–	–	–
Empress 1A	154041	803.00	–	0.12	–	–	–	–	–	–	–	–
Empress 1A	154040	808.20	–	0.12	–	–	–	–	–	–	–	–
Empress 1A	154038	821.15	–	0.03	–	–	–	–	–	–	–	–
Empress 1A	154037	826.00	–	0.06	–	–	–	–	–	–	–	–
Empress 1A	154036	829.50	–	0.19	–	–	–	–	–	–	–	–
Empress 1A	154035	830.30	–	0.30	–	–	–	–	–	–	–	–
Empress 1A	154034	834.00	–	0.07	–	–	–	–	–	–	–	–
Empress 1A	154033	838.70	–	0.25	–	–	–	–	–	–	–	–
Empress 1A	154032	842.80	–	0.11	–	–	–	–	–	–	–	–
Empress 1A	154031	843.90	–	0.11	–	–	–	–	–	–	–	–
Empress 1A	154028	971.70	–	0.03	–	–	–	–	–	–	–	–
Empress 1A	154027	973.60	–	0.07	–	–	–	–	–	–	–	–
Empress 1A	154608	974.20	–	0.06	–	–	–	–	–	–	–	–
Empress 1A	154609	1 072.30	–	1.07	–	0.01	0.05	0.04	0.06	0.17	5	4
Empress 1A	154026	1 074.70	–	0.90	–	0.03	0.11	0.43	0.14	0.21	12	48
Empress 1A	154025	1 077.50	–	0.37	–	–	–	–	–	–	–	–
Empress 1A	154024	1 083.30	–	0.10	–	–	–	–	–	–	–	–
Empress 1A	106439	1 089.80	–	0.07	–	–	–	–	–	–	–	–
Empress 1A	106440	1 100.00	–	0.05	–	–	–	–	–	–	–	–
Empress 1A	154020	1 142.00	–	0.02	–	–	–	–	–	–	–	–
Empress 1A	154019	1 144.10	–	0.02	–	–	–	–	–	–	–	–
Empress 1A	154018	1 155.50	–	0.03	–	–	–	–	–	–	–	–
Empress 1A	154017	1 165.80	–	0.01	–	–	–	–	–	–	–	–

Table 9.3. (continued)

Well	*GSWA number*	*Depth 1 (m)*	*Depth 2 (m)*	*TOC (%)*	T_{max} (°C)	S_1	S_2	S_3	$S_1 + S_2$	*PI*	*HI*	*OI*
Empress 1A	154016	1 174.40	–	0.02	–	–	–	–	–	–	–	–
Empress 1A	154015	1 209.50	–	0.03	–	–	–	–	–	–	–	–
Empress 1A	154012	1 226.00	–	0.02	–	–	–	–	–	–	–	–
Empress 1A	154011	1 448.70	–	0.02	–	–	–	–	–	–	–	–
Empress 1A	154007	1 507.00	–	0.09	–	–	–	–	–	–	–	–
Empress 1A	154006	1 522.00	–	0.01	–	–	–	–	–	–	–	–
Empress 1A	154005	1 539.30	–	0.26	450	0.13	0.69	0.15	0.82	0.16	265	58
Empress 1A	154004	1 551.00	–	0.04	–	–	–	–	–	–	–	–
Empress 1A	106445	1 560.90	–	0.02	–	–	–	–	–	–	–	–
Empress 1A	154003	1 563.90	–	0.01	–	–	–	–	–	–	–	–
Empress 1A	154002	1 569.80	–	0.01	–	–	–	–	–	–	–	–
Empress 1A	145001	1 602.30	–	0.03	–	–	–	–	–	–	–	–

NOTES: TOC: total organic carbon
T_{max}: temperature of maximum pyrolytic yield (S_2)
S_1: existing hydrocarbons (HC)
S_2: pyrolytic yield (HC)
S_3: organic carbon dioxide
$S_1 + S_2$: potential yield
PI: production index
HI: hydrogen index
OI: oxygen index

generating potential. Twenty of the 88 samples screened by TOC analysis were analysed by Rock-Eval pyrolysis to assess their hydrocarbon-generating potential. The Rock-Eval pyrolysis showed that six samples from the Kanpa Formation have fair to good hydrocarbon-generating potential. Their organic richness ranges between 0.51 and 1.52% TOC and potential yields between 1.62 and 6.44 mg/g rock. They are classified as fair to good in hydrocarbon-generating potential (Table 9.3; Figs 9.1 and 9.2). These source beds are of centimetre thickness and interbedded with dolomite between 587.5 – 588.5 and 737.4 – 768.2 m (Fig. 9.1).

Kerogen type

Pyrolysis-gas chromatography (PGC) and extract analyses were used to supplement the Rock-Eval pyrolysis to determine the type of kerogen present. A plot of Rock-Eval parameters, hydrogen index (HI) versus T_{max}, for the six source-rock samples from the Kanpa Formation indicate that the bulk chemical character of kerogen present is of oil- and gas-generating type II (Fig. 9.3).

PGC was used to evaluate the detailed molecular configuration of a kerogen to assess oil- versus gas-generating potential of three source-rock samples (588.3, 737.4, and 768.2 m). Tables 9.4 to 9.6 provide PGC data and Figure 9.4 shows pyrograms for three analysed samples. The normalized composition of pyrolysate indicates that the concentration of hydrocarbons is high with the predominance of aromatic hydrocarbons (Fig. 9.5a). High concentration of hydrocarbons indicate that the kerogen is hydrogen rich, thus hydrocarbon generating. However, a relative increase in aromatic compounds indicates a decrease in kerogen quality. This is because type III kerogens have the highest relative aromatic content (Larter, 1985). The aliphatic compounds (alkane + alkene) in the pyrolysate is limited up to 14 carbon atoms, representing mainly the gasoline to kerosene hydrocarbon range (Fig. 9.5b). The aliphatic carbon content of a kerogen, and its distribution within various structural elements, dictate the type of product, oil versus gas. In Figure 9.5c, oil proneness, expressed as C_5 to C_{31} alkanes plus alkenes (values as a percentage of S_2 from Rock-Eval), is plotted against the gas-oil generation index (GOGI), expressed as $(C_1–C_5)/C_{6+}$, and confirms that the type of kerogen present is oil and gas generating. However, cores from 588.3 and 737.4 m are more oil prone compared to core from 768.2 m.

Table 9.7 provides extract analysis data and Figure 9.6 shows their gas chromatograms. The predominance of C_{17} in n-alkane distribution of 588.3 m core indicates an algal (cyanobacteria) source (Fig. 9.7a). The high extract yields (2500 ppm) and high hydrocarbon yields as a function of TOC content indicate that core 588.3 m is a very good oil source rock (Fig. 9.7b). The lower extract yields from core 737.4 m (472 ppm) and core 768.2 m (731.5 ppm) confirm their fair source potential as suggested by their TOC content. A plot of isoprenoid/n-alkane ratios, pristane/nC_{17} versus phytane/nC_{18}, for the three samples suggest that the environment of deposition was reducing and the kerogen is type II (Fig. 9.7c).

Organic petrology confirms that the type of organic matter is liptinite type II of algal origin (lamalginite).

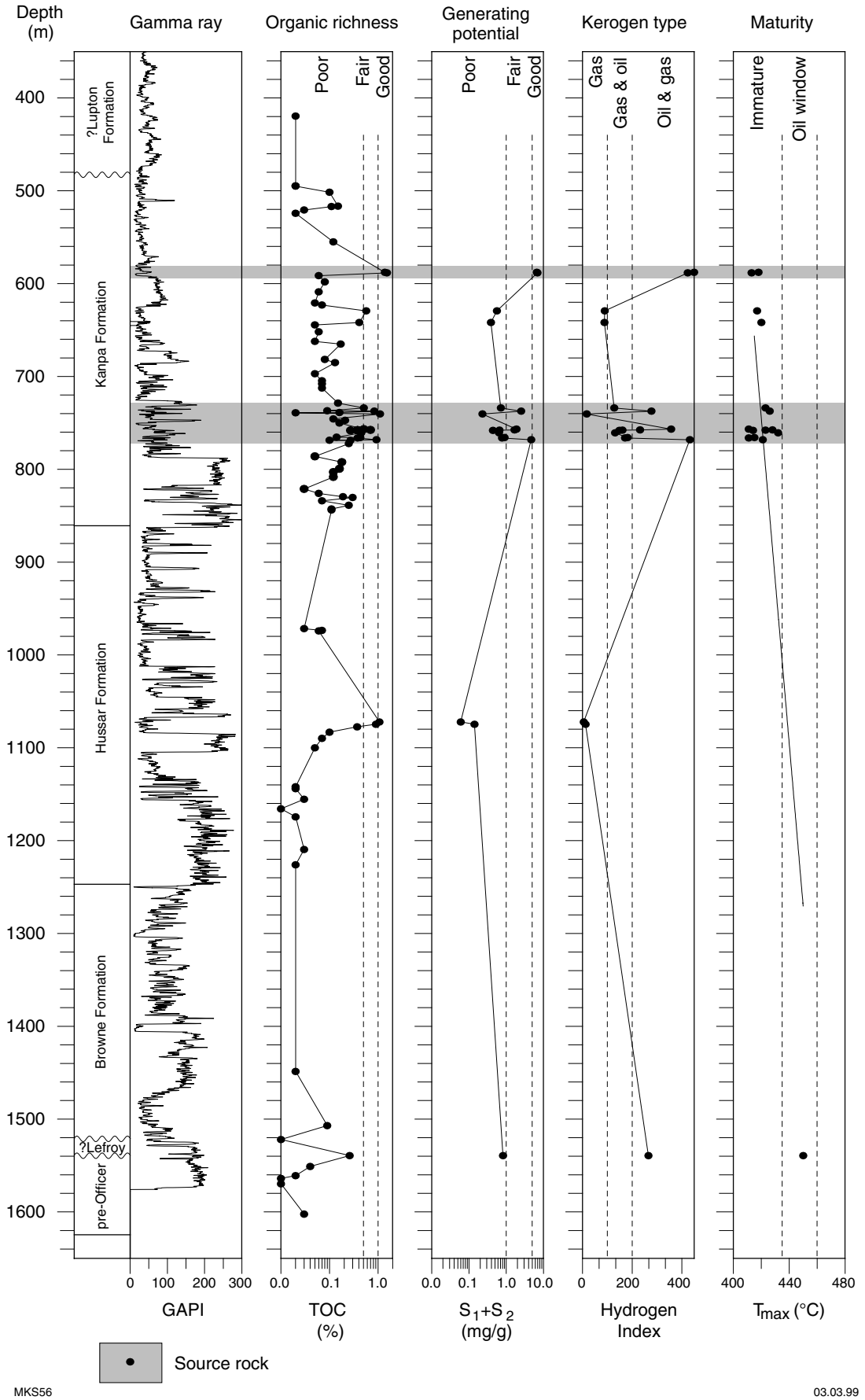

Figure 9.1. Petroleum source potential of rocks in Empress 1A

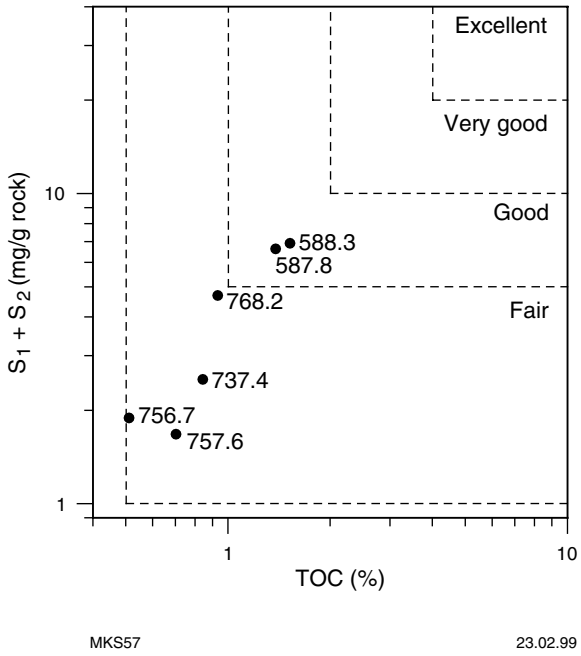

Figure 9.2. Petroleum-generating potential of source rocks in Empress 1A

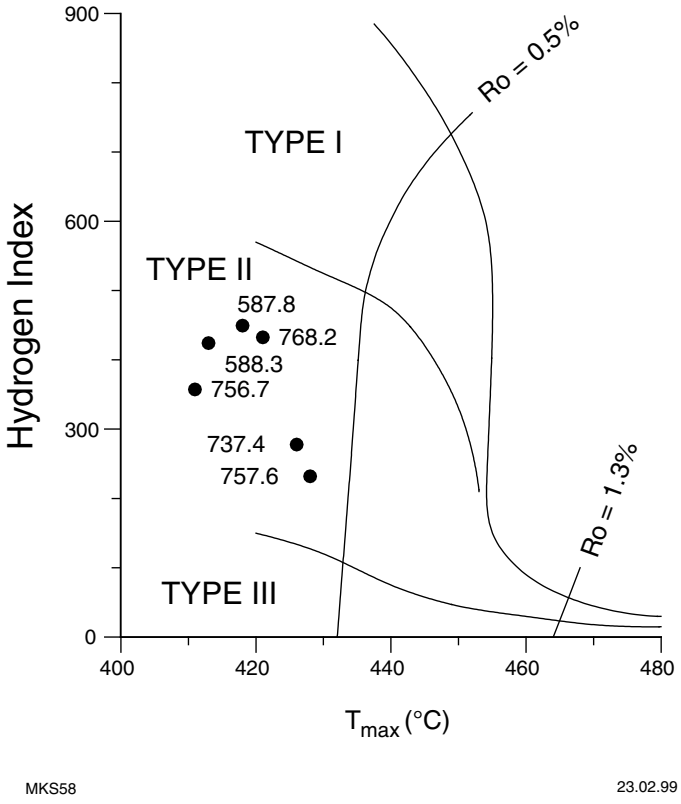

Figure 9.3. Rock-Eval kerogen typing for source rocks in Empress 1A

Table 9.4. Pyrolysis-gas chromatography data of core samples from Empress 1A: alkane and alkene component

Depth (m)	Carbon number	Alkane A	Alkane B	Alkane C	Alkene A	Alkene B	Alkene C	Alkane + Alkene A	Alkane + Alkene B	Alkane + Alkene C	Alkane/ Alkene
588.3	1	–	–	–	–	–	–	–	–	–	–
	2	–	–	–	–	–	–	–	–	–	–
	3	–	–	–	–	–	–	–	–	–	–
	4	–	–	–	–	–	–	–	–	–	–
	5	3.810	0.245	0.161	3.810	0.245	0.161	7.620	0.491	0.323	1.00
	6	2.535	0.163	0.107	1.342	0.086	0.057	3.877	0.250	0.164	1.89
	7	1.754	0.113	0.074	1.139	0.073	0.048	2.893	0.186	0.123	1.54
	8	0.940	0.061	0.040	0.916	0.059	0.039	1.856	0.120	0.079	1.03
	9	0.466	0.030	0.020	0.610	0.039	0.026	1.076	0.069	0.046	0.76
	10	0.488	0.031	0.021	0.548	0.035	0.023	1.036	0.067	0.044	0.89
	11	0.819	0.053	0.035	0.000	0.000	0.000	0.819	0.053	0.035	–
	12	0.349	0.022	0.015	0.000	0.000	0.000	0.349	0.022	0.015	–
	13	0.343	0.022	0.015	0.000	0.000	0.000	0.343	0.022	0.015	–
	14	0.310	0.020	0.013	0.000	0.000	0.000	0.310	0.020	0.013	–
	15	0.000	0.000	0.000	0.000	0.000	0.000	0.000	0.000	0.000	–
	16	0.000	0.000	0.000	0.000	0.000	0.000	0.000	0.000	0.000	–
	17	0.000	0.000	0.000	0.000	0.000	0.000	0.000	0.000	0.000	–
	18	0.000	0.000	0.000	0.000	0.000	0.000	0.000	0.000	0.000	–
	19	0.000	0.000	0.000	0.000	0.000	0.000	0.000	0.000	0.000	–
	20	0.000	0.000	0.000	0.000	0.000	0.000	0.000	0.000	0.000	–
	21	0.000	0.000	0.000	0.000	0.000	0.000	0.000	0.000	0.000	–
	22	0.000	0.000	0.000	0.000	0.000	0.000	0.000	0.000	0.000	–
	23	0.000	0.000	0.000	0.000	0.000	0.000	0.000	0.000	0.000	–
	24	0.000	0.000	0.000	0.000	0.000	0.000	0.000	0.000	0.000	–
	25	0.000	0.000	0.000	0.000	0.000	0.000	0.000	0.000	0.000	–
	26	0.000	0.000	0.000	0.000	0.000	0.000	0.000	0.000	0.000	–
	27	0.000	0.000	0.000	0.000	0.000	0.000	0.000	0.000	0.000	–
	28	0.000	0.000	0.000	0.000	0.000	0.000	0.000	0.000	0.000	–
	29	0.000	0.000	0.000	0.000	0.000	0.000	0.000	0.000	0.000	–
	30	0.000	0.000	0.000	0.000	0.000	0.000	0.000	0.000	0.000	–
	31	0.000	0.000	0.000	0.000	0.000	0.000	0.000	0.000	0.000	–
737.4	1	–	–	–	–	–	–	–	–	–	–
	2	–	–	–	–	–	–	–	–	–	–
	3	–	–	–	–	–	–	–	–	–	–
	4	–	–	–	–	–	–	–	–	–	–
	5	2.025	0.047	0.056	2.025	0.047	0.056	4.050	0.094	0.112	1.00
	6	1.766	0.041	0.049	1.966	0.046	0.055	3.732	0.087	0.104	0.90
	7	2.134	0.050	0.059	1.313	0.031	0.036	3.447	0.080	0.096	1.63
	8	1.103	0.026	0.031	0.855	0.020	0.024	1.958	0.046	0.054	1.29
	9	0.660	0.015	0.018	0.562	0.013	0.016	1.222	0.028	0.034	1.17
	10	1.077	0.025	0.030	0.374	0.009	0.010	1.451	0.034	0.040	2.88
	11	0.664	0.015	0.018	0.501	0.012	0.014	1.165	0.027	0.032	1.33
	12	0.380	0.009	0.011	0.417	0.010	0.012	0.797	0.019	0.022	0.91
	13	0.471	0.011	0.013	0.236	0.005	0.007	0.707	0.016	0.020	2.00
	14	0.313	0.007	0.009	0.302	0.007	0.008	0.615	0.014	0.017	1.04
	15	0.481	0.011	0.013	0.109	0.003	0.003	0.590	0.014	0.016	4.41
	16	0.263	0.006	0.007	0.000	0.000	0.000	0.263	0.006	0.007	–
	17	0.246	0.006	0.007	0.000	0.000	0.000	0.246	0.006	0.007	–
	18	0.110	0.003	0.003	0.000	0.000	0.000	0.110	0.003	0.003	–
	19	0.089	0.002	0.002	0.000	0.000	0.000	0.089	0.002	0.002	–
	20	0.039	0.001	0.001	0.000	0.000	0.000	0.039	0.001	0.001	–
	21	0.061	0.001	0.002	0.000	0.000	0.000	0.061	0.001	0.002	–
	22	0.036	0.001	0.001	0.000	0.000	0.000	0.036	0.001	0.001	–
	23	0.035	0.001	0.001	0.000	0.000	0.000	0.035	0.001	0.001	–
	24	0.020	0.000	0.001	0.000	0.000	0.000	0.020	0.000	0.001	–
	25	0.018	0.000	0.000	0.000	0.000	0.000	0.018	0.000	0.000	–
	26	0.015	0.000	0.000	0.000	0.000	0.000	0.015	0.000	0.000	–
	27	0.007	0.000	0.000	0.000	0.000	0.000	0.007	0.000	0.000	–
	28	0.000	0.000	0.000	0.000	0.000	0.000	0.000	0.000	0.000	–
	29	0.000	0.000	0.000	0.000	0.000	0.000	0.000	0.000	0.000	–
	30	0.000	0.000	0.000	0.000	0.000	0.000	0.000	0.000	0.000	–
	31	0.000	0.000	0.000	0.000	0.000	0.000	0.000	0.000	0.000	–

Table 9.4. (continued)

Depth (m)	Carbon number	Alkane A	Alkane B	Alkane C	Alkene A	Alkene B	Alkene C	Alkane + Alkene A	Alkane + Alkene B	Alkane + Alkene C	Alkane/ Alkene
768.2	1	–	–	–	–	–	–	–	–	–	–
	2	–	–	–	–	–	–	–	–	–	–
	3	–	–	–	–	–	–	–	–	–	–
	4	–	–	–	–	–	–	–	–	–	–
	5	2.428	0.098	0.105	3.291	0.132	0.142	5.719	0.230	0.247	0.74
	6	1.733	0.070	0.075	0.726	0.029	0.031	2.459	0.099	0.106	2.39
	7	1.107	0.045	0.048	1.831	0.074	0.079	2.938	0.118	0.127	0.60
	8	0.572	0.023	0.025	0.405	0.016	0.018	0.977	0.039	0.042	1.41
	9	0.250	0.010	0.011	0.145	0.006	0.006	0.395	0.016	0.017	1.72
	10	0.578	0.023	0.025	0.113	0.005	0.005	0.691	0.028	0.030	5.12
	11	0.461	0.019	0.020	0.300	0.012	0.013	0.761	0.031	0.033	1.54
	12	0.000	0.000	0.000	0.000	0.000	0.000	0.000	0.000	0.000	–
	13	0.000	0.000	0.000	0.000	0.000	0.000	0.000	0.000	0.000	–
	14	0.000	0.000	0.000	0.000	0.000	0.000	0.000	0.000	0.000	–
	15	0.000	0.000	0.000	0.000	0.000	0.000	0.000	0.000	0.000	–
	16	0.000	0.000	0.000	0.000	0.000	0.000	0.000	0.000	0.000	–
	17	0.000	0.000	0.000	0.000	0.000	0.000	0.000	0.000	0.000	–
	18	0.000	0.000	0.000	0.000	0.000	0.000	0.000	0.000	0.000	–
	19	0.000	0.000	0.000	0.000	0.000	0.000	0.000	0.000	0.000	–
	20	0.000	0.000	0.000	0.000	0.000	0.000	0.000	0.000	0.000	–
	21	0.000	0.000	0.000	0.000	0.000	0.000	0.000	0.000	0.000	–
	22	0.000	0.000	0.000	0.000	0.000	0.000	0.000	0.000	0.000	–
	23	0.000	0.000	0.000	0.000	0.000	0.000	0.000	0.000	0.000	–
	24	0.000	0.000	0.000	0.000	0.000	0.000	0.000	0.000	0.000	–
	25	0.000	0.000	0.000	0.000	0.000	0.000	0.000	0.000	0.000	–
	26	0.000	0.000	0.000	0.000	0.000	0.000	0.000	0.000	0.000	–
	27	0.000	0.000	0.000	0.000	0.000	0.000	0.000	0.000	0.000	–
	28	0.000	0.000	0.000	0.000	0.000	0.000	0.000	0.000	0.000	–
	29	0.000	0.000	0.000	0.000	0.000	0.000	0.000	0.000	0.000	–
	30	0.000	0.000	0.000	0.000	0.000	0.000	0.000	0.000	0.000	–
	31	0.000	0.000	0.000	0.000	0.000	0.000	0.000	0.000	0.000	–

NOTES: A: % of resolved compounds in S_2
B: mg/g rock (Rock-Eval)
C: (mg/g rock)/TOC
TOC: total organic carbon
S_2: pyrolytic yield

Thermal maturity

Organic petrology, Rock-Eval pyrolysis, and AFTA provide levels of thermal maturation for Empress 1 and 1A.

Organic petrology: Lamalginite and bitumen reflectance data can provide maturity levels for rocks older than the Devonian (Crick et al., 1988). The reflectance values of lamalginite are more reliable for moderate to high maturation levels (Cook, 1995). Thucholitic bitumen (solid bitumen), which encases radioactive minerals, shows that reflectance values on the outer rim are very similar to those of the co-existing vitrinite. Fluorescing lamalginite becomes non-fluorescing at higher levels of maturation, and both forms can occur in a single sample.

Thirteen samples were subjected to reflectance measurements on fluorescing and non-fluorescing lamalginite, reservoir and thucholitic bitumen, and their fluorescence intensity (Table 9.8; Fig. 9.8). Most of the organic matter consists of lamalginite (alginite). The reflectance values of non-fluorescing lamalginite are plotted versus depth in Figure 9.9. This plot indicates that the basal interbedded volcanic section is overmature, whereas the remaining samples are either immature, or within the oil-generative window.

Rock-Eval pyrolysis: T_{max} is a maturation parameter, in °C, at which the pyrolytic yield of hydrocarbons (from a rock sample) reaches its maximum. Production index (PI) is also a maturation parameter; that is, the ratio of already generated hydrocarbon (S_1) to potential hydrocarbon (S_2). Fifteen T_{max} and 19 PI values (Table 9.3) are plotted versus depth on Figure 9.9. This suggests that all the samples are either immature or within the oil-generative window. However, the T_{max} values are comparatively lower than the PI values.

Table 9.5. Pyrolysis-gas chromatography data of core samples from Empress 1A: aromatic and phenolic component

Depth (m)	*Type*	*Compound*	*Value*		
			A	*B*	*C*
588.3	aromatic	Benzene	1.936	0.125	0.082
		Toluene	0.638	0.041	0.027
		Ethylbenzene	0.875	0.056	0.037
		m- + p-xylene	1.679	0.108	0.071
		Styrene	0.500	0.032	0.021
		o-xylene	0.941	0.061	0.040
	phenolic	Phenol	1.193	0.077	0.051
		o-cresol	0.358	0.023	0.015
		m- + p-cresol	0.244	0.016	0.010
		C_2 phenol	0.194	0.012	0.008
		C_2 phenol	0.393	0.025	0.017
737.7	aromatic	Benzene	2.092	0.049	0.058
		Toluene	2.412	0.056	0.067
		Ethylbenzene	0.853	0.020	0.024
		m- + p-xylene	1.845	0.043	0.051
		Styrene	0.350	0.008	0.010
		o-xylene	0.957	0.022	0.027
	phenolic	Phenol	1.124	0.026	0.031
		o-cresol	0.000	0.000	0.000
		m- + p-cresol	0.000	0.000	0.000
		C_2 phenol	0.000	0.000	0.000
		C_2 phenol	0.000	0.000	0.000
768.2	aromatic	Benzene	4.122	0.166	0.178
		Toluene	0.202	0.008	0.009
		Ethylbenzene	0.661	0.027	0.029
		m- + p-xylene	2.333	0.094	0.101
		Styrene	0.181	0.007	0.008
		o-xylene	0.994	0.040	0.043
	phenolic	Phenol	1.937	0.078	0.084
		o-cresol	0.349	0.014	0.015
		m- + p-cresol	0.455	0.018	0.020
		C_2 phenol	0.432	0.017	0.019
		C_2 phenol	0.219	0.009	0.009

NOTES: A: % of resolved compounds in S_2
B: mg/g rock (Rock-Eval)
C: (mg/g rock)/TOC
TOC: total organic carbon
S_2: pyrolytic yield

Apatite fission-track analysis (AFTA): The fission-track age is largely a function of fission-track annealing in response to increasing temperature between 70 and 120°C, whereas fission-track length reflects the style of cooling. Therefore, AFTA is useful in understanding the geothermal history of the host rocks. Tables 9.9 to 9.11 summarizes AFTA data of three samples from Empress 1A. Figure 9.10a shows chlorine weight percent, fission-track lengths, and fission-track ages for the analysed samples. The AFTA data indicate that the samples were hotter than the present-day temperature at some time after deposition (Figure 9.10b), and two cooling events were recognized (Fig. 9.10c); 600–300 Ma and 40 Ma to present day (Hegarty et al., 1998).

The 600–300 Ma palaeothermal event (Table 9.9) encompasses two major tectonic events of the basin: the Petermann Ranges Orogeny (570–540 Ma) and the Alice Springs Orogeny (~290 Ma). The Petermann Ranges Orogeny is considered to be the most intense structuring event of the basin (Lambeck, 1984; Perincek, 1996), and was used as the major erosional episode in maturity modelling of Empress 1A.

Present-day temperature: The present-day temperature is available from two runs of 4 wireline logs: dual resistivity, gamma ray, and caliper; density, neutron, gamma ray, and caliper; multi-channel sonic, gamma ray, and caliper; and 4 arm dipmeter.

Table 9.6. Pyrolysis-gas chromatography data of core samples from Empress 1A: parameter summary

Depth (m)	*Parameter*	*A*	*B*	*C*	*D*
588.3	C_1–C_4 abundance (all compounds)	23.32	1.50	0.99	–
	C_5–C_8 abundance (all resolved compounds)	36.28	2.34	1.54	–
	C_5–C_8 abundance (alkanes + alkenes)	16.25	1.05	0.69	–
	C_9–C_{14} abundance (all resolved compounds)	34.99	2.25	1.48	–
	C_9–C_{14} abundance (alkanes + alkenes)	3.93	0.25	0.17	–
	C_{15}–C_{31} abundance (all resolved compounds)	5.51	0.35	0.23	–
	C_{15}–C_{31} abundance (alkanes + alkenes)	0.00	0.00	0.00	–
	C_9–C_{31} abundance (all resolved compounds)	40.50	2.61	1.72	–
	C_9–C_{31} abundance (alkanes + alkenes)	3.93	0.25	0.17	–
	C_5–C_{31} abundance (all resolved compounds)	76.78	4.94	3.25	–
	C_5–C_{31} abundance (alkanes + alkenes)	20.18	1.30	0.85	–
	C_5–C_{31} alkane abundance	11.81	0.76	0.50	–
	C_5–C_{31} alkene abundance	8.36	0.54	0.35	–
	C_5–C_8 alkane/alkene	–	–	–	1.25
	C_9–C_{14} alkane/alkene	–	–	–	2.40
	C_{15}–C_{31} alkane/alkene	–	–	–	–
	C_5–C_{31} alkane/alkene	–	–	–	1.41
	$(C_1$–$C_5)/C_{6+}$	–	–	–	0.46
	R (m + p-xylene/n-octene)	–	–	–	1.83
737.4	C_1–C_4 abundance (all compounds)	17.43	0.41	0.48	–
	C_5–C_8 abundance (all resolved compounds)	45.13	1.05	1.25	–
	C_5–C_8 abundance (alkanes + alkenes)	13.19	0.31	0.37	–
	C_9–C_{14} abundance (all resolved compounds)	32.78	0.76	0.91	–
	C_9–C_{14} abundance (alkanes + alkenes)	6.01	0.14	0.17	–
	C_{15}–C_{31} abundance (all resolved compounds)	4.65	0.11	0.13	–
	C_{15}–C_{31} abundance (alkanes + alkenes)	1.53	0.04	0.04	–
	C_9–C_{31} abundance (all resolved compounds)	37.44	0.87	1.04	–
	C_9–C_{31} abundance (alkanes + alkenes)	7.54	0.18	0.21	–
	C_5–C_{31} abundance (all resolved compounds)	82.57	1.92	2.29	–
	C_5–C_{31} abundance (alkanes + alkenes)	20.73	0.48	0.58	–
	C_5–C_{31} alkane abundance	12.01	0.28	0.33	–
	C_5–C_{31} alkene abundance	8.71	0.20	0.24	–
	C_5–C_8 alkane/alkene	–	–	–	1.14
	C_9–C_{14} alkane/alkene	–	–	–	1.46
	C_{15}–C_{31} alkane/alkene	–	–	–	13.03
	C_5–C_{31} alkane/alkene	–	–	–	1.38
	$(C_1$–$C_5)/C_{6+}$	–	–	–	0.37
	R (m + p-xylene/n-octene)	–	–	–	2.16
768.2	C_1–C_4 abundance (all compounds)	31.50	1.27	1.36	–
	C_5–C_8 abundance (all resolved compounds)	44.03	1.77	1.90	–
	C_5–C_8 abundance (alkanes + alkenes)	12.09	0.49	0.52	–
	C_9–C_{14} abundance (all resolved compounds)	20.21	0.81	0.87	–
	C_9–C_{14} abundance (alkanes + alkenes)	1.85	0.07	0.08	–
	C_{15}–C_{31} abundance (all resolved compounds)	4.25	0.17	0.18	–
	C_{15}–C_{31} abundance (alkanes + alkenes)	0.00	0.00	0.00	–
	C_9–C_{31} abundance (all resolved compounds)	24.45	0.98	1.06	–
	C_9–C_{31} abundance (alkanes + alkenes)	1.85	0.07	0.08	–
	C_5–C_{31} abundance (all resolved compounds)	68.48	2.75	2.96	–
	C_5–C_{31} abundance (alkanes + alkenes)	13.94	0.56	0.60	–
	C_5–C_{31} alkane abundance	7.13	0.29	0.31	–
	C_5–C_{31} alkene abundance	6.81	0.27	0.29	–
	C_5–C_8 alkane/alkene	–	–	–	0.93
	C_9–C_{14} alkane/alkene	–	–	–	2.31
	C_{15}–C_{31} alkane/alkene	–	–	–	–
	C_5–C_{31} alkane/alkene	–	–	–	1.05
	$(C_1$–$C_5)/C_{6+}$	–	–	–	0.78
	R (m + p-xylene/n-octene)	–	–	–	5.76

NOTES: A: % of resolved compounds in S_2
B: mg/g rock (Rock-Eval)
C: (mg/g rock)/TOC
D: ratio, no unit
TOC: total organic carbon
S_2: pyrolytic yield

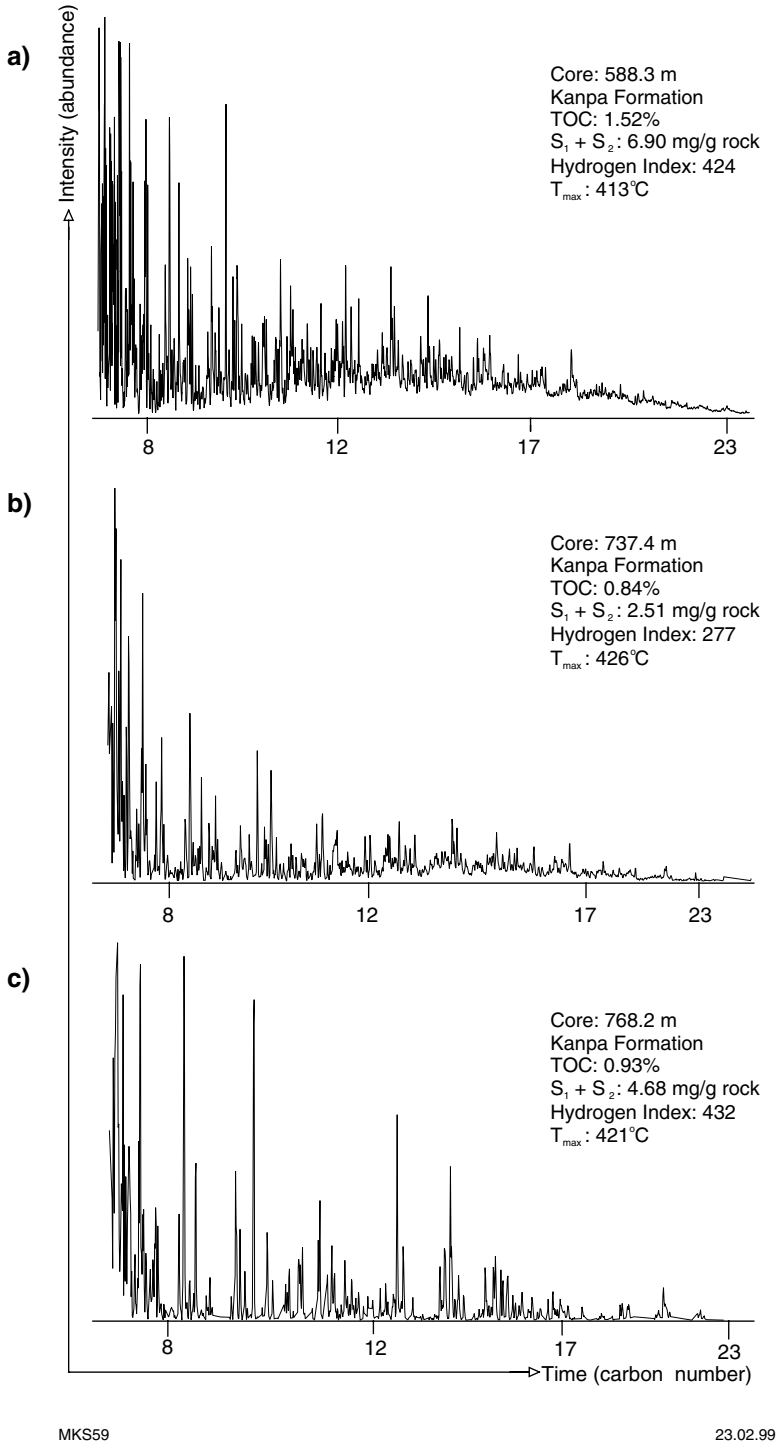

Figure 9.4. Pyrolysis-gas chromatograms for samples from Empress 1A: a) 588.3 m; b) 737.4 m; c) 768.2 m

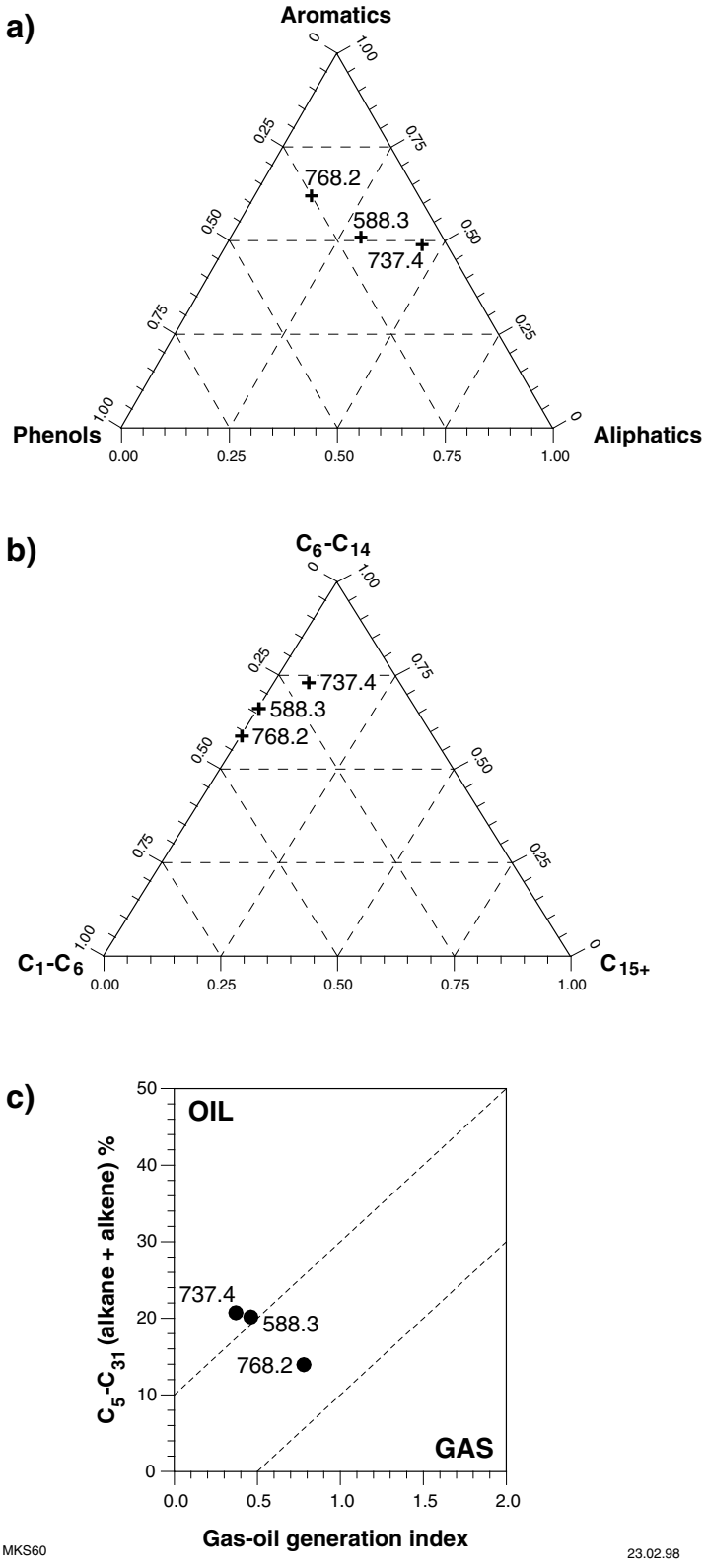

Figure 9.5. Pyrolysis-gas chromatographic kerogen typing in Empress 1A: a) normalized phenolic, aromatic, and aliphatic compounds in pyrolysate; b) normalized alkane and alkene compound distribution in pyrolysate; c) gas–oil generation index versus C_5–C_{31} alkane plus alkane percent plot

Table 9.7. Saturate-gas chromatography data of core samples from Empress 1A: alkane composition and n-alkane distribution

Parameter	*Unit*	*Sample 1*	*Sample 2*	*Sample 3*
Depth	m	588.3	737.4	768.2
Rock extracted	g	19.4	14.8	10.0
Total extract	ppm	2500.0	472.0	731.5
Loss on column	ppm	390.9	–	–
Saturates	ppm	838.5	–	–
Aromatics	ppm	524.7	–	–
NSOs	ppm	745.9	–	–
Saturates	%	39.8	–	–
Aromatics	%	24.8	–	–
NSOs	%	34.4	–	–
EOM (mg)/TOC (g)	ratio	164.5	–	–
SAT. (mg)/TOC (g)	ratio	55.2	–	–
SAT./AROM.	ratio	1.6	–	–
HC/Non-HC	ratio	1.8	–	–
Pristane/Phytane	ratio	2.51	1.55	1.52
Pristane/n-C_{17}	ratio	0.29	1.34	0.26
Phytane/ n-C_{18}	ratio	0.34	1.18	0.40
CPI (1)	ratio	1.34	1.19	1.43
CPI (2)	ratio	1.42	1.18	1.35
$(C_{21}+C_{22})/(C_{28}+C_{29})$	ratio	1.67	1.69	2.00
n-C_{12}	%	2.7	7.1	11.4
n-C_{13}	%	4.7	10.5	23.5
n-C_{14}	%	5.4	10.2	19.3
n-C_{15}	%	9.0	8.1	8.9
n-C_{16}	%	7.1	6.7	5.6
n-C_{17}	%	19.9	7.1	8.2
i-C_{19}	%	5.8	9.5	2.1
n-C_{18}	%	6.8	5.2	3.5
i-C_{20}	%	2.3	6.1	1.4
n-C_{19}	%	7.1	4.8	3.2
n-C_{20}	%	3.5	3.9	2.1
n-C_{21}	%	4.4	3.1	2.1
n-C_{22}	%	2.1	2.5	1.4
n-C_{23}	%	2.7	2.3	1.3
n-C_{24}	%	1.9	1.8	0.9
n-C_{25}	%	2.2	1.9	1.0
n-C_{26}	%	1.8	1.8	0.7
n-C_{27}	%	2.7	1.8	0.7
n-C_{28}	%	1.6	1.3	0.6
n-C_{29}	%	2.3	2.0	1.1
n-C_{30}	%	2.0	1.2	0.4
n-C_{31}	%	2.2	1.0	0.4

NOTES: CPI: carbon preference index
NSOs: nitrogen, sulfur, and oxygen compounds
EOM: extractable organic matter
TOC: total organic carbon
SAT.: saturates
AROM.: aromatics
HC: hydrocarbons
n: normal
i: iso

$$\text{CPI (1)} = \frac{(C_{23} + C_{25} + C_{27} + C_{29}) \text{ wt \%} + (C_{25} + C_{27} + C_{29} + C_{31}) \text{ wt \%}}{2 \times (C_{24} + C_{26} + C_{28} + C_{30}) \text{ wt \%}}$$

$$\text{CPI (2)} = \frac{(C_{23} + C_{25} + C_{27}) \text{ wt \%} + (C_{25} + C_{27} + C_{29}) \text{ wt \%}}{2 \times (C_{24} + C_{26} + C_{28}) \text{ wt \%}}$$

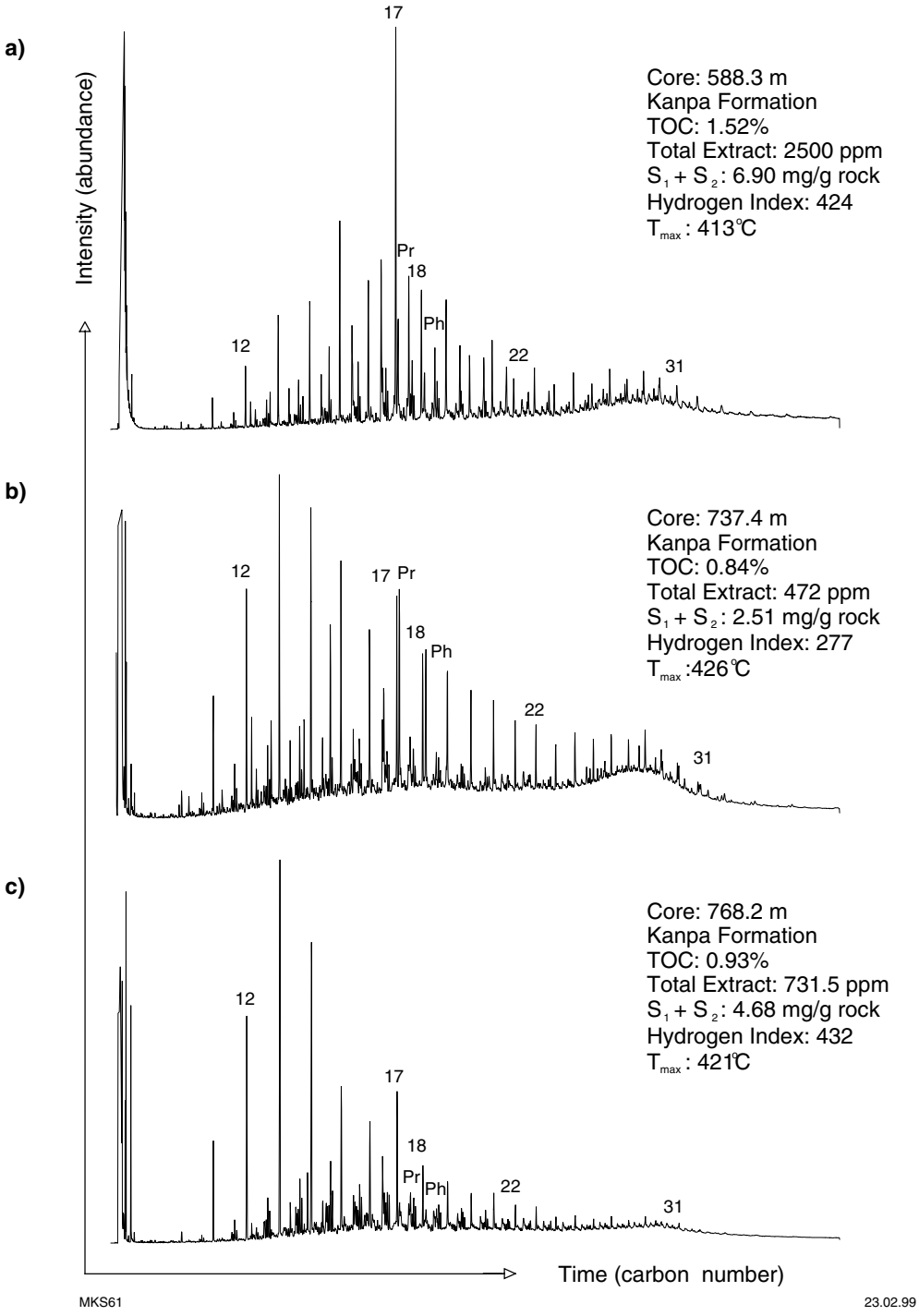

Figure 9.6. Gas chromatograms for samples from Empress 1A: a) 588.3 m; b) 737.4 m; c) 768.2 m

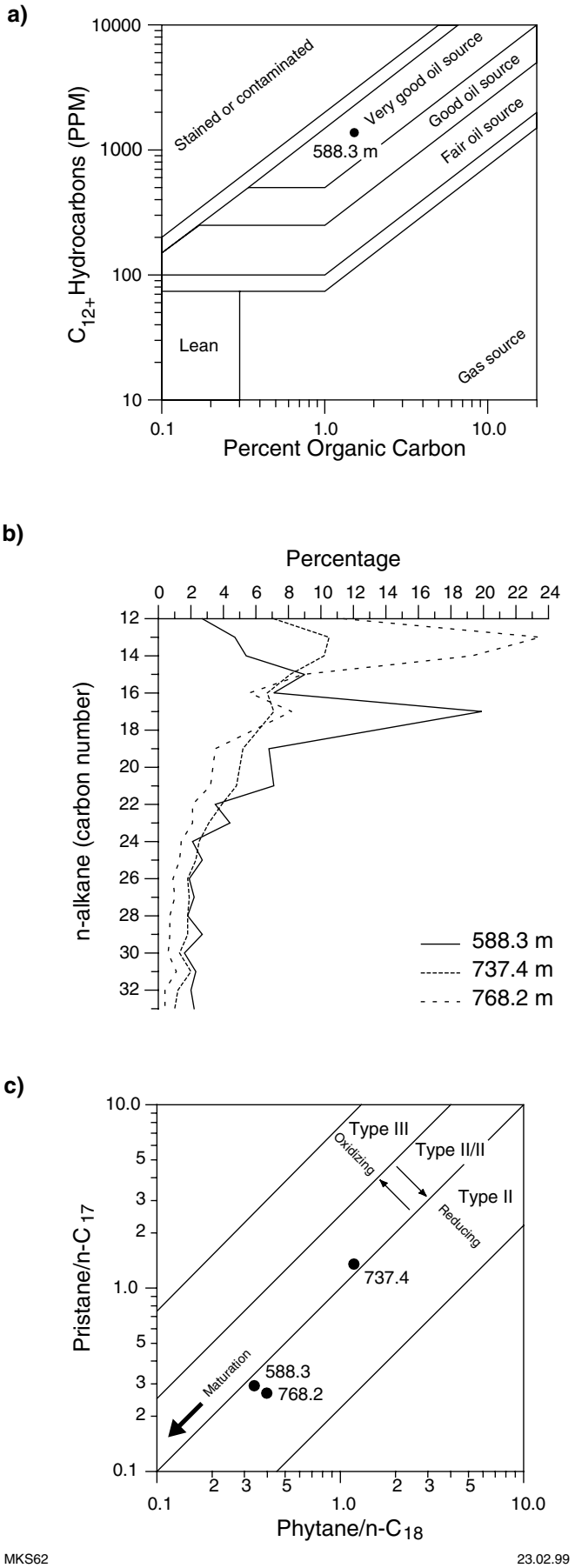

Figure 9.7. Liquid-gas chromatographic kerogen typing in Empress 1A: a) source rock rating as a function of C_{12+} hydrocarbon yields versus TOC content; b) n-alkane distribution in C_{12}–C_{31} chain length; c) kerogen type and environment of deposition as a function of pristane/n-C_{17} versus phytane/n-C_{18} plot

Table 9.8. Vitrinite reflectance data for core samples from Empress 1 and 1A

Well	*Depth (m)*	*Mean (% Ro)*	*Minimum (% Ro)*	*Maximum (% Ro)*	*Number of readings*	*Description including liptinite fluorescence characteristics*
Empress 1A	360.3	?0.95	0.67	1.029	?4	Liptinite absent (Impure sandstone. DOM spare, ?bitumen only, ??bitumen rare, macerals absent. Iron oxide present in the matrix of the sandstone. Mineral fluorescence strong from some composite sand grains, weak dull orange from matrix outside dark patch, absent from matrix in dark patch. These minerals show strong bireflectance and probably represent hematite. The absence of fluorescence from the matrix within the dark patch is associated with the iron oxides and is probably due to quenching of secondary fluorescence by these oxides. The dark patch seems to be of secondary origin and related to mineralization, and not the presence of organic matter)
Empress 1	516.6	0.56	0.52	0.60	2	Rare lamalginite and liptodetrinite, bright yellow to orange (silty claystone with igneous fragments; DOM rare to sparse; L>V; liptinite rare to sparse. FGV vitrinite and inertinite absent. Rare ?bitumen, possibly thucholitic. Rare vitrinite contaminants with Rv of around 0.4%. Mineral fluorescence pervasive dull orange. Iron oxide rare. Pyrite common)
Empress 1	602.1	1.00	0.80	1.16	5	Fluorescing liptinite absent (silty claystone; DOM rare; L only. Non-fluorescing lamalginite rare and vitrinite and inertinite absent. Rare vitrinite contaminants with Rv of around 0.4%. Mineral fluorescence pervasive dull orange. Iron oxides commonly form both disseminated in claystone and as recrystallized specks)
Empress 1A	629.4	0.53 0.15	0.41 0.11	0.63 0.18	5 2	Common lamalginite, yellow to orange and dull brown (siltstone; DOM common; L only. Liptinite common. The lamalginite forms mainly as relatively extensive thin to moderately thick layers. Some smaller lenses are present that probably correspond with single algal tests. Some non-fluorescing lamalginite is present and the sample is probably close to where non-fluorescing lamalginite becomes prominent in these Proterozoic section. Mineral fluorescence is patchy and weak dull orange. Pyrite abundant)
Empress 1A	737.4	0.57 0.19 0.64	0.46 0.05 0.53	0.68 0.35 0.74	8 7 3	Common lamalginite, bright yellow to orange and dull brown (siltstone; DOM common; L only. Liptinite common. The lamalginite forms mainly as as relatively extensive thin layers but some thick lenses are present similar in morphology to megaspores. The extensive layers range from yellowish orange to dull orange. The bright-yellow lamalginite forms smaller lenses that probably correspond with single algal tests. Some non-fluorescing lamalginite is present and the sample is probably close to where non-fluorescing lamalginite becomes prominent in these Proterozoic section. A rare organic component of uncertain origin shows a reflectance of 1.05%. Mineral fluorescence is patchy bright orange to moderate dull orange. The brighter orange patches could include some dead oil. Pyrite abundant)
Empress 1A	745.7	0.52	0.38	0.74	6	Rare lamalginite and liptodetrinite, yellow to orange (siltstone; DOM rare; liptinite only; liptinite rare, vitrinite and inertinite absent. Non-fluorescing lamalginite. Most of the lamalginite shows yellow to orange fluorescence but a proportion is non-fluorescing and the reflectance of this component is reported here. Small specks of liptodetrinite are probably derived from lamalginite, there are yellow fluorescing oil drops also present and some occurrences are difficult to distinguish from liptodetrinite. Mineral fluorescence pervasive dull orange. Pyrite abundant)
Empress 1A	768.2	– – 0.82	– – 0.77	– – 0.88	– – 3	Common lamalginite, bright yellow to orange and dull orange (calcareous siltstone interbedded with carbonate; DOM common; L only; liptinite common. The lamalginite occurs mainly as relatively extensive thin layers ranging in colour

Table 9.8. (continued)

Well	*Depth (m)*	*Mean (% Ro)*	*Minimum (% Ro)*	*Maximum (% Ro)*	*Number of readings*	*Description including liptinite fluorescence characteristics*
						from yellowish orange to dull orange. The bright-yellow lamalginite forms small lenses that probably correspond with single algal tests. Non-fluorescing lamalginite is not present. Estimation of maturation level depends on measurements of thucholitic bitumens. Mineral fluorescence variable and patchy bright orange to moderate dull orange. Pyrite common to abundant)
Empress 1A	792.2	0.87	0.56	1.13	5	Rare lamalginite yellowish orange (calcareous siltstone; DOM rare; liptinite only; liptinite rare, vitrinite and inertinite absent. Non-fluorescing lamalginite. Lamalginite showing fluorescence is less common compared with 745.7 m core and fluorescence intensities are weaker in this sample. The non-fluorescing lamalginite component is present and shows a mixed range of reflectance. Mineral fluorescence pervasive dull orange. Iron oxide rare. Pyrite common)
Empress 1A	830.3	0.57 0.31	– 0.24	– 0.43	1 10	Sparse lamalginite, rare yellow, some orange but most dull orange (siltstone; DOM sparse; L only; liptinite sparse. The lamalginite occurs mainly as very thin extensive layers up to 0.01 mm thick. Mineral fluorescence pervasive weak dull orange but rapid positive alteration on prolonged irradiation. Pyrite common to abundant)
Empress 1A	1 074.7	– –	– –	– –	– –	Fluorescing liptinite seems to be absent (siltstone, calcareous, ?dolomitic; DOM probably absent, possible rare liptinite; liptinite rare or absent. Some orange-fluorescing lines are present but these seem to represent grain boundaries rather than liptinite. Mineral fluorescence pervasive very weak dull orange, slightly brighter dull orange from ?dolomite. Very weak positive alteration on prolonged irradiation. Pyrite common)
Empress 1A	1 089.9	0.90	0.66	1.26	4	Rare liptodetrinite yellowish orange (fine-grained siltstone; DOM rare; liptinite only; liptinite rare, vitrinite and inertinite absent. Non-fluorescing lamalginite. Lenses of diffuse organic matter are present and the fluorescing liptodetrinite is associated with some of the diffuse organic matter. Organic matter is less abundant compared with the other samples from Empress 1A. Mineral fluorescence very weak to absent. Iron oxide common. Pyrite common to abundant)
Empress 1A	1 539.3	3.27 2.14	2.88 1.74	4.26 4.03	22 5	Fluorescing liptinite absent (siltstone, calcareous, dolomitic; DOM sparse, highly coalified; liptinite sparse, vitrinite and inertinite absent. Rmin is 2.14% and bireflectance ratio is about 0.40 with bireflectance being distinct on rotation of the stage. Mineral fluorescence is extremely weak to absent. Pyrite common)
Empress 1A	1 560.9	–	–	–	–	Fluorescing liptinite absent (fine-grained siltstone; DOM absent. Fine-grained, recrystallized iron oxides abundant to major, possible magnetite, no bireflectance being detected. Lesser amounts of diffuse ferric oxides are also present showing red internal reflectance. The black colour of the rock in hand specimen is due to the presence of iron oxides. This lithology is markedly different from that at 602.1 m. Mineral fluorescence pervasive, weak dull orange. Pyrite abundant)

NOTES: DOM: dispersed organic matter; L: liptinite; V: vitrinite; I: inertinite

The dark patch (360.3 m) and the black sample (1560.9 m) both owe their colouration to the presence of iron oxides rather than the presence of organic matter. Organic matter is doubtful in the sample from 360.3 m, is present in the samples from 516.6 and 602.1 m, and absent in the sample from 1560.9 m. The sample from 516.6 m contains rare, near-spherical grey inclusions that represent a bitumen phase, possibly thucholitic in character. Small amounts of moderate- to bright-fluorescing lamalginite is present. The sample from 602.1 m contains no fluorescing liptinite but does contain rare lamellae that represent non-fluorescing lamalginite. The sample from 516.6 m is mid- to late-mature, and the sample from 602.1 m is late to marginally overmature for oil.

From the liptinite fluorescence, the sample from 745.7 m is late mature for oil generation and an equivalent vitrinite reflectance of about 0.7 – 0.8% can be inferred from the fluorescence colour and intensity, and the reflectance. The sample from 792.2 m seems to represent a horizon from close to the effective end of oil-generation window with the lamalginite present being interpreted as the more resistant component of the alginite population. In the sample from 1089.9 m, it is concluded that all of the fluorescing lamalginite has been altered and that the liptodetrinite found represents moieties not broken down during oil generation. A reflectance equivalent for the sample from 1089.9 m of about 1.1 – 1.3% is inferred. The mineral fluorescence in the sample from 1089.9 m could indicate an even higher level of maturation, but this would be difficult to reconcile with the fluorescing liptodetrinite.

The upper part of the section examined is probably mid mature but tends towards being early mature for oil. Over the interval from about 700 to 1000 m, the section is late mature. The sample from 1074.7 m is barren but the mineral fluorescence suggests that this interval is probably overmature and it is possible that the material identified as liptodentrinite in a sample from 1089.9 m, may be a contaminant. The sample from 1539.3 m is undoubtedly overmature being beyond the conventional floor for gas reservoirs (it should, however, be noted that some large gas reservoirs occur in fracture porosity at this level of rank). The high level of maturation inferred from the maximum reflectance is confirmed by the large differences found between the Rmax and Rmin values – see histogram.

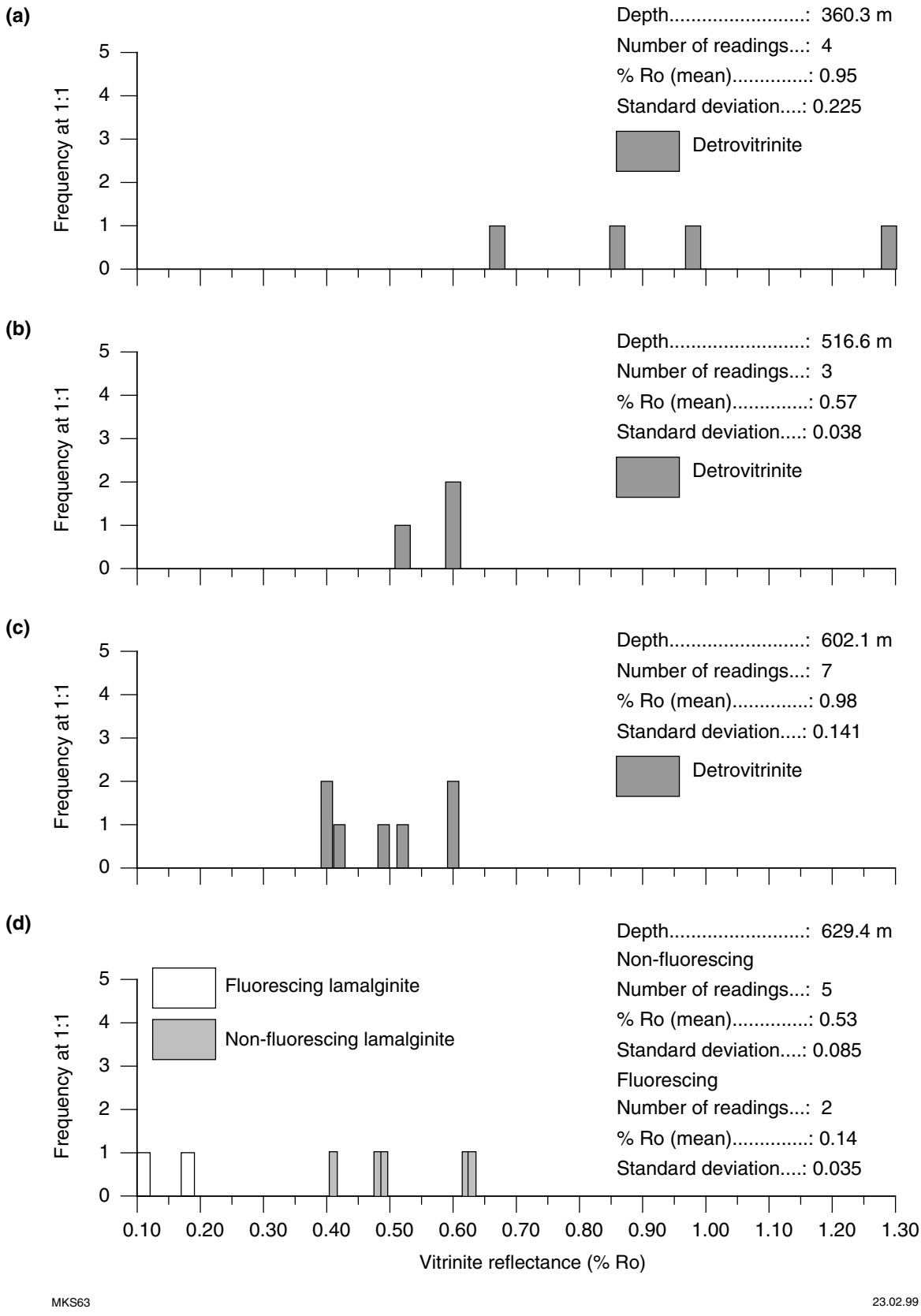

Figure 9.8. Percent reflectance histograms for samples from Empress 1A: a) 360.3 m; b) 516.6 m; c) 602.1 m; d) 629.4 m; e) 737.4 m; f) 745.7 m; g) 768.2 m; h) 792.2 m; i) 830.3 m; j) 1089.9 m; k) 1539.3 m

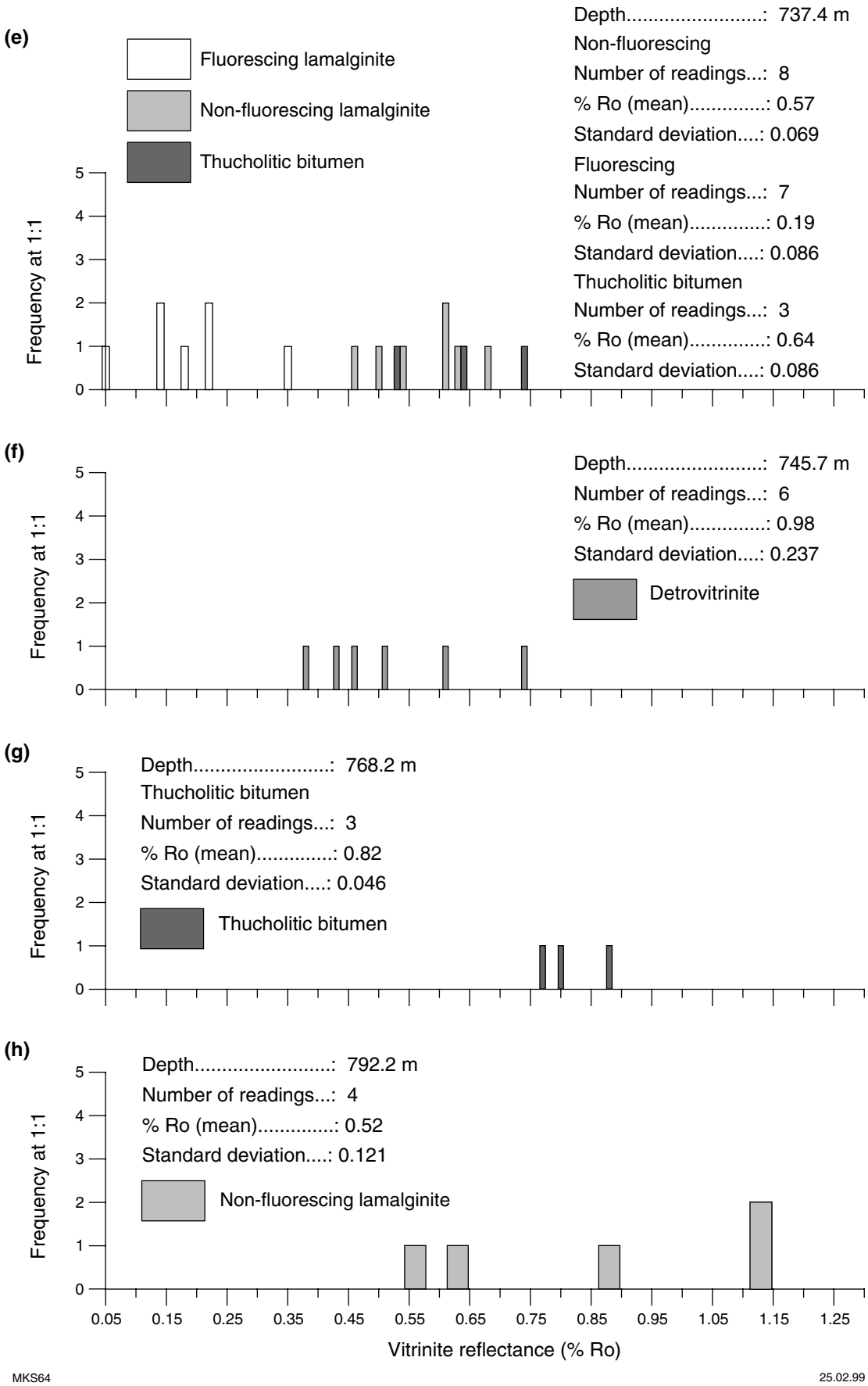

Figure 9.8. (continued)

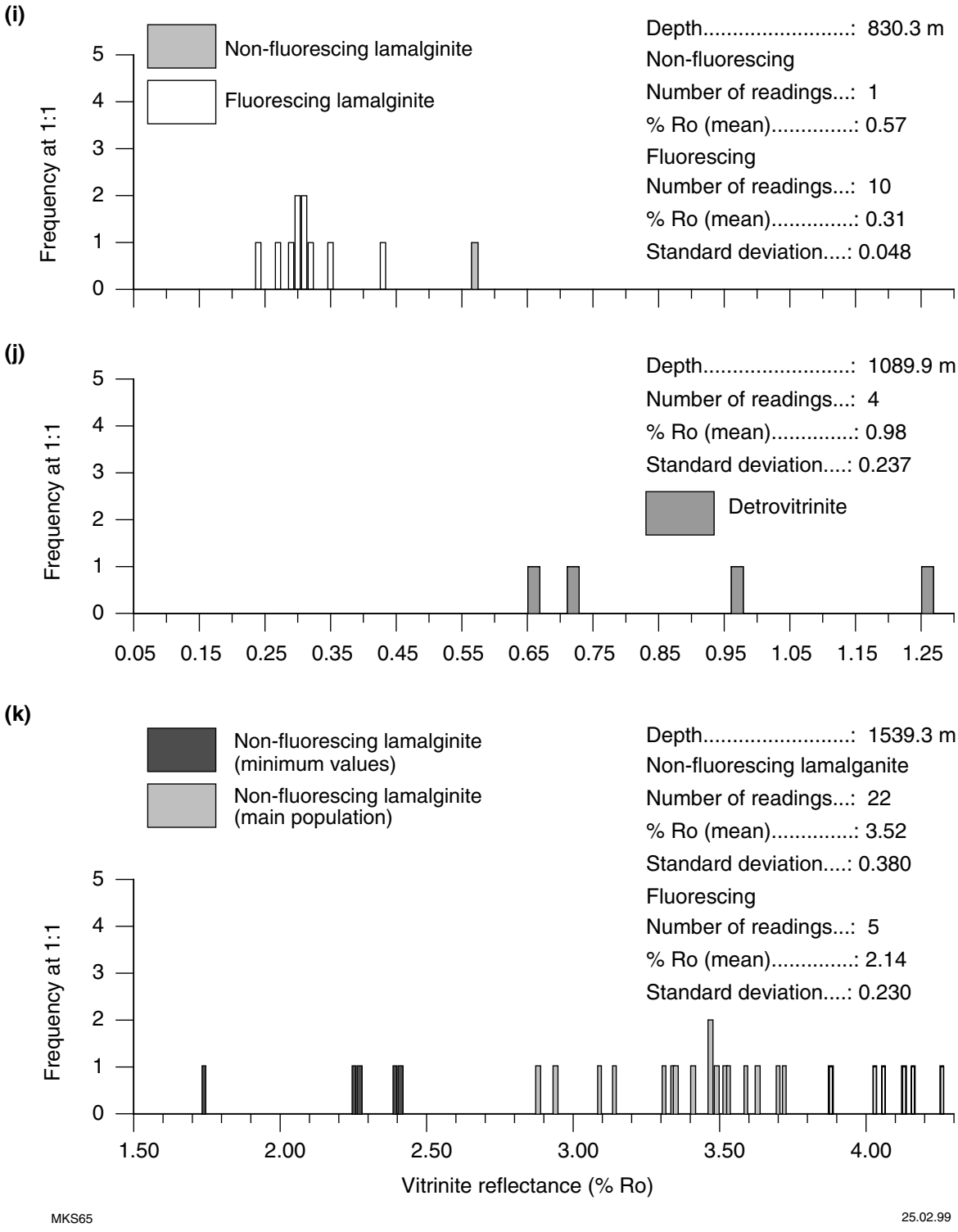

Figure 9.8. (continued)

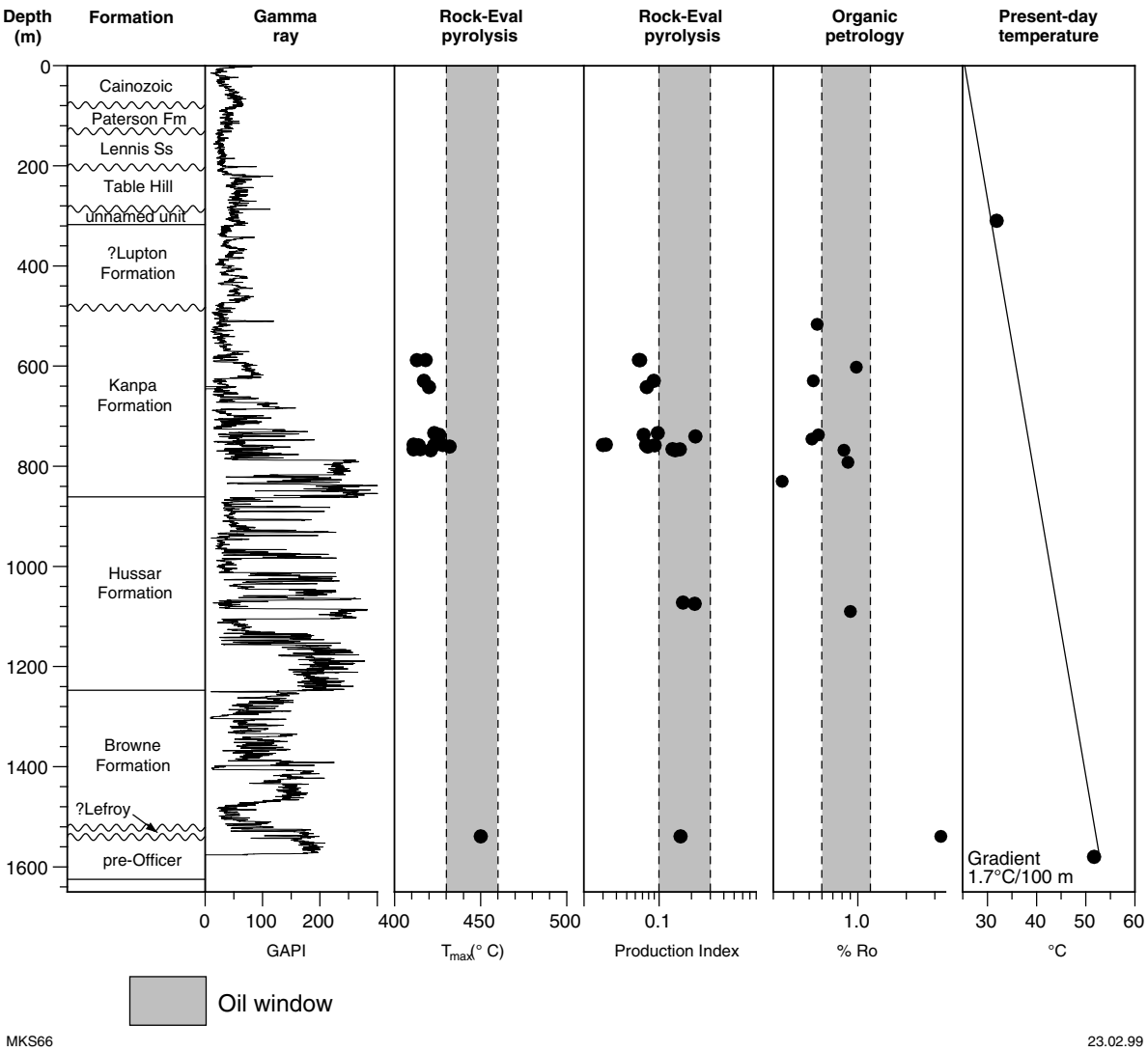

Figure 9.9. Maturation and present-day temperature as a function of depth in Empress 1A

Table 9.9. Summary of apatite fission-track data of core samples from Empress 1A (Hegarty et al., 1988)

Parameter	*Unit*	*Sample 1*	*Sample 2*[(c)]	*Sample 3*
Depth	m	123–125	318–320	557–560
Formation		Paterson	?Lupton	Kanpa
Stratigraphic age	Ma	300–270	560–530	780–750
Present-day temperature	°C	27	30	35
Mean track length	µm	11.40 ± 0.13	12.11 ± 0.14	12.19 ± 0.42
Default mean track length	µm	14.12	13.8	13.5
Apatite fission-track age	Ma	523.4 ± 44.4	588.4 ± 53.7	413.6 ± 33.7
Default fission-track age	Ma	282	569	708
Maximum palaeotemperature[(a)]	°C	n/a	90–100	>100
Onset of cooling[(a)]	Ma	n/a	640–200	600–300
Maximum palaeotemperature[(b)]	°C	75–85	70–80	80–105
Onset of cooling[(b)]	Ma	40–0	120–0	300–0

NOTES: Overlapping timing constraints from AFTA include 600–300 Ma for onset of cooling[(a)] and 40–0 Ma for onset of cooling[(b)]
(c) sample 2 designated as of ?Lupton Formation (640–600 Ma) when supplied to Geotrack International

Ma: million years before present
n/a: not applicable

Table 9.10. Apatite fission-track age data for individual apatite grains in core samples from Empress 1A (Hegarty et al., 1988)

Depth 1 (m)	*Depth 2 (m)*	*Grain*	*Ns*	*Ni*	*Na*	*RHOs (10^6)*	*RHOi (10^6)*	*Ratio*	*U (ppm)*	*Cl (wt%)*	*FT age (Ma)*
123	125	3	285	113	100	4.5290	1.7960	2.522	15.0	0.08	622.1 ± 71.0
		8	42	9	36	1.8540	0.3973	4.666	3.3	0.00	1107.6 ± 407.8
		9	79	42	40	3.1380	1.6690	1.880	14.0	0.00	469.5 ± 90.5
		10	140	107	48	4.6350	3.5420	1.309	29.7	0.02	330.2 ± 43.3
		11	25	10	16	2.4830	0.9932	2.500	8.3	0.00	616.9 ± 231.4
		12	54	15	45	1.9070	0.5297	3.600	4.4	0.00	870.6 ± 255.1
		13	26	21	49	0.8432	0.6810	1.238	5.7	0.01	312.9 ± 92.2
		14	54	26	60	1.4300	0.6886	2.077	5.8	0.00	516.5 ± 124.0
		15	78	38	45	2.7540	1.3420	2.052	11.2	0.00	510.7 ± 101.9
		16	313	265	70	7.1050	6.0160	1.181	50.4	0.02	298.8 ± 26.1
		17	32	16	30	1.6950	0.8475	2.000	7.1	0.04	498.1 ± 153.1
		18	38	20	24	2.5160	1.3240	1.900	11.1	0.00	474.1 ± 131.6
		19	110	57	100	1.7480	0.9058	1.930	7.6	0.00	481.3 ± 79.5
		20	165	50	100	2.6220	0.7945	3.300	6.7	0.00	802.4 ± 131.2
		21	67	21	35	3.0420	0.9534	3.191	8.0	0.24	777.3 ± 195.5
		22	58	24	20	4.6080	1.9070	2.416	16.0	0.00	597.2 ± 145.8
		24	136	90	40	5.4030	3.5750	1.511	29.9	0.04	379.9 ± 52.6
		25	260	136	64	6.4560	3.3770	1.912	28.3	0.03	476.9 ± 52.0
		26	75	20	48	2.4830	0.6621	3.750	5.5	0.00	904.5 ± 228.8
		27	101	43	80	2.0060	0.8541	2.349	7.2	0.01	581.2 ± 106.9
318	320	3	27	7	15	2.8600	0.7416	3.857	6.2	0.01	932.5 ± 396.2
		5	115	63	18	10.1500	5.5620	1.825	46.4	0.00	458.1 ± 72.8
		8	61	10	40	2.4230	0.3973	6.099	3.3	0.66	1418.5 ± 485.3
		10	143	58	30	7.5750	3.0720	2.466	25.6	0.00	611.4 ± 96.5
		11	93	54	24	6.1580	3.5750	1.723	29.8	0.03	433.1 ± 74.9
		13	25	6	40	0.9932	0.2384	4.166	2.0	0.02	1001.8 ± 456.1
		14	51	22	18	4.5020	1.9420	2.318	16.2	0.00	576.4 ± 147.8
		15	61	13	18	5.3850	1.1480	4.691	9.6	0.33	1117.8 ± 342.7
		16	91	34	35	4.1320	1.5440	2.676	12.9	0.00	661.1 ± 134.0
		17	128	42	32	6.3560	2.0860	3.047	17.4	0.24	747.6 ± 134.4
		18	42	21	35	1.9070	0.9534	2.000	7.9	0.03	500.3 ± 134.3
		19	71	23	35	3.2240	1.0440	3.088	8.7	0.10	756.7 ± 182.6
		21	86	26	32	4.2710	1.2910	3.308	10.8	0.19	807.6 ± 182.0
		22	123	53	50	3.9090	1.6840	2.321	14.0	0.05	577.0 ± 96.0
		23	64	53	25	4.0680	3.3690	1.207	28.1	0.00	306.7 ± 57.5
		24	18	15	15	1.9070	1.5890	1.200	13.2	0.02	304.8 ± 106.9
		26	22	20	18	1.9420	1.7660	1.100	14.7	0.01	280.0 ± 86.8
		29	168	61	35	7.6280	2.7700	2.754	23.1	0.05	679.3 ± 103.1
		31	73	24	32	3.6250	1.1920	3.041	9.9	0.01	746.3 ± 176.7
		33	123	74	21	9.3070	5.6000	1.662	46.7	0.00	418.5 ± 62.5
557	560	1	65	33	18	5.7380	2.9130	1.970	24.2	0.08	495.1 ± 106.6
		2	12	10	8	2.3840	1.9860	1.200	16.5	0.00	306.1 ± 131.3
		5	49	44	12	6.4890	5.8270	1.114	48.3	0.00	284.6 ± 59.6
		6	76	65	24	5.0320	4.3040	1.169	35.7	0.00	298.5 ± 51.0
		53	78	36	25	4.9580	2.2880	2.167	19.0	0.04	542.6 ± 110.2
		54	46	24	24	3.0460	1.5890	1.917	13.2	0.09	482.3 ± 122.1
		56	38	17	20	3.0190	1.3510	2.235	11.2	0.00	559.1 ± 163.8
		57	33	12	15	3.4960	1.2710	2.751	10.5	0.00	681.2 ± 230.3
		59	31	22	12	4.1050	2.9130	1.409	24.2	0.01	358.0 ± 100.2
		60	15	8	20	1.1920	0.6358	1.875	5.3	0.00	472.2 ± 207.1

NOTES:
Ns: number of spontaneous tracks
Ni: number of induced tracks
Na: number of grid squares counted in each grain
RHOs: spontaneous track density
RHOi: induced track density
U (ppm): uranium in parts per million
Cl (wt%): chlorine in weight percent
FT: fission-track
Ma: million years

Table 9.11. Summary of apatite fission-track data of core samples from Empress 1A (Hegarty et al., 1988)

Parameter	*Unit*	*Sample 1*	*Sample 2*[(c)]	*Sample 3*
Depth	m	123–125	318–320	557–560
Formation		Paterson	?Lupton	Kanpa
Stratigraphic age		Early Permian	Ediacaran–Cambrian	Neoproterozoic
	Ma	300–270	560–530	780–750
Present-day temperature	°C	27	30	35
Chi squared (9° freedom)	χ^2	91.745	60.666	15.063
P(chi squared)	$P(\chi^2)$	0.0	0.0	8.9
Correlation coefficient		0.902	0.830	0.836
Variance of SQR(Ns)		14.65	6.53	3.41
Variance of SQR(Ni)		11.59	3.63	2.77
Age dispersion	%	29.717	31.792	19.122
Ns/Ni		1.904 ± 0.070	2.334 ± 0.1070	1.635 ± 0.126
Mean ratio		2.364 ± 0.205	2.728 ± 0.283	1.781 ± 0.172
RHOd (ND = 2200)	$\times 10^6$	1.362	1.368	1.374
RHOs (Ns)	$\times 10^6$	3.236 (2138)	4.434 (1585)	**3.955 (443)**
RHOi (Ni)	$\times 10^6$	1.700 (1123)	1.900 (679)	**2.419 (271)**
Pooled age	Ma	475.0 ± 21.4	580.3 ± 30.6	**413.6 ± 33.7**
Central age	Ma	**523.4 ± 44.4**	**588.4 ± 53.7**	420.8 ± 44.0
Grain's (chlorine weight percent)	0.0 – 0.1	19	15	10
	0.1 – 0.2	–	2	–
	0.2 – 0.3	1	1	–
	0.3 – 0.4	–	1	–
	0.6 – 0.7	–	1	–
Total grains		**20**	**20**	**10**
Track-length interval	8 (µm)	2	–	–
	9 (µm)	3	–	–
	10 (µm)	9	2	1
	11 (µm)	15	7	1
	12 (µm)	36	29	5
	13 (µm)	29	20	3
	14 (µm)	7	15	2
	15 (µm)	1	–	–
	16 (µm)	–	–	1
	17 (µm)	–	2	–
Total tracks		**102**	**75**	**13**
Mean track length	µm	11.40 ± 0.13	12.11 ± 0.14	12.19 ± 0.42
Standard deviation	µm	1.31	1.18	1.51
Default mean track length	µm	14.12	13.8	13.5
Apatite fission-track age	Ma	523.4 ± 44.4	588.4 ± 53.7	413.6 ± 33.7
Default fission-track age	Ma	282	569	708
Maximum palaeotemperature[(a)]	°C	n/a	90–100	>100
Onset of cooling[(a)]	Ma	n/a	640–200	600–300
Maximum palaeotemperature[(b)]	°C	75–85	70–80	80–105
Onset of cooling[(b)]	Ma	40–0	120–0	300–0

NOTES:

SQR:	square root
Ns:	number of spontaneous tracks
Ni:	number of induced tracks
d:	density from standard
RHOd:	track density from uranium standard glass
RHOs:	spontaneous track density
RHOi:	induced track density
ND:	total number of tracks counted
P(chi squared):	probability of obtaining chi squared values
Mean ratio:	mean of (Ns/Ni) for individual grains
Ma:	million years before present
n/a:	not applicable

Overlapping timing constraints from AFTA include 600–300 Ma for onset of cooling[(a)] and 40–0 Ma for onset of cooling[(b)]

(c) sample 2 designated as of ?Lupton Formation (640–600 Ma) when supplied to Geotrack International

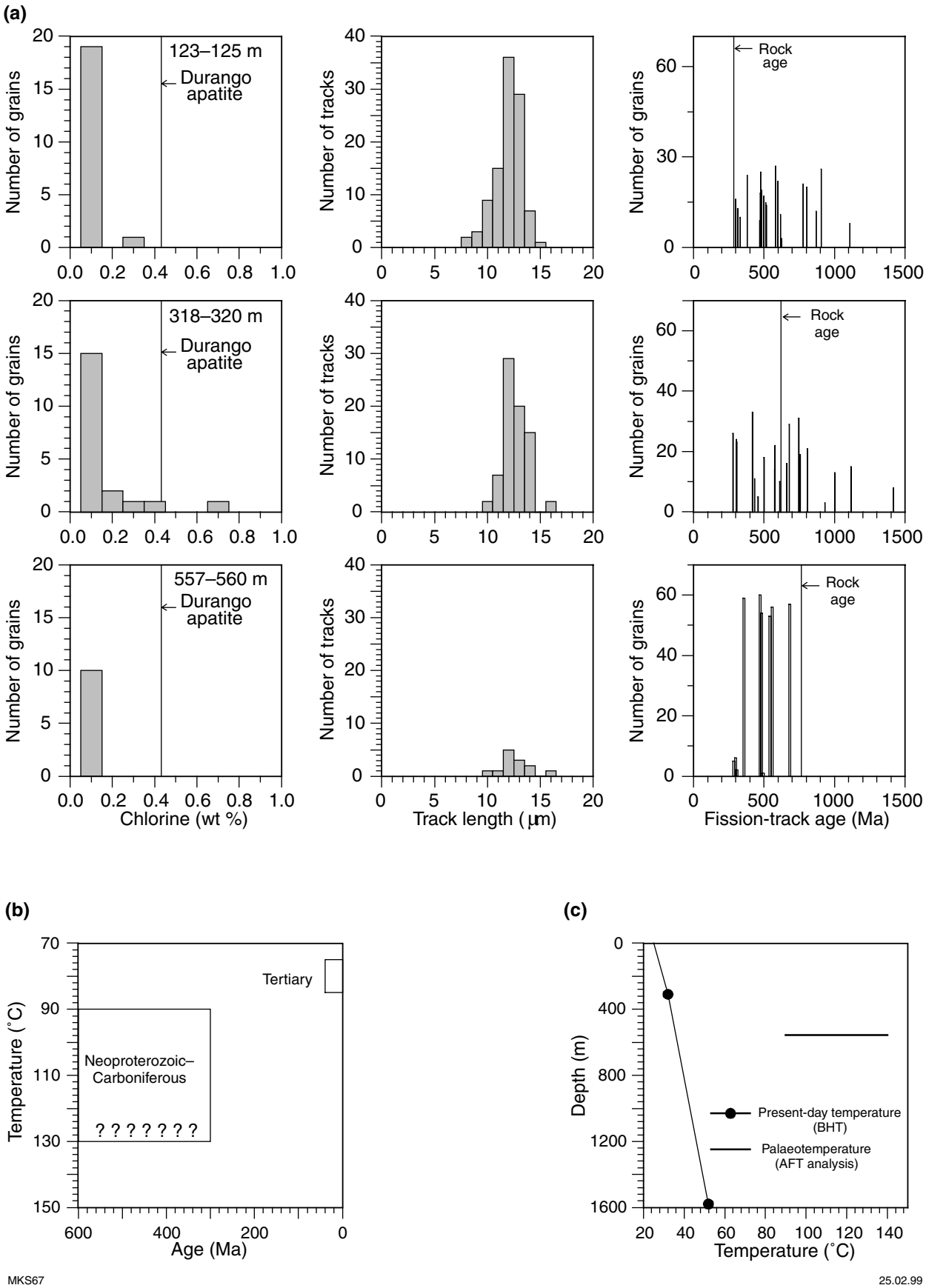

Figure 9.10. Results of apatite fission-track analysis (AFTA) for three cores from Empress 1A: a) chlorine content, fission-track length, and fission-track age; b) magnitude and timing of palaeotemperatures from AFTA; c) present-day temperature from BHT and palaeotemperatures from AFTA

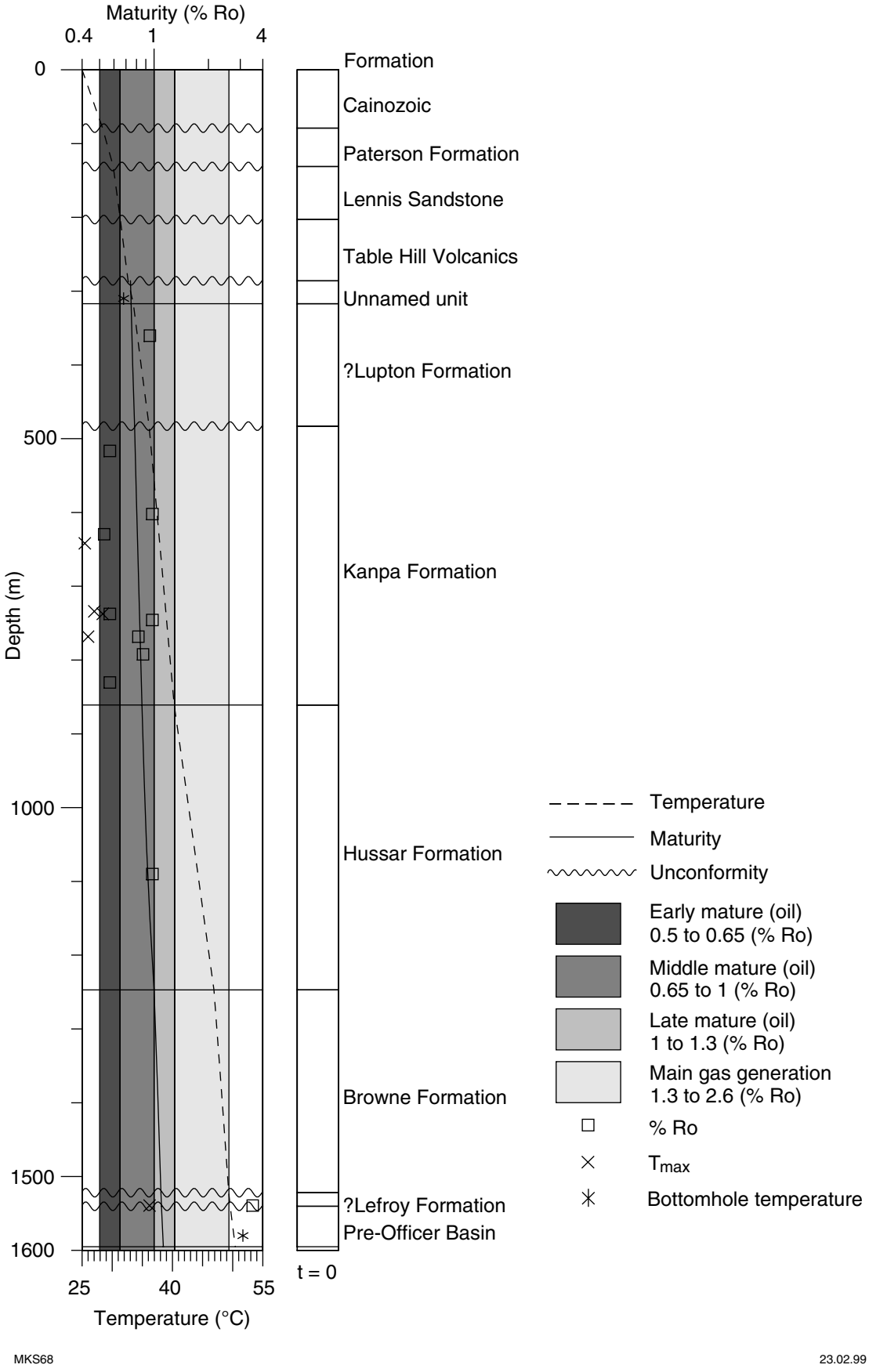

Figure 9.11. Calibration of measured versus calculated temperatures and maturity in Empress 1A

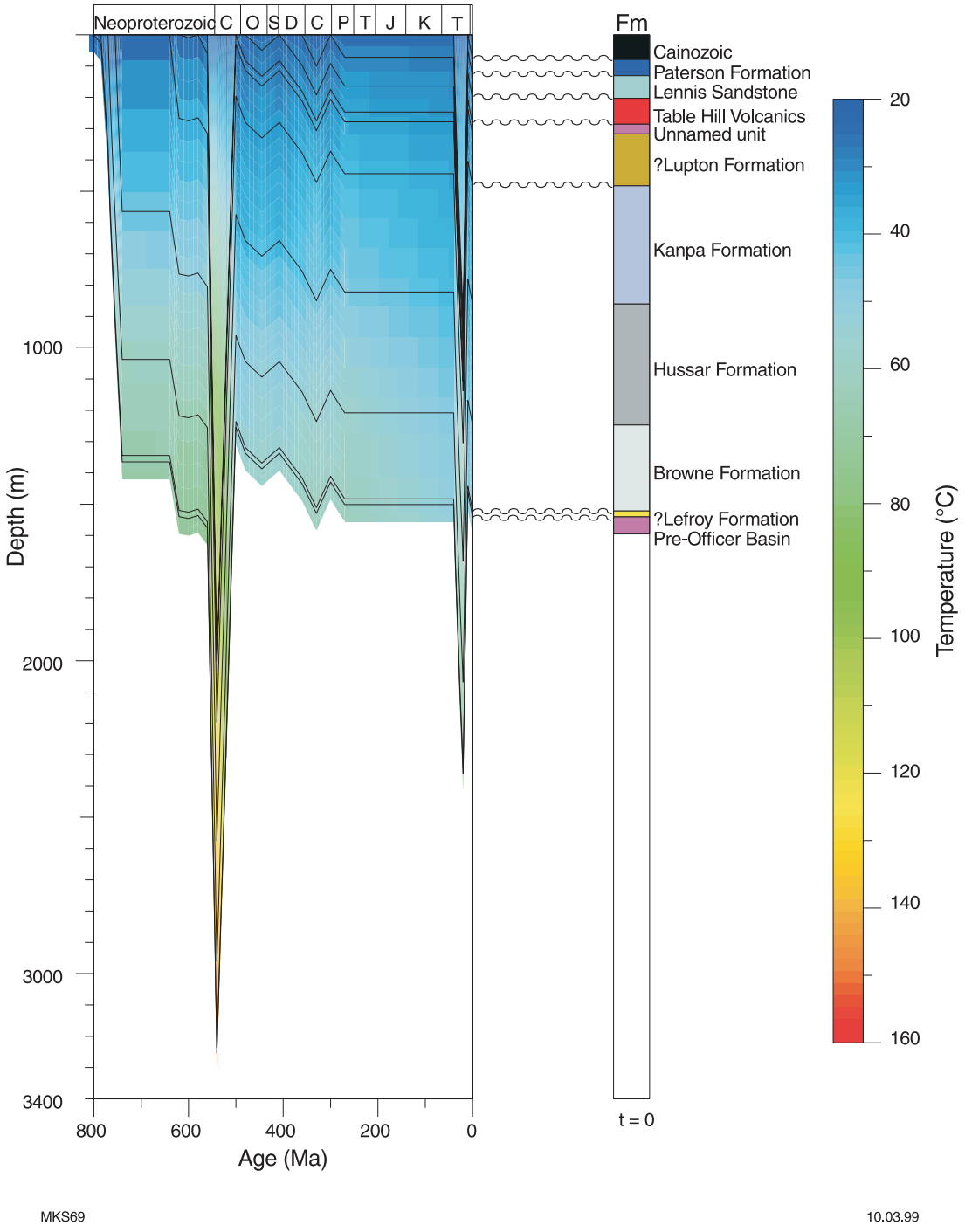

Figure 9.12. Calibration of palaeotemperature as a function of burial and erosional histories in Empress 1A

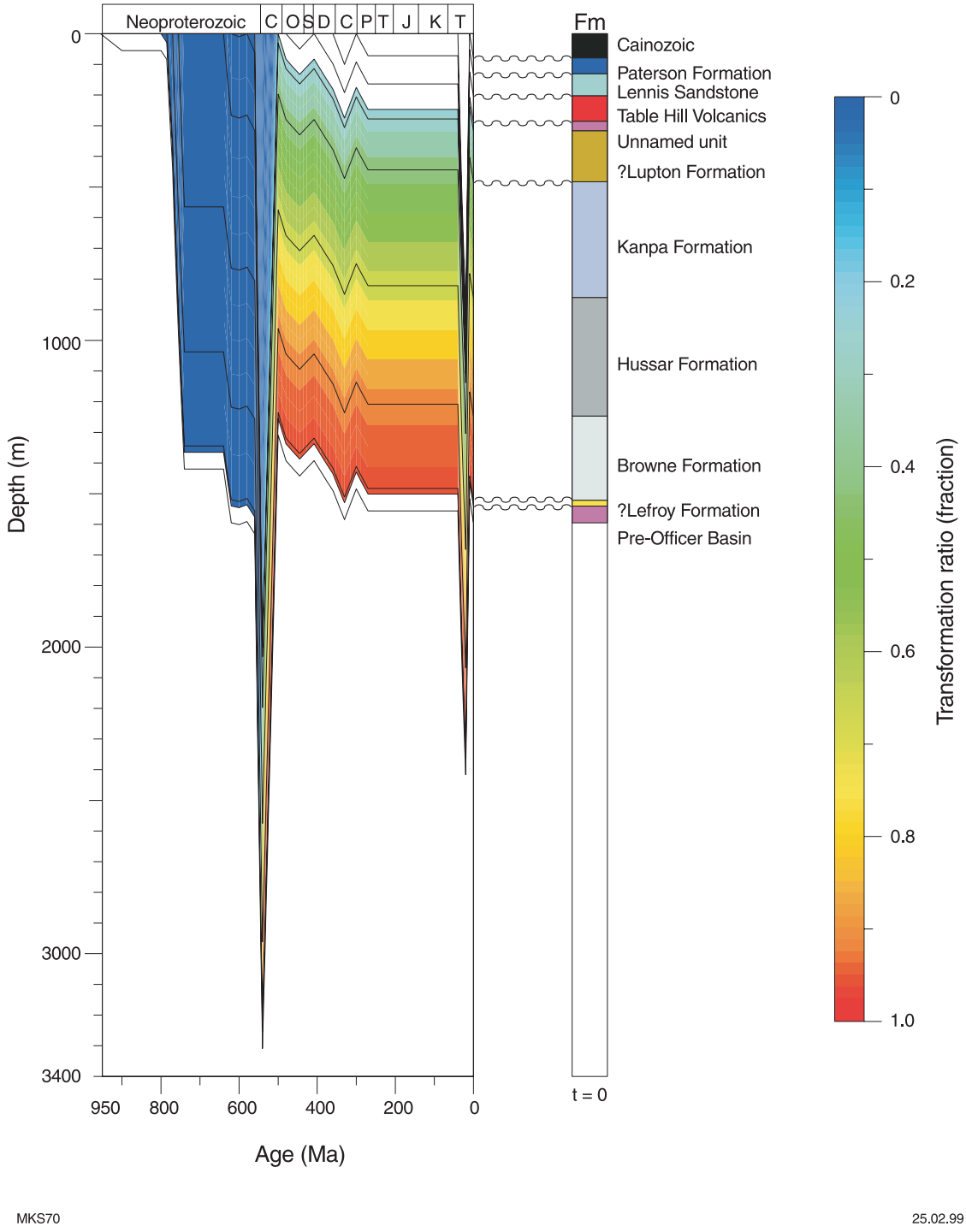

Figure 9.13. Oil window as a function of transformation ratio of kerogen to petroleum in Empress 1A

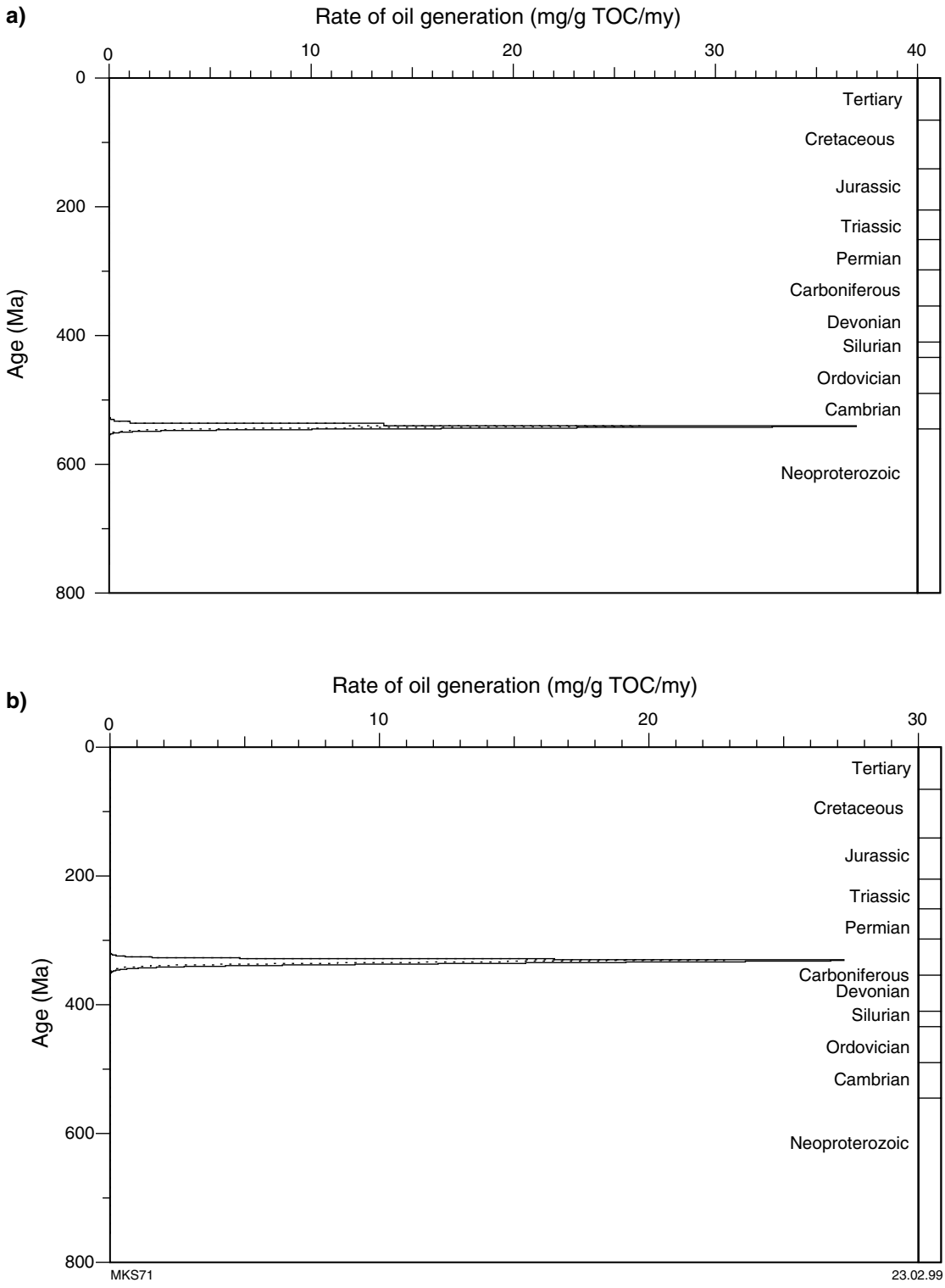

Figure 9.14. Timing of peak hydrocarbon generation as a function of oil and gas generation rate versus time for top and base of the Kanpa Formation in Empress 1A: a) if the major erosional event is assumed to be during the Petermann Ranges Orogeny; b) if the major erosional event is assumed to be during the Alice Springs Orogeny

Table 9.12. Present-day subsurface temperature in Empress 1A

RT (m)	*GL (m)*	*Recorded (°C)*	*Estimated (°C)*	*Surface (°C)*	*Gradient (°C/100 m)*	*Log*	*Date*
310.0	309.6	29.0	31.9	25	2.2	Dual resistivity, gamma ray, and caliper	27/08/97
1 580.0	1 579.6	47.0	51.7	25	1.7	Dual resistivity, gamma ray, and caliper	25/08/97

NOTES: RT: rotary table
GL: ground level

Run one was recorded between 1580 and 650 m, whereas run two was between 310 and 210 m. The time gap between mud circulation and logging was 4 hours and 40 minutes for the dual resistivity, 7 hours for density, 18 hours and 30 minutes for sonic, and 23 hours and 25 minutes for the dipmeter. Although these logs were run at different times since circulation, only one bottomhole temperature (BHT) was recorded for each depth. Therefore, an arbitrary factor of plus 10% for converting BHT to equilibrium temperature is applied. The estimated present-day geothermal gradient in Empress 1A is 1.7ºC/100 m (Table 9.12).

Petroleum generation modelling

Kinetic modelling of petroleum generation as a function of geothermal history and type and amount of kerogen was used to determine the oil window utilizing the BasinMod package of Platte River Associates. A vitrinite reflectance value of 0.65% has been adopted for the onset of the oil window. This value is based on the kerogen type estimated from geochemical data as 10% type I kerogen, 70% type II, and 20% type III. The depth of the oil window is taken to be equivalent to burial depths required for the conversion of 10–90% of the available kerogen to petroleum. The thermal history was constructed by adjusting thermal conductivities and heat flow to constrain maturity models versus measured data. Corrected BHTs, equivalent % Ro, T_{max}, and information from AFTA were used to constrain present-day temperatures and palaeotemperatures. Predicted maturity and oil windows are based on Lawrence Livermore National Laboratory (LLNL) vitrinite and kerogen kinetics respectively.

Figure 9.11 shows the calibration of the maturity model and compares measured with calculated temperatures and maturity, whereas Figure 9.12 shows the calibration of temperatures as a function of burial and erosional histories. Figure 9.13 illustrates the oil window as a function of the transformation ratio of kerogen to petroleum, and indicates that the recognized oil source beds within the Kanpa Formation are at main stages of oil generation with ratios up to 0.5 (fraction). The time of petroleum generation is a function of kerogen conversion to petroleum over a period of time and is shown as rate of generation versus time (Fig. 9.14).

The maturation and hydrocarbon generation modelling of Empress 1A shows that the source beds within the Kanpa Formation are presently at the main stages of oil generation, and the timing for peak generation was during the Cambrian, if the major erosional event was assumed to be the Petermann Ranges Orogeny (Fig. 9.14a). However, if the Alice Springs Orogeny is assumed to be the major erosional event, then the peak time for oil generation was during the Carboniferous (Fig. 9.14b).

Conclusions

TOC, Rock-Eval, PGC, extract liquid-gas chromatography, organic petrology, and AFTA of core samples from Empress 1 and 1A suggest that the Neoproterozoic Kanpa Formation penetrated in the Empress 1A drillhole contains fair to good, fully mature, oil-prone source beds between 587.85 and 588.35 and 737.4 and 768.2 m. These source beds are of centimetre thickness at this location. The maximum palaeotemperatures were reached some time between 600 and 300 Ma. The basal section of interbedded clastic and volcanic rocks is overmature.

References

COOK, A. C., 1995, Report on source rock type, maturation levels, thermal history and hydrocarbon occurrence in suites of samples from four wells in the Officer Basin, W.A. by Keiraville Konsultants Pty Ltd: Western Australia Geological Survey (unpublished), 40p.

CRICK, I. H., BOREHAM, C. J., COOK, A. C., and POWELL, T. G., 1988, Petroleum geology and geochemistry of the Middle Proterozoic McArthur Basin, Northern Australia II — assessment of source rock potential: American Association of Petroleum Geologists, Bulletin, v. 72, p. 1495–1514.

HEGARTY, K. A., O'BRIEN, C., and WATSON, P. G. F., 1988, Thermal history reconstruction for the Empress 1A well (Officer Basin) using apatite fission track analysis and reflectance by Geotrack International Pty Ltd (Geotrack), Report 681: Western Australia Geological Survey (unpublished).

LAMBECK, K., 1984, Structure and evolution of the Amadeus, Officer and Ngalia Basins of central Australia: Australian Journal of Earth Sciences, v. 31, p. 25–48.

LARTER, S. R., 1985, Integrated kerogen typing in the recognition and quantitative assessment of petroleum source rocks, *in* Petroleum geochemistry in exploration of Norwegian Shelf *edited by* B. M. THOMAS: London, Norwegian Petroleum Society, p. 269–286.

PERINCEK, D., 1996, The age of Neoproterozoic–Palaeozoic sediments within the Officer Basin of the Centralian Superbasin can be constrained by major sequence-bounding unconformities: APPEA Journal, v. 36, pt 1, p. 61–79.

Appendix 10
Core and log analysis
(by P. Havord)

Core analysis

Porosity and permeability measurements were made on three core plug samples from the Paterson Formation, one from the Lennis Sandstone, four from the Table Hill Volcanics, three from the unnamed unit (between the Table Hill Volcanics and ?Lupton Formation), two from the ?Lupton Formation, two from the Steptoe Formation (now included in the Kanpa Formation), ten from the Kanpa Formation, 18 from the Hussar Formation, 24 from the Browne Formation, and four from the pre-Browne unit. Helium porosity and air and Klinkenberg (liquid equivalent) permeabilities were determined for each core sample at confining pressures of 800 and 1000 psi (CoreLab, 1997). Core analysis results are presented in Table 10.1 and shown in Figures 10.1 and 10.2. In addition, permeability measurements were obtained by profile permeametry on intervals within the Hussar and Browne Formations (see Plate 1).

Log analysis

The density, neutron, sonic, and gamma-ray logs were used to calculate effective (clay corrected) porosities using the complex-lithology processing module of the Petrolog computer log analysis program. Effective porosities were computed for the Table Hill Volcanics, the upper part of the unnamed unit, and Kanpa, Hussar, Browne, and ?Lefroy Formations. The interval above the Table Hill Volcanics, as well as the upper part of the Kanpa Formation, ?Lupton

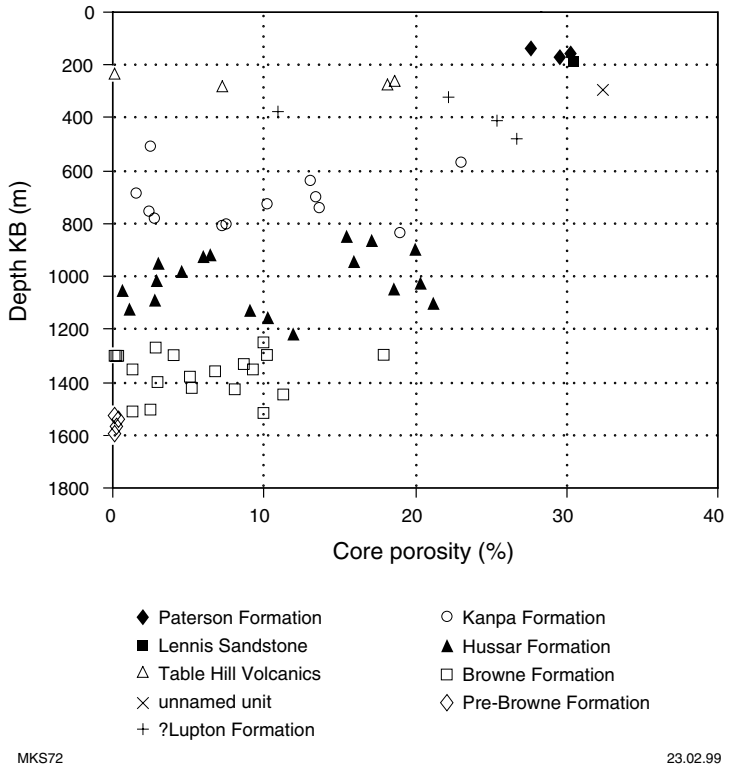

Figure 10.1. Relationship between core porosity and depth for Empress 1 and 1A

Table 10.1. Empress 1 and 1A core analysis results (including reanalysed samples)

Formation	Depth (m)	800 psi nob pressure — Permeability — Kinf (mD)	800 psi nob pressure — Permeability — Kair (mD)	Porosity (%)	Grain density (g/cc)
Paterson Formation	136.70	5 730	5 770	27.7	2.63
	159.90	5 890	5 950	30.3	2.62
	173.00	6 050	6 110	29.5	2.62
Lennis Sandstone	191.10	6 240	6 300	30.5	2.64
Table Hill Volcanics	231.60	<0.001	<0.001	<0.1	2.78
	257.40	0.037	0.050	18.7	2.63
	275.10	0.219	0.291	18.2	2.67
	282.30	0.001	0.004	7.2	2.59
unnamed unit	294.70	810	831	32.4	2.63
?Lupton Formation	322.10	10.7	12.4	22.2	2.66
	375.70	0.025	0.044	10.9	2.68
	412.70	80.1	85.3	25.4	2.65
	480.00	62.1	75.2	26.8	2.67
Kanpa Formation	503.60	<0.001	<0.001	2.5	2.83
	567.50	30.5	31.8	23.0	2.68
	639.30	0.001	0.002	13.1	2.67
	685.80	<0.001	<0.001	1.6	2.97
	696.50	0.470	0.684	13.5	2.67
	724.80	0.955	1.19	10.2	2.68
	741.50	1.56	1.98	13.7	2.68
	752.80	0.001	0.003	2.4	2.75
	782.50	0.001	0.003	2.7	2.85
	800.00	0.010	0.020	7.5	2.69
	804.40	1.64	1.83	7.21	2.66
	832.00	361	371	19.0	2.64
Hussar Formation	864.30	252	300	15.3	2.64
	877.40	261	265	17.0	2.63
	911.80	1 270	1 400	19.8	2.64
	932.70	0.025	0.040	6.3	2.76
	937.80	0.137	0.199	5.8	2.65
	958.40	107	113	15.8	2.66
	967.10	0.001	0.003	2.9	2.68
	991.60	0.023	0.037	4.4	2.69
	1 024.90	0.002	0.004	2.7	2.79
	1 042.40	146	161	20.2	2.64
	1 058.00	65.0	73.1	18.4	2.62
	1 070.80	0.001	0.003	0.5	2.95
	1 102.70	<0.001	0.001	2.7	2.86
	1 116.20	2 690	2 770	21.0	2.63
	1 137.20	0.002	0.004	1.0	2.87
	1 142.60	0.967	0.999	9.0	2.70
	1 170.70	2.71	2.86	10.1	2.69
	1 232.40	0.048	0.088	11.7	2.69
Browne Formation	1 251.00	0.721	0.915	10.0	2.54
	1 274.90	14.5	15.3	2.8	2.19
	1 298.3	<0.001	<0.001	0.1	2.59
	1 298.9	<0.001	<0.001	0.1	2.59
	1 299.6	<0.001	<0.001	<0.1	2.34
	1 299.8	<0.001	<0.001	<0.1	2.52
	1 300.2	<0.001	<0.001	0.1	2.44
	1 301.4	<0.001	<0.001	0.3	2.53
	1 302.3	<0.001	<0.001	0.2	2.63
	1 301.40	372	383	18.0	2.58
	1 302.30	0.789	0.940	10.2	2.58
	1 303.40	0.061	0.085	4.0	2.64
	1 335.40	0.743	0.829	8.7	2.62
	1 353.40	3.76	4.37	9.2	2.63
	1 358.20	0.009	0.012	1.3	2.80
	1 365.00	42.7	46.6	6.8	2.71
	1 382.90	0.104	0.137	5.1	2.78

Table 10.1. (continued)

Formation	Depth (m)	800 psi nob pressure — Permeability — Kinf (mD)	Permeability — Kair (mD)	Porosity (%)	Grain density (g/cc)
Browne Formation (cont.)	1 400.20	0.300	0.354	3.0	2.67
	1 422.30	0.035	0.048	5.2	2.70
	1 430.60	8.94	9.69	8.0	2.62
	1 452.70	6.04	6.16	11.3	2.62
	1 506.00	0.838	0.891	2.5	2.54
	1 514.50	0.211	0.226	1.3	2.18
	1 521.20	396	421	9.9	2.53
?Lefroy Formation	1 524.90	<0.001	<0.001	0.1	2.71
Pre-Officer Basin	1 542.70	<0.001	<0.001	0.3	2.72
	1 569.80	<0.001	<0.001	0.2	2.82
	1 593.30	<0.001	<0.001	0.1	2.96

NOTES: Kinf: Klinkenberg permeability
Kair: Permeability to air

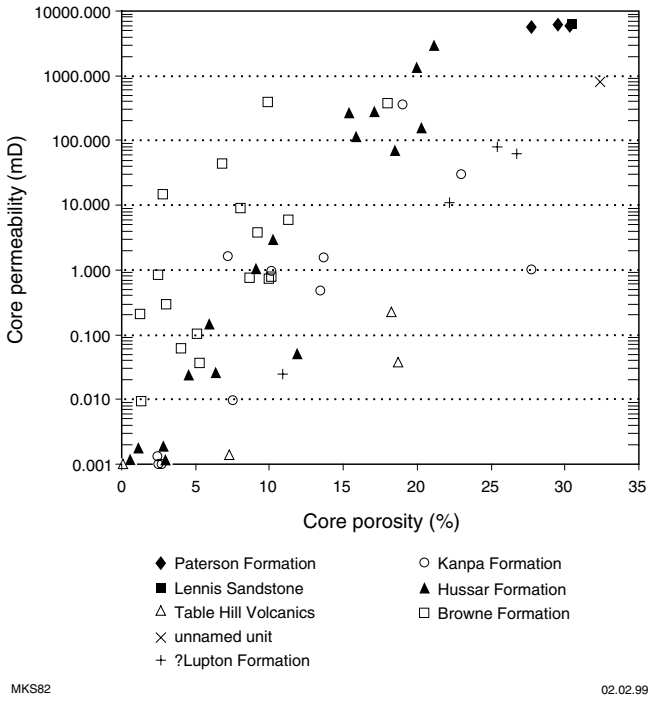

Figure 10.2. Relationship between core porosity and core permeability for Empress 1 and 1A

Table 10.2. Log analysis zone input parameters and results for Empress 1A

Formation	*Lennis Sandstone*	*Table Hill Volcanics*	*Unnamed unit*	*Kanpa Formation*				*Hussar Formation*					*Browne Formation*					*Unnamed unit*
				Unit A	*Unit B*	*Unit C*	*Unit D*	*Unit A*	*Unit B*	*Unit B*	*Unit C*	*Unit D*	*Unit A*	*Unit A*	*Unit A*	*Unit A*	*Unit B*	
Zone number	*1*	*2*	*3*	*4*	*5*	*6*	*7*	*8*	*9*	*10*	*11*	*12*	*13*	*14*	*15*	*16*	*17*	*18*
Top depth	200.0	203.1	286.9	652.0	686.9	726.1	787.7	862.8	1 045.2	1 078.0	1 104.6	1 157.7	1 249.3	1 299.5	1 306.1	1 320.0	1 406.1	1 524.1
Bottom depth	203.0	286.8	302.0	686.8	726.0	787.6	862.7	1 045.1	1 077.9	1 104.5	1 157.6	1 249.2	1 299.4	1 306.0	1 319.9	1 406.0	1 524.0	1 585.0
RHOMA	2.64	2.78	2.63	3.00	2.92	2.85	2.64	2.64	2.64	2.7	2.65	2.64	2.1	2.673	2.1	2.1	2.1	2.7
Tma	55.5	55.5	55.5	60.0	50.0	60.0	70.0	55.5	55.5	80.0	55.5	60.0	67.0	60.0	67.0	55.0	67.0	60.0
Sonic Option	RHG	RHG	RHG	RHG	RHG	RHG	RHG	RHG	RHG	RHG	RHG	RHG	RHG	RHG	RHG	RHG	RHG	RHG
No clay	–	–	–	–	–	–	–	–	–	–	–	–	–	–	–	–	–	–
GR clean	20	20	20	20	20	20	20	20	20	20	20	20	20	20	20	20	20	20
GR clay	120	120	120	120	120	120	120	120	120	120	120	120	120	120	120	120	120	120
RHOBclay	2.450	2.509	2.241	2.450	2.537	2.528	2.582	2.325	2.708	2.908	2.688	2.649	2.645	2.615	2.545	2.512	2.344	2.799
$PHIN_{clay}$	0.400	0.477	0.410	0.398	0.307	0.302	0.313	0.293	0.280	0.284	0.245	0.294	0.201	0.286	0.224	0.256	0.294	0.299
t_{clay}	101.0	87.7	109.2	109.2	104.3	92.9	98.5	86.4	97.0	92.0	85.3	85.8	69.1	76.3	69.4	71.2	68.5	67.3
M_{clay}	0.617	0.681	0.655	0.559	0.532	0.638	0.601	0.787	0.545	0.514	0.612	0.634	0.739	0.707	0.785	0.790	0.911	0.684
N_{clay}	0.420	0.352	0.484	0.422	0.450	0.463	0.456	0.542	0.427	0.380	0.453	0.434	0.492	0.448	0.509	0.499	0.534	0.394
$PHIN_{2.2}$	0.235	0.221	0.200	0.235	0.266	0.244	0.204	0.222	0.269	0.261	0.217	0.235	0.245	0.235	0.292	0.287	0.264	0.299
$t_{2.2}$	90.0	90.0	90.0	90.0	90.0	90.0	90.0	90.0	90.0	90.0	90.0	90.0	90.0	90.0	90.0	90.0	90.0	90.0
PHImax	0.314	0.319	0.371	0.4	0.3	0.286	0.355	0.303	0.227	0.278	0.263	0.239	0.212	0.271	0.212	0.266	0.245	0.218
PHImaxcalc	nd	0.311	0.371	0.349	0.3	0.256	0.262	0.282	0.259	0.047	0.240	0.207	0.129	0.115	0.026	0.160	0.146	0.106
CLAY meancalc	0.536	0.129	0.343	0.315	0.123	0.137	0.272	0.184	0.114	0.337	0.120	0.470	0.024	0.001	0.001	0.053	0.127	0.081

NOTES:

Abbreviation	**Definition**	**Units**	**Data Source**
CLAY meancalc	Calculated mean clay volume	fraction	Petrolog calculation
GR	Gamma ray	API	Coburn 1 log suite
GR clay	100% clay formation gamma ray cutoff	API	Petrolog user specification
GR clean	Clay-free gamma ray cutoff API		Petrolog user specification
M_{clay}	$(t_{fluid}–t_{clay})/(RHOB_{clay}–RHO_f)$		Petrolog crossplots
N_{clay}	$(PHIN_{fluid}–PHIN_{clay})/(RHOB_{clay}–RHO_{fluid})$		Petrolog crossplots
No clay	Switch for undesired clay indicators		Petrolog user specification
PHImax	Crossplot-limited maximum porosity	fraction	Petrolog user specification
PHImaxcalc	Calculated maximum effective porosity	fraction	Petrolog calculation
$PHIN_{clay}$	Clay neutron value	fraction	Petrolog crossplots
$PHIN_{fluid}$	Fluid neutron value	fraction	Petrolog calculation
$PHIN_{2.2}$	Clean point on density-neutron crossplot		Petrolog crossplots
RHG	Raymer–Hunt–Gardner porosity equation		Petrolog user specification
$RHOB_{clay}$	Clay density	g/cm^3	Petrolog crossplots
RHO_{fluid}	Fluid density	g/cm^3	Petrolog calculation
RHOMA	Rock solids density	g/cm^3	Core analysis (CoreLab, 1997)
Sonic Option	Sonic porosity equation		Petrolog user specification
t_{clay}	Clay transit time	us/ft	Petrolog crossplots
$t_{2.2}$	Clean point on density-sonic crossplot		Petrolog crossplots
t_{fluid}	Formation fluid transit time	us/ft	Petrolog calculation
Tma	Average formation transit time	us/ft	Petrolog user specification

Formation, and most of the unnamed unit, were cased, thereby precluding analysis. Core porosity and grain-density data were used to calibrate the computation of effective porosity.

The computed maximum-effective log porosities are:

- 31.1% for the Table Hill Volcanics
- 37.1% for the unnamed unit
- 34.9% for the Kanpa Formation
- 28.2% for the Hussar Formation
- 16.0% for the Browne Formation
- 10.6% for the ?Lefroy Formation

The log-derived mean clay volume for each zone was also calculated (Table 10.2). Effective log porosity for the uncased portion of Empress 1A is presented as a curve in the WCR composite log (see Plate 1).

Reference

CORELAB, 1997, Routine core analysis wells Empress 1 and 1A: Western Australia Geological Survey, S-series S20424 A1 (unpublished).

Appendix 11
Chemical analysis of drillcore from Empress 1 and 1A to assess potential for base metals and phosphate
(by I. Ruddock)

Twenty-two drillcore samples were collected from Ordovician, Neoproterozoic, and ?Mesoproterozoic successions in Empress 1 and 1A to check the potential for sedimentary-hosted base metal mineralization and phosphate mineralization, and also for base metal mineralization associated with contact zones between mafic volcanics and sedimentary rocks. The samples were analysed for the following nine elements: Ag, As, Ba, Co, Cu, Mn, P, Pb, and Zn.

Core samples were obtained as 2 m intervals of quarter-slabbed PQ core and half-slabbed HQ core except in zones of friable shales, at 608–610 and 678–680 m, where the sampled material was rock chips. Sampled intervals were selected to provide a spot check of lithologies that had the most likely mineral potential.

Sample preparation and analysis were carried out by Genalysis Laboratory Services, Maddington, Perth. Crushing and pulverizing were carried out using a jaw crusher and a chrome-steel ring grinder. Sample dissolution was by digestion in a multi-acid mixture of hydrofluoric, hydrochloric, nitric, and perchloric acids. Sample solutions were analysed by inductively coupled plasma optical-emission spectrography (ICP–OES).

Sample analyses are shown in Table 11.1. Although none of the sampled intervals show encouraging results for base metal or phosphate mineralization, this does not necessarily downgrade the mineral potential of the units intersected. In particular, the sabkha to shallow-marine deposits of the Neoproterozoic Kanpa and Hussar Formations could still be prospective for base metals. More comprehensive sampling of these successions (using continuous 'fillets' of core from Empress 1A) may yield more encouraging results. Also, drilling of these successions elsewhere in the region may locate base metal mineralization in fault zones or other structural corridors, which have acted as conduits for large volumes of metal-rich basinal fluids.

Some samples show relatively high values for Mn, Cu, Co, and P, but these reflect higher background values expected for particular lithologies. The samples from mafic volcanics show slightly high values for Cu, Co, and Mn due to the presence of pyroxenes, amphiboles, and chlorite, which commonly contain relatively high concentrations of these elements. Highest Mn values are shown in chlorite-rich intervals of sheared mafic volcanics and adjacent siltstones of the pre-Officer Basin strata (1562 – 1624.6 m total depth). The highest value for P (3515 ppm) is from the arenaceous interval at the base of the ?Lefroy Formation (1536–1538 m), which has been interpreted as an unconformity. Offsetting this value is the knowledge that phosphorus often shows concentrations above erosional breaks (e.g. basal phosphatic-nodule horizons).

Table 11.1. Drillcore analyses

Drillhole	*Unit*	*Depth*	*Ag*	*As*	*Ba*	*Co*	*Cu*	*Mn*	*P*	*Pb*	*Zn*
						Parts per million					
Empress 1	Table Hill Volcanics	204.0 – 206.0	<2	10	164	46	8	510	263	20	48
		240.0 – 242.0	<2	5	251	43	20	1209	291	27	59
		246.0 – 248.0	<2	<5	245	42	73	994	308	30	63
		254.0 – 256.0	<2	<5	272	41	72	1186	323	25	61
		256.0 – 269.0	<2	<5	202	40	19	634	312	19	66
Empress 1A	Table Hill Volcanics	275.0 – 277.0	<2	5	117	44	13	582	293	15	92
		284.0 – 286.0	<2	<5	288	48	11	346	294	26	223
	Kanpa Formation	608.0 – 610.0	<2	<5	271	37	44	187	977	18	64
		678.0 – 680.0	<2	<5	156	37	32	821	806	26	63
		737.0 – 739.0	<2	8	199	5	1	311	122	16	35
		654.0 – 766.0	<2	<5	225	5	1	272	114	14	19
		810.0 – 812.0	<2	<5	473	21	8	251	346	29	80
		836.0 – 838.0	<2	<5	610	12	19	157	251	20	44
	Hussar Formation	1 098.0 – 1 100.0	<2	<5	378	25	90	209	285	38	75
	Browne Formation/ ?Lefroy Formation contact	1 521.0 – 1 523.0	<2	<5	711	11	2	522	1418	19	66
	?Lefroy Formation	1 536.0 – 1 538.0	<2	<5	733	13	8	448	3515	14	109
	Pre-Officer Basin strata (sedimentary rocks)	1 562.0 – 1 564.0	<2	<5	555	27	21	1600	452	24	88
	Pre-Officer Basin strata (mafic volcanic rocks)	1 570.0 – 1 572.0	<2	<5	467	37	40	4060	650	17	79
		1 574.0 – 1 576.0	<2	<5	449	53	81	1148	982	15	71
		1 578.0 – 1 580.0	<2	<5	442	45	111	1112	989	16	74
		1 600.0 – 1 602.0	<2	<5	467	40	138	1224	1017	17	84
		1 622.0 – 1 624.0	<2	<5	418	52	106	2356	979	14	75
Detection limit			2	5	2	2	1	1	20	5	1

Appendix 12
Well index sheet

ORGANIZATION: Geological Survey of Western Australia
S no.: 20424
SPUDDED: 21 June 1997
WELL: GSWA Empress 1
TYPE: Stratigraphic
COMPLETED: 13 July 1997
BASIN: Officer Basin **TD:** 615 m
ELEV. GL: 461 m AHD (differential GPS) note: 0.7 m upward shift of drill floor at 294.2 m
LAT: 27°03'13.3"S; **LONG:** 125°09'24.5"E
STATUS: Abandoned
NORTHING: 7005774; **EASTING:** 713917 (AGD84 Zone 51J)

FORMATION	TOPS (m) DRILL	TOPS (m) SUBSEA	LITHOLOGICAL SUMMARY
Cainozoic	surface	+461	Clay, sandstone, gravel
Paterson Formation	79	+382	Mudstone, sandstone, conglomerate
Lennis Sandstone	131.9	+329.1	Sandstone, conglomerate
Table Hill Volcanics	201.3	+259.7	Basalt, dolerite
Unnamed unit	285	+176	Sandstone, conglomerate, mudstone
?Lupton Formation	316.9	+144.1	Diamictite, sandstone, mudstone, conglomerate
Kanpa Formation	482.6	-21.6	Dolomite, sandstone, mudstone, conglomerate
Base of core	612.9	-151.9	

CORES	Fully cored: PQ: 105 – 294.2 m (94% recovery) HQ: 294.9 – 612.9 m (93% recovery)
LOGS	No wireline logs acquired
CASING	VAM 7" 0 – 11.5 m PW 5.5" 0 – 105 m (all recovered) PF 4.5" 0 – 294.2 m (recovered above 129 m)
FISH	HMQ drillstring, HQ barrel, and drillbit 615–494 m

ORGANIZATION: Geological Survey of Western Australia **S no.:** 20424
SPUDDED: 13 July 1997 **WELL:** GSWA Empress 1A **TYPE:** Stratigraphic
COMPLETED: 28 August 1997 **BASIN:** Officer Basin **TD:** 1624.6 m
ELEV. GL: 461 m AHD (differential GPS) note: rig shifted by 6 m to 300° from Empress 1
LAT: 27°03'13.26"S; **LONG:** 125°09'24.30"E
STATUS: Abandoned **NORTHING:** 7005777; **EASTING:** 713912 (AGD84 Zone 51J)

FORMATION	TOPS (m) DRILL	TOPS (m) SUBSEA	LITHOLOGICAL SUMMARY
Cainozoic	Surface	+461	Clay, sand, sandstone, gravel
Paterson Formation	79	+382	Mudstone, sandstone, conglomerate
Lennis Sandstone	131	+330	Sandstone, conglomerate
Table Hill Volcanics	203	+258	Basalt, dolerite
Unnamed unit	286	+175	Sandstone, conglomerate, mudstone
?Lupton Formation	317.1	+143.9	Diamictite, sandstone, mudstone, conglomerate
Kanpa Formation	483	-22	Dolomite, sandstone, mudstone, siltstone, conglomerate, evaporites
Hussar Formation	860.8	-399.8	Sandstone, mudstone, dolomite
Browne Formation	1247.1	-786.1	Mudstone, salt, dolomite, sandstone
?Lefroy Formation	1521.8	-1060.8	Mudstone, sandstone, basalt
Pre-Officer Basin	1540.2	-1079.2	Mudstone, sandstone, basalt
Total depth	1624.6	-1163.6	

CORES	Fully cored:	PQ: 210.5 – 650 m	(98% recovery)
		HQ: 650 – 1624.6 m	(100% recovery)

LOGS	Compensated density, Gamma ray, caliper	650–1580 m
	Compensated density, Gamma ray, caliper	210–310 m
	Multi-channel sonic	650–1580 m
	Multi-channel sonic	210–310 m
	Dual resistivity	650–1580 m
	Dual resistivity	210–310 m
	Dipmeter (4 arm)	650–1580 m
	Dipmeter (4 arm)	210–310 m
	Limestone-neutron porosity, gamma ray	0–1580 m
	Limestone-neutron porosity, gamma ray	0–310 m

CASING
VAM 7" 0 – 11.5 m
PW 5.5" 0 – 105 m (all recovered)
PF 4.5" 0 – 294.2 m (recovered above 129 m)

GSWA RECORD 1999/4 Plate 1

GOVERNMENT OF WESTERN AUSTRALIA
HON. NORMAN MOORE, M.L.C.
MINISTER FOR MINES

DEPARTMENT OF
MINERALS AND ENERGY
L.C. RANFORD, DIRECTOR GENERAL

GEOLOGICAL SURVEY
OF WESTERN AUSTRALIA
DAVID BLIGHT, DIRECTOR

GSWA Empress 1/1A

Composite well log

Composite well log

Well Name	GSWA Empress 1 & 1A
Field	Officer Basin
Country	Australia
State	Western Australia
Latitude	027 03' 13.298" S DMS
Longitude	125 09' 24.313" E DMS
Permanent Datum	MSL
Elevation of PD	461.00 M
Elevation of KB	461.40 M
Elevation Ground lv	461.00 M
Elevation Log Zero	461.40 M
Log measured from	KB
Drill measured from	KB
Services	Drilling: Western Deep Hole Drilling
Other Services Ln 1	Mud: Australian Mud Company
Other Services Ln 2	Logging: BPB Wireline Services
Date plotted	27-02-1999
Time plotted	19:01:57

PETROLOG SOFTWARE Revision 6.31 — CROCKER DATA PROCESSING

Run number	One	Two
Log date	25 August 1997	27 August 1997
Depth-Driller	1624.60 M	1624.60 M
Depth-Logger	1583.00 M	1583.00 M
Bottom log interval	1580.00 M	310.00 M
Top log interval	0.00 M	210.00 M
Casing-Driller	650.00 M	210.00 M
Casing-Logger	651.00 M	211.10 M
Casing Diameter		5.5000 inch
Bit Size	3.7800 inch	4.8000 inch
Hole Fluid type	KCL/POLY	KCL/POLY
Fluid Density	1.2000 gm/cc	1.2000 gm/cc
Fluid Viscosity	40	40
Fluid PH	10	10
Fluid Loss	7.5	7.5
Mud Sample Source	Mud Tank	Mud Tank
RM (ohmm) Surface	0.046	0.046
Mud temp Surface	17.00 degC	17.00 degC
Mud Sample Temp		
Bottom hole temp	47.00 degC	
Max recorded temp	47.00 degC	29.00 degC
Logging unit No	V337	V337
Logging unit Loc	Perth	Perth
Recorded by	R Tench	R Tench
Witness	P Havord	P Havord
Logs run	RR3-DD3-NN1-DIP4	RR3-DD3-NN1-DIP4
Hours since circulation	18.5 hours	

LITHOLOGIES

Mudstone | Sandstone | Conglomerate
Claystone | Basalt | Breccia
Dolomite | Siltstone | Anhydrite
Halite

TADPOLE AZIMUTH ROSE LEGEND

High Quality — 1 2 3 4 5 6 7 8 9 10 — Low Quality

LEGEND

GOVERNMENT OF WESTERN AUSTRALIA
HON. NORMAN MOORE, M.L.C.
MINISTER FOR MINES

DEPARTMENT OF
MINERALS AND ENERGY
L. C. RANFORD, DIRECTOR GENERAL

GEOLOGICAL SURVEY
OF WESTERN AUSTRALIA
DAVID BLIGHT, DIRECTOR

STRUCTURAL CORRELATION OF THE OFFICER BASIN SEQUENCES, KINGSTON SHELF–YOWALGA SUB-BASIN

LEGEND

Claystone
Siltstone
Sandstone
Conglomerate
Basalt
Dolomite
Shales
Chert
Halite
Anhydrite
Limestone

Vertical scale 1:5000
Horizontal scale 1:500,000
DATUM: SEA LEVEL

SW NE

WESTWOOD 2 — 14 km — WESTWOOD 1 — 33 km — EMPRESS 1/1A — 74 km — KANPA 1A

GR 0 API 200 | DEPTH M | DT 140 US/F 40

Lennis Sandstone
Cainozoic
Paterson Formation
Lennis Sandstone
Table Hill Volcanics
unnamed unit
? Lupton Formation
Kanpa Formation
Hussar Formation
Browne Formation
? Lefroy Formation
Pre-Officer Basin
Townsend Quartzite
SUPERSEQUENCE 2
SUPERSEQUENCE 1
PALAEOZOIC
DATUM: SEA LEVEL

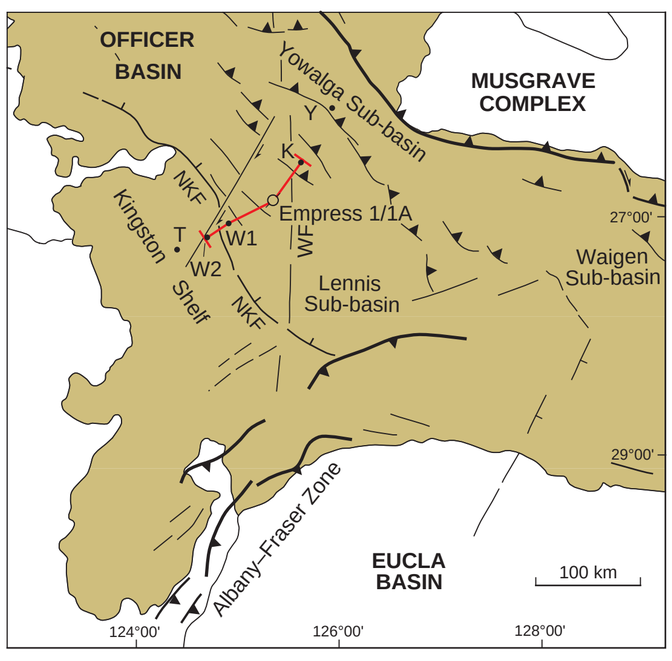

Cross section location

GSWA RECORD 1999/4 PLATE 3

GOVERNMENT OF WESTERN AUSTRALIA
HON. NORMAN MOORE, M.L.C.
MINISTER FOR MINES

DEPARTMENT OF
MINERALS AND ENERGY
L. C. RANFORD, DIRECTOR GENERAL

GEOLOGICAL SURVEY
OF WESTERN AUSTRALIA
DAVID BLIGHT, DIRECTOR

GSWA Empress 1A
Biostratigraphic range chart

Stromatolites
Acritarchs
Filaments
Miscellaneous

FDOM Finely dispersed organic matter
LOAF Large organic amorphous fragments
CO Core sample

Well Name : Empress 1A
Interval : 250.00m - 1630.00m
Scale : 1:1500

Style : Presence/Absence
Author : Kath Grey
Date : 16-December-1998